2011

Regulation of Polarized Protein Transport to Axons, Dendrites, and Sensory Cilia in Caeborhabditis Elegans Neurons

Tapan Apurva Maniar

REGULATION OF POLARIZED PROTEIN TRANSPORT TO AXONS, DENDRITES, AND SENSORY CILIA IN CAEBORHABDITIS ELEGANS NEURONS

A Thesis Presented to the Faculty of

The Rockefeller University

in Partial Fulfillment of the Requirements for

the degree of Doctor of Philosophy

By

Tapan Apurva Maniar

June 2011

REGULATION OF POLARIZED PROTEIN TRANSPORT TO AXONS, DENDRITES AND SENSORY CILIA IN *CAENORHABDITIS ELEGANS* NEURONS

Tapan Apurva Maniar, Ph.D.

The Rockefeller University 2011

Neurons are highly polarized cells, capable of receiving, processing and transmitting information, with the help of their specialized domains, an axon and one or more dendrites. The molecular dissimilarities between these domains are critical for neuronal function, and are a result of asymmetric trafficking of a large number of cellular components including ion channels, neurotransmitter receptors, synaptic vesicles, and signaling proteins. Yet, despite the significance of asymmetric protein transport in neuronal polarity, the molecules and mechanisms that direct polarized transport to axons, dendrites and cilia in neurons are only partly understood. In this thesis, I describe my effort at understanding how neuronal proteins are asymmetrically localized. I pursued a genetic approach, employing the *C. elegans* nervous system as an *in vivo* model system for protein transport to axons, dendrites and cilia.

Having established a system to visualize axon-dendrite compartmentalization in PVD mechanosensory neurons, I identified the microtubule-binding protein UNC-33/CRMP and the ankyrin homolog UNC-*44* as major regulators of polarized protein transport in *C. elegans* neurons. In both *unc-33* and *unc-44* mutants, axonal proteins are distributed randomly between axons and dendrites, and dendritic proteins are partly mislocalized to axons. In both mutants, the axonal kinesin UNC-104/KIF1A actively

misdelivers axonal proteins to both axons and dendrites. An altered distribution of neuronal microtubules in *unc-33* and *unc-44* mutants suggests that a primary defect in microtubule organization underlies defective protein targeting. *unc-44* is required for UNC-33 localization to axons, where its enrichment in a proximal axonal segment suggests analogies with the vertebrate axon initial segment.

In parallel experiments, I analyzed *odr-8* mutants, which were previously identified in screens for chemotaxis-defective mutants and shown to affect GPCR localization. *odr-8* mutants fail to localize a subset of odorant receptors including the ODR-10 diacetyl receptor to sensory cilia. I found that *odr-8* encodes the *C. elegans* homolog of mammalian UfSP2, which acts as a cysteine-protease specific for UFM1, a ubiquitin-like molecule. ODR-10::GFP is retained in the ER in *odr-8* mutants, whereas cilia localization of ODR-10::GFP is enhanced in *ufm-1* mutants. *ufm-1* function is required for ER retention of ODR-10::GFP in *odr-8* animals. Thus, ODR-8 and UFM-1 may act antagonistically to regulate ER exit and cilia localization of chemoreceptors such as ODR-10.

This thesis is dedicated to my
family and friends

Acknowledgements

I am extremely grateful to my advisor, Cori Bargmann, for her constant support throughout my graduate work. She has created a wonderful environment in the lab for a graduate student, and has taught me how to be a good scientist and an independent thinker. I am constantly awed by the breadth of her scientific knowledge. Her work ethic, her creativity and her desire to constantly challenge herself and explore new scientific areas are all qualities I find inspiring. I cannot thank her enough for the time and energy she has spent guiding me through my thesis.

I would like to thank my committee members, Paul Nurse and Shai Shaham, for their advice and helpful suggestions. Our scientific discussions, combined with their enthusiasm and support, played an important role in my progress as a graduate student. I am also grateful to Bettina Winckler for agreeing to be the external reviewer on my thesis committee. Her outstanding work on the role of AIS as a membrane diffusion barrier, and her careful analysis of L1/NgCAM transport are excellent examples of what neuronal cell biology should be, and have been a source of inspiration.

I would like to thank all the members of the Bargmann Lab, past and present, who throughout the years have made the lab an intellectually stimulating and a friendly working environment. I would like to thank Makoto Tsunozaki, Yasunori Saheki and Manuel Zimmer for their insight and advice. My special thanks to Carrie Adler, Yun Zhang and Massimo Hilliard for their guidance during the initial stages of my project. Jennifer Garrison has been extremely generous with her time and in sharing her biochemistry expertise. Special thanks to members of the night shift (Makoto, Jason Kennerdell, Yifan Xu, Christine Cho) for making it fun and productive to work at night;

to lab members (Navin Pokala, Andrew Gordus, Steve Flavell and Greg Lee) for interesting and useful discussions over coffee and for their friendship. Conversations with my past and present baymates, Andy Chang, Chiou-Fen Chuang, Dirk Albrecht and Heeun Jiang, have made my time in the lab fun and enjoyable.

Special thanks to Holly Hunnicutt for always willing to go out of her way to help members of the lab. She makes the lab a lively and wonderful place. Thanks to Hernan Jaramillo for freezing and thawing strains for me on innumerable occasions, and for Spanish lessons where I need much practice. Aside from providing the lab with plates and medium, Manoush Ardzivian is central to the lab environment as she is much like our lab grandmother. I thank her for her delicious Mediterranean dishes and for her yogurt cultures. Christian Woods and Priscilla Kong have been excellent lab managers, ordering reagents and aiding the progress of my project in many ways.

Scott Dewell at the Rockefeller Genomics Resource Center and Patrick McGrath in the lab helped me analyze the data obtained from Illumina/Solexa sequencing. Their help was critical in making sense of the data and in making progress with the *odr-8* project. I am indebted to Alison North and Shiva Bhuvanendran at the Bioimaging Resource Center for their advice and for sharing with me their technical expertise.

I would like to thank Hiro Funabiki for being a great rotation mentor, for many wonderful discussions during and after my rotation, and for always being welcoming on my frequent visits to the lab. Special thanks also to the past and present members of the Funabiki lab. To Cristina Ghenoiu for her biochemistry and microscopy expertise, for her patience and support throughout my project given my late night experiments, and for her insanity that made my time during graduate school enjoyable. To Christian Zierhut

for his scientific advice, for his sympathetic ear, and for good times at Kati Roll. To the Sri Twins for making my rotation experience an educational and fun rotation like no other, and for their continuous support and wisdom. To Alex Kelly for his biochemical expertise as well as his insight and advice regarding science. To John Xue, Andy Chang and Evan Feinberg for being formidable squash opponents and for many stimulating discussions.

I am especially grateful to Max Heiman for sharing with me his passion for science, his expertise in the field, and for being incredibly supportive as I make important choices about the future. Sandhya Koushika and Kang Shen provided us with reagents as well as scientific input that were critical for the progress of my project. I am ever grateful to them for their suggestions.

Members of the Dean's Office, Sid Strickland, Kristen Cullen, Emily Harms, Marta Delgado and Cristian Rosario have been extremely helpful at various stages during my graduate school, particularly with the paperwork when I visit home, and I thank them for all their support.

Without the support of my friends, this thesis would not have been possible. Away from India, they have made New York like a second home for me, and have provided me with encouragement, advice and most importantly their friendship. I thank them for that. My family has always been extremely supportive of me, from the early days of schooling and skating in India, to Singapore and then to the U.S. Despite being an only child, my parents made the difficult decision of allowing me to leave for Singapore while in high school, and have showed their trust in me throughout the years. I cannot thank them enough for all their support, patience, advice and guidance.

Table of Contents

List of Figures Page #

Chapter 1

Introduction

Polarization of cells into functionally and morphologically specialized subcellular domains is a critical property for most cell types. Neurons are prime examples of such polarization, with highly specialized substructures that execute distinct functions (Barnes and Polleux, 2009). At the simplest and most fundamental level, neurons are divided into two major compartments, a single long axon and one or more dendrites with variable degrees of branching. Reflecting the complexity of neurons, these domains are often organized into further subspecializations such as the axon initial segment, presynaptic sites, nodes of Ranvier, dendritic spines and chemosensory or primary cilia (Lasiecka et al., 2009). Axons contain presynaptic vesicles filled with neurotransmitters and specialize in releasing these chemicals for signal propagation to downstream neurons in neural circuits. Dendrites contain numerous organelle systems such as Golgi outposts and molecules such as neurotransmitter receptors and ion channels that allow them to sense and propagate these signals through the neuron. Efficient flow of information in neural circuits relies on the proper functioning of axonal and dendritic domains, whose properties are defined by their constituent proteins (Arnold, 2009). A greater understanding of the mechanisms that underlie proper targeting of neuronal proteins to their corresponding destinations has the potential to significantly improve knowledge of neuronal development and function.

Accurate localization of neuronal proteins is the outcome of a host of cellular processes, which can be divided into two main events. The first of these is the proper establishment of neuronal polarity resulting in well-defined axon-dendrite domains, and

the second is the subsequent process of protein transport, which is guided by the spatial information laid out by the polarization event.

1.) Neuronal compartmentalization into axons and dendrites

1.1.) Primary hippocampal neurons: Conceptual foundation and molecular contributions

Much effort has been dedicated towards understanding the process of neuronal polarization, using cultured mammalian neurons. The employment of dissociated rodent hippocampal neurons established an ideal *in vitro* system (Dotti et al., 1988) that has been used for studies over the past two decades, and has enriched our understanding of neuronal polarity. Cultured hippocampal neurons progress through multiple stages of morphological transition, starting out as round cells with lamellipodial protrusions (Stage 1), followed shortly by growth of simple, immature neurites (Stage 2). One of these neurites, which will eventually become an axon, initiates rapid and persistent outgrowth (Stage 3). Subsequently, the other processes also start to grow and develop into dendrites, as the axon continues its elongation (Stage 4). Ultimately, both sets of processes develop further specializations such as presynaptic sites, dendritic branches and dendritic spines (Stage 5) (Baas et al., 1989).

Experiments have primarily focused on the transition from Stage 2 to Stage 3, the earliest visual representation of the decision as to which process will develop into an axon. Through these studies, extracellular cues such as laminin, BDNF and NT3 have been shown to affect neuronal polarity and promote axon development (Esch et al., 1999; Morfini et al., 1994; Shelly et al., 2007). However, the main drive towards polarity in this

system is cell-intrinsic. It is thought that these cells start out as symmetric cells that undergo minor local fluctuations in signaling molecules or pathways, generating weak intracellular asymmetry. A large enough spontaneous fluctuation is subsequently amplified through positive feedback and establishes a lasting asymmetry within the neuron, eventually developing into axon-dendrite polarity (Arimura and Kaibuchi, 2007).

In addition, a large set of signaling molecules can affect the morphological development of axons or dendrites, as described below.

1.1.1.) PI3-Kinase and PTEN

Members of the PI3K family of kinases phosphorylate phosphatidylinositol-(4,5)-bisphosphate (PIP2) to generate phosphatidylinositol-(3,4,5)-trisphosphate (PIP3) and have well-established roles in cell polarity and cell migration (Swaney et al., 2010). Growing evidence from multiple groups point towards an important role of PI3K and its lipid product PIP3 in regulation of neuronal polarity. Pharmacological inhibition of PI3K using Wortmannin or LY294002 disrupts proper formation of an axon (Jiang et al., 2005; Shi et al., 2003; Yoshimura et al., 2005), whereas overexpression of a constitutive active catalytic subunit (p110α) results in the development of multiple axons (Jiang et al., 2005). These results suggest that PI3K activity is necessary and sufficient for specification and development of axon identity. Consistent with this model, PIP3 accumulation and therefore PI3K activity show higher levels in developing axons compared to dendrites in Stage 3 neurons (Menager et al., 2004; Shi et al., 2003).

Studies on PTEN (phosphatase and tensin homolog deleted on chromosome 10), an antagonist of PI3K function, provide further support for the role of PI3K and PIP3 in

neuronal polarization. PTEN is a protein and lipid phosphatase that dephosphorylates PIP3 to convert it back to PIP2, and thereby provides a spatial and temporal control on PI3K-PIP3 signaling (Arimura and Kaibuchi, 2007). Overexpression of PTEN leads to defects in axon formation, whereas knocking down its expression results in multiple axons (Jiang et al., 2005; Shi et al., 2003), opposite effects of the abovementioned effects of PI3K. Thus, a balance in PI3K and PTEN activity may specify axon-dendrite development. Recent studies in *C. elegans in vivo* have provided support for this general concept, as they have demonstrated the significance of PI3K in the initial events of neuronal polarization (Adler et al., 2006; Chang et al., 2006).

1.1.2.) GSK-3β

One of the targets through which PI3K signaling may regulate neuronal polarity is the serine/threonine kinase GSK-3β, or Glycogen Synthase Kinase 3β. Unlike most kinases, GSK-3β is constitutively active until phosphorylated. In cultured hippocampal neurons the phosphorylated form of GSK-3β shows greater accumulation in developing axons than in dendrites (Jiang et al., 2005; Yoshimura et al., 2005). Overexpression of a non-phosphorylatable form of GSK-3β results in neurons lacking axons, and suppresses the supernumerary axon formation phenotype of overactive PI3K signaling. Conversely, inhibition of GSK-3β using multiple peptide inhibitors or siRNAs leads to supernumerary axon formation (Gartner et al., 2006; Jiang et al., 2005; Yoshimura et al., 2005). GSK-3β phosphorylates a diversity of proteins including microtubule-binding proteins such as MAP1b, Tau, CRMP-2 (discussed below) and APC (Adenomatous Polyposis Coli) (Hur

and Zhou, 2010), and may act through one or more of these targets to regulate axon-dendrite formation.

1.1.3.) PAR proteins

The PAR proteins, conserved regulators of cell polarity, were originally identified in a pioneering screen for mutants with defects in asymmetric cell division of the *C. elegans* zygote (Guo and Kemphues, 1996). PAR-3, PAR-6, and aPKC proteins localize at the anterior edge of the single-celled embryo and are required for, whereas PAR-1 and PAR-2 proteins are enriched at the posterior edge, and are required for establishing and maintaining posterior specification. The PAR3-PAR6-aPKC complex is also required for the polarity of epithelial cells and dividing *Drosophila* neuroblasts (Nance and Zallen, 2011). In cultured hippocampal neurons, PAR3, PAR6 and aPKC accumulate in the developing axon, and overexpression of PAR3 or PAR6 perturbs neuronal polarization, and inhibition of aPKC activity leads to defects in axon formation (Shi et al., 2003).

Of the 13 mammalian kinases similar to the *C. elegans* PAR-1 kinase, three have been shown to be important for neuronal polarity (Lizcano et al., 2004). Two of these, SAD-A and SAD-B kinases, are mammalian homologs of *C. elegans* SAD-1 (Kishi et al., 2005), discussed in greater detail below along with its upstream regulator LKB1/PAR-4. The third PAR-1-like protein implicated in axon formation is MARK2 or microtubule-affinity-regulating kinase 2. Overexpression of MARK2 prevents axon formation, whereas knocking-down its expression results in excess axons, suggesting the regulated inhibition of MARK2 may be critical for the proper development of axon-dendrite polarity (Biernat et al., 2002; Chen et al., 2006).

1.1.4) Summary of hippocampal polarity

In addition to the proteins mentioned above, cyclic nucleotides, calcium, calcium chloride and cytoskeletal effectors regulating actin or microtubules affect the number of axons per neurons (Arimura and Kaibuchi, 2007; Shelly and Poo, 2011). The cytoskeletal systems will be discussed further below.

Analyses using the *in vitro* hippocampal system have provided a conceptual framework for future experiments and with identities of numerous putative regulators. However, certain caveats associated with these experiments have also been recognized and are worth noting (Barnes and Polleux, 2009; Jiang and Rao, 2005). For example, most of these experiments relied on neurite length as the single marker of axon identity, thereby not making the distinction between molecules that are required for specification of axons, and those that only affect axon elongation. Furthermore, identification of regulatory molecules through overexpression or dominant negative approaches, while revealing, can be associated with ectopic activation of pathways not normally used by neurons, or with non-specific inactivation of an undesired pathway, respectively. Lastly, given that the system employs dissociation of E17-E18 neurons that were already polarized, it is possible that at least a part of the analysis may be specific to repolarization of cells with some remaining memory of the previous polarization event. These limitations highlight the importance of parallel studies of *in vivo* regulatory mechanisms.

1.2.) The development of axon-dendrite polarity in vivo

The emerging theme from *in vivo* analyses of axon-dendrite specification indicates that this process involves four basic steps. 1.) The first step involves generation of intracellular asymmetry in an unpolarized neuron. A number of recent studies have elegantly demonstrated that extracellular cues in the vicinity of postmitotic neurons play an instructive role in this process through asymmetric activation of downstream signaling pathways, leading to directed intracellular asymmetry in these neurons (Adler et al., 2006; Hilliard and Bargmann, 2006; Pan et al., 2006). 2.) The second step, the morphological elaboration of this initial intracellular asymmetry, involves directed outgrowth of axons and dendrites. This visually striking and important step in neuronal polarization is likely to involve coordinated regulation of the cytoskeleton and membrane addition. Indeed, a growing number of molecules are implicated in this morphogenetic process of growth (Tahirovic and Bradke, 2009). 3.) The third step is the molecular differentiation of axons and dendrites enabling them to serve their respective functions. This process involves the regulated and polarized transport of constituent proteins to the two compartments, providing each with its molecular and functional properties. Cell biological and genetic studies indicate that the microtubule cytoskeleton, which is known to differ between axons and dendrites, plays a major role in defining the directionality of protein transport. 4.) The morphological and molecular compartmentalization of neurons is maintained by a number of processes. An actin- and ankyrin-dependent diffusion barrier exists between the axonal and somatodendritic domains (Nakada et al., 2003; Song et al., 2009; Winckler et al., 1999), playing a pivotal role in maintaining axon-dendrite molecular distinctions

(Hedstrom et al., 2008; Sobotzik et al., 2009). Furthermore, continued directional sorting and transport of proteins, as well as selective retention or endocytosis of other proteins, are required to maintain the functional properties of these compartments.

1.2.1.) Regulation of axon-dendrite polarity by extracellular cues

Analysis of *C. elegans unc-6*/netrin mutants have provided striking evidence for the role of netrin signaling in generating neuronal polarity. The generation of initial asymmetry can be visualized directly in the HSN egg-laying neurons whose stereotyped anatomy is defined by a ventrally guided axon. From their original spherical morphology, HSN neurons consistently initiate polarized outgrowth in the ventral direction. UNC-6, which is secreted from ventral sources, plays an instructive role in directing this step (Adler et al., 2006). HSN neurons in *unc-6* mutants no longer restrict their outgrowth ventrally, and instead direct filopodia and nascent neurites in all directions. Ultimately, however, HSN develops a single axon that grows anteriorly, indicating *unc-6*/netrin is required for the initial cellular asymmetry and for defining the direction of axon development, but not for axon development per se. In absence of *unc-6*, intrinsic or external mechanisms may provide spatial information that polarize the cell anteriorly. Ventral UNC-6 leads to ventral localization of the UNC-6 receptor, UNC-40/DCC, in HSN neurons. UNC-40 in turn triggers a signaling pathway involving MIG-10/lamellipodin and UNC-34/Enabled, which can act on the actin cytoskeleton. Mammalian homologs of MIG-10 and UNC-34 also play important roles in lamellipodia and filopodia formation in neuritogenesis (Dent et al., 2007; Krause et al., 2004; Kwiatkowski et al., 2007).

Interestingly, *unc-6*/netrin, originally identified for its early roles in cell migration and axon guidance, also acts at later stages in neuronal development, promoting synaptogenesis in one cell type (Colon-Ramos et al., 2007), and inhibiting accumulation of presynaptic proteins in dendrites in another (Poon et al., 2008). These activities can be considered to be components of axon differentiation and neuronal polarity.

Complementing the significance of UNC-6/netrin along the dorsoventral axis, *C. elegans* WNT proteins act along the anterioposterior axis in neuronal polarity and other aspects of development (Hilliard and Bargmann, 2006; Pan et al., 2006). The PLM mechanosensory neurons, positioned near the *C. elegans* tail, extend a long anterior process with a branch containing synaptic vesicles, and an unbranched and shorter posterior process. In *lin-44*/WNT mutant animals, as well as in animals defective for its receptor LIN-17/Frizzled, the PLM neuron reverses its polarity along the A-P axis, directing a long process with its synaptic branch posteriorly, and extending a short unbranched process in the anterior direction. Thus, while WNT signaling may not be essential for initiation and elaboration of PLM polarity, it is important in the organization of polarity along the body axis. The source of LIN-44 expression is situated in the tail, posterior to PLM neurons (Hilliard and Bargmann, 2006). These experiments suggest that WNT signaling orients PLM polarity along the A-P axis by directing the site of axon initiation away from the WNT source.

An activity analogous to that of netrin and WNTs in *C. elegans* neuronal polarity has been identified for the mammalian semaphorin Sema3A. Dissociated rodent cortical neurons when cultured on cortical brain slices extend their axons towards the ventricular surface of the slice, as is the case *in vivo*. Sema3A in the underlying slice directs this

polarity axis by promoting dendrite growth apically, and orienting the site of axon initiation away from its source (Polleux et al., 1998; Polleux et al., 2000). Disrupting the function of Sema3A receptor Neuropilin-1 leads to defects in this bias oriented growth (Polleux et al., 1998), suggesting that Neuropilin-1 signaling downstream of Sema3A directs the development of axon-dendrite polarity.

While a number of extracellular cues can affect axon development *in vitro*, recent work from Ehlers and Polleux labs may have identified the first extracellular signal in the mammalian nervous system important for neuronal polarity *in vivo* (Yi et al., 2010). Using conditional knockout mice, they observed that TβR2, a receptor for TGF-β, is required in neurons for axonogenesis. Neurons knocked out for TβR2 remained bipolar but failed to elaborate an axon, suggesting a specific defect in axon formation and development, rather than a defect in neuronal asymmetry. *In vitro* experiments suggest that the TβR2 ligand TGF-β can promote axonal development.

In summary, significant progress has been made in identifying cues that regulate neuronal polarity *in vivo*. A lesson from these experiments is that extracellular cues identified for different roles in neurons or other tissues can act in neurons to regulate neuronal polarity. *unc-6*/netrin, WNTs, or the TGF-β receptor may regulate distinct processes such as cell migration, axon-dendrite development and guidance, and synapse formation, in distinct cell types or even in the same cell in which they regulate neuronal polarity.

1.2.2.) SAD and LKB1 kinases regulate axon-dendrite compartmentalization in vivo

Among the intracellular signaling molecules, the SAD-1 (SAD A/B) kinase and LKB-1/PAR-4 kinase are the best characterized and conserved regulators of neuronal polarity *in vivo*. Genetic screens in *C. elegans* originally identified *sad-1* mutants based on defects in presynaptic vesicle organization (Crump et al., 2001). In addition to the defect in presynaptic vesicle clustering, *sad-1* mutants also showed neuronal polarity defects, mislocalizing synaptic vesicle proteins to dendrites in sensory and motor neurons. SAD-1 encodes a serine/threonine kinase that is similar to the polarity protein PAR-1, identified for its role in the embryonic polarity of *C. elegans* zygote and subsequently found to be important for the polarity of numerous cell types, hinting at similarities between mechanisms controlling neuronal polarity and those controlling embryonic or epithelial cell polarity. Subsequent knockout studies demonstrated that SAD A and SAD B kinases, mammalian homologs of SAD-1, are required for neuronal polarity in mice (Kishi et al., 2005). While it is not clear how SAD kinases regulate neuronal polarity or synapse development, it is believed that part of this effect is mediated by phosphorylation of microtubule-associated proteins (MAPs) such as tau (Kishi et al., 2005). In addition, the identification of Neurabin (NAB-1) as a binding partner of SAD kinase, along with studies of the *C. elegans nab-1* mutant, have led to the model where SAD-1 acts in concert with NAB-1 to regulate neuronal polarity (Hung et al., 2007).

Acting upstream of mammalian SAD kinases, the mammalian homolog of the polarity protein PAR-4, the LKB1 kinase, is required for neuronal polarity and axon formation in mouse brain (Barnes et al., 2007). Phosphorylated LKB1 in the presumptive axon phosphorylates and activate SAD kinases leading to polarization of neurons and axon

formation (Barnes et al., 2007; Shelly et al., 2007). Providing further support to the role of LKB1 in neuronal polarity, *C. elegans par-4* (*LKB1)* mutants also mislocalize synaptic vesicle proteins to dendrites, as seen in the case of *sad-1*. However, in case of *C. elegans*, *par-4* seems to act in the same pathway as *par-1* rather than *sad-1*, whereas *strd-1* (STRDα), a binding partner of LKB1, appears to act in a parallel pathway with *sad-1* (Kim et al., 2010). It remains to be seen how extracellular cues such as TGF-β, *unc-6*/netrin or WNTs lead to the asymmetric activation of LKB1.

In addition to LKB1 and SAD kinases, additional signaling molecules such as PIP3, cGMP, cAMP and many others have also been implicated in neuronal polarity through *in vitro* studies (Arimura and Kaibuchi, 2007; Barnes and Polleux, 2009). Now, with improved techniques for visualizing neuronal development and manipulating genes, the *in vivo* requirement and functions of these molecules with respect to axon-dendrite development can be better understood.

1.3) Neuronal cytoskeleton: an active player orchestrating axon-dendrite compartmentalization

Axons and dendrites exhibit striking differences in their microtubule cytoskeleton. Axonal microtubules are generally oriented with their plus ends away from the cell body, whereas dendritic microtubules of mammalian neurons as well as *Drosophila* neurons exhibit the opposite orientation, or mixed polarity, depending on the cell type (Baas et al., 1988; Burton and Paige, 1981; Heidemann et al., 1981; Kwan et al., 2008; Rolls et al., 2007). Furthermore, dendrites, but not axons, exhibit subcompartment specific and age-dependent changes. Microtubules in basal dendrites of pyramidal neurons display a mixed

orientation at all stages of neuronal development, whereas microtubules in apical dendrites of developing pyramidal neurons have a mixed polarity initially, but acquite a uniform orientation later in development (Kwan et al., 2008). These differences in microtubule orientation are likely to be critical for neuronal function, given that they determine the directionality of cargo transport, executed by microtubule-dependent motors, discussed further below.

In addition to microtubule orientation, axonal microtubules are also distinct from dendritic microtubules in terms of their stability, post-translational modifications and the complement of their MAPs, with the former being more stable, showing greater pools of acetylated and detyrosinated tubulin than the latter, and being enriched in the MAP tau as opposed to MAP2 (Binder et al., 1985; Caceres et al., 1984a; Caceres et al., 1984b; Dotti et al., 1987; Witte et al., 2008).

Notably, the cytoskeletal differenes between axons and dendrites are not limited to mature neurons, but are also detectable in developing neurons. The process that develops into an axon is marked by a more dynamic actin cytoskeleton and more stable microtubules compared to the other neurites (Bradke and Dotti, 1999; Witte et al., 2008). Rather than just being markers of axon versus dendrite identities, both actin and microtubule cytoskeleton play critical roles in establishing as well as maintaining neuronal polarity (Tahirovic and Bradke, 2009). Pharmacological manipulations have shown that actin destabilization and microtubule stabilization play instructive roles in neuronal polarity and bias the fate of a nearby neurite, inducing it to develop and acquire axonal identity (Bradke and Dotti, 1999, 2000; Witte et al., 2008).

Instability of the actin cytoskeleton was first suggested to promote axon formation by allowing the progressive advancement and stabilization of microtubules in a given neurite towards its growth cone (Forscher and Smith, 1988). A variety of actin nucleators and modulators have been shown to affect neuronal polarization, suggesting, however, a more subtle model. For example, a result consistent with the earlier model is that the actin severing protein Cofilin is highly active in axonal growth cones, leading to a more destabilized actin network compared to presumptive dendrite processes. Cofilin knockdown results in disrupted axon formation, whereas Cofilin constitutive activation leads to increased outgrowth (Garvalov et al., 2007; Jacobs et al., 2007). A contrasting result was obtained by examining triple knockout of all three mammalian Ena/VASP proteins that promote actin polymerization. Ena/VASP proteins, which are required for filopodia formation and neuritogenesis, are essential for axon formation (Dent et al., 2007; Kwiatkowski et al., 2007). The emerging picture based on studies of actin modulators indicates that the determination of axonal identity may not be as simple as inhibiting actin depolymerization. It will be important to understand which aspects of actin dynamics are regulated at which stages in neuronal development to bias a process towards becoming an axon or a dendrite.

In addition to the structural foundation provided by actin and microtubules, they also serve as tracks for protein transport by actin-dependent myosin motors, and microtubule-dependent kinesin and dynein motors. Indeed, microtubule-based transport plays a critical role in the establishment of neuronal polarity, and continues to do so in maintaining molecular distinctions. For instance, the signaling molecule PIP2 and the polarity protein PAR3, discussed above, play important roles in axon specification and

elongation in cultured mammalian neurons, and they require the kinesins GAKIN and KIF3A for their polarized accumulation in the nascent axon during the initial stages of axon-dendrite development (Horiguchi et al., 2006; Shi et al., 2004). Given the instructive role of microtubules and the significance of protein transport in the establishment of axon-dendrite polarity, the asymmetric nature of kinesin-dependent transport from an early stage in neuronal development is likely to be a major factor in determining and developing axon-dendrite identities.

Once axon-dendrite polarity is established through coordinated regulation of the cytoskeleton and membrane/protein transport, the resulting differences in the compositions of these two domains are actively maintained, and to some extent plastic. Axotomy in mature neurons either leads to regrowth of the axon, or can induce an existing dendrite to elongate and differentiate into an axon, depending on the site of axotomy (Gomis-Ruth et al., 2008). Furthermore, pharmacological perturbations to actin and microtubule cytoskeleton can convert an existing dendrite in a mature neuron to an axon (Bradke and Dotti, 2000; Witte et al., 2008), highlighting the continued significance of the cytoskeleton in the maintenance of polarity.

1.4) C. elegans UNC-33 and mammalian CRMPs (Collapsin Response Mediator Proteins)

The *C. elegans unc-33* gene encodes the founding member of the CRMP family, and is the sole *C. elegans* homolog of mammalian CRMP proteins. *unc-33* was first identified as a mutant with abnormal locomotion, and subsequently found to have axon elongation and guidance defects (Brenner, 1974; Desai et al., 1988; Hedgecock et al., 1985; Li et al., 1992; Siddiqui and Culotti, 1991; Tsuboi et al., 2005) and abnormal

organization of microtubules within and near sensory cilia (Hedgecock et al., 1985). The *unc-33* gene encodes three protein isoforms that vary in the lengths of their N-termini, while sharing a 523 amino acid C-terminal sequence and (Li et al., 1992). Immunofluorescence experiments demonstrated that UNC-33 isoforms are primarily expressed in neurons and are localized along neuronal processes, showing enrichment in axons compared to dendrites (Tsuboi et al., 2005).

The first mammalian CRMP was identified as an UNC-33-like protein acting as a potential mediator of growth cone collapse caused by Semaphorin (Goshima et al., 1995); however, this activity has not been validated *in vivo*. Subsequently, CRMPs came to attention for their roles in neuronal polarity. CRMP-2 is enriched in the distal part of growing axons of cultured hippocampal neurons. Overexpression of CRMP-2 leads to elongation of axons, as well as formation of multiple axon-like processes (Inagaki et al., 2001). Conversely, perturbing CRMP-2 activity through dominant negative and knockdown approaches results in shorter axons or cells with no axon-like processes (Inagaki et al., 2001; Nishimura et al., 2003). These results implicate CRMP-2 in axon elongation and formation.

The Collapsin Response Mediator Protein (CRMP) family, also known as Ulip, TOAD, DRP or TUC, is broadly expressed in the developing mammalian nervous system (Quinn et al., 1999). Members of this family bear sequence as well as structural similarity to liver diydropyrimidinases (DHPase), enzymes involved in the catabolism of uracil and thymine (Deo et al., 2004; Hamajima et al., 1996; Stenmark et al., 2007; Wang and Strittmatter, 1997). Like DHPases, murine CRMP1 as well as human CRMP2 form tetramers (Deo et al., 2004; Fukata et al., 2002; Stenmark et al., 2007; Wang and

Strittmatter, 1997). Similarly, *C. elegans* UNC-33 proteins are also able to interact with each other (Tsuboi et al., 2005), although the significance of oligomerization is not known. Unlike DHPases, however, CRMPs do not exhibit any catalytic activity towards any DHPase substrates, likely due to the fact that histidine residues critical for catalytic activity are not conserved in CRMP sequences (Hamajima et al., 1996; Wang and Strittmatter, 1997). Interestingly, mammalian CRMPs as well *C. elegans* UNC-33 can bind to tubulin heterodimers and with a lower affinity to microtubules (Fukata et al., 2002), and these interactions are regulated by phosphorylation events. GSK-3β, mentioned above, as well as another kinase, Rho kinase, can phosphorylate CRMP-2 near its C-terminus leading to a reduction in its microtubule-binding affinity (Cole et al., 2004; Yoshimura et al., 2005). Furthermore, CRMP-2 can also promote microtubule assembly *in vitro* (Fukata et al., 2002), suggesting a possible role in neuronal polarity through regulation of the cytoskeleton. However, the presence of five CRMP members in mammals has meant a significant hurdle in elucidating the roles of this group of proteins in neuronal development *in vivo*. Moreover, each of the five mammalin CRMPs encode multiple isoforms, and most of the work in the field has focused on the shorter isoform for each gene (Quinn et al., 2003; Quinn et al., 1999).

1.5.) Motors executing axonal and dendritic transport, and their regulation

There are three classes of molecular motors involved in intracellular transport of proteins, namely kinesins, dyneins and myosins. Myosins move along actin filaments and are mostly involved in short range transport beneath the plasma membrane (Hirokawa and Noda, 2008). Kinesins and dyneins on the other hand are microtubule-dependent motors

that orchestrate long-range transport from the soma to the axon or dendrite periphery and back.

The kinesin superfamily comprises of fifteen subfamilies of kinesin proteins (also known as KIFs). Almost all kinesins, except for members of the KIF14 family, move towards the plus-end of microtubules, and are primarily responsible for the 'anterograde traffic' of cargoes moving away from the cell body in both compartments (Hirokawa and Takemura, 2005). In contrast, dyneins identified thus far are minus-end directed motors (Kardon and Vale, 2009). While there is a multitude of kinesins orchestrating anterograde transport, cytosplasmic dynein is the primary motor responsible for retrograde transport from axonal tip to the soma (Schnapp and Reese, 1989). Given the mixed or opposite orientation of microtubules in dendrites, however, dynein may function as an anterograde motor as well as a retrograde transporter in subsections of this compartment, whereas in distal dendrites, it primarily acts a retrograde motor.

Observations of transport in real time has demonstrated that cargoes do not move unidirectionally or continuously, and instead pause as well as switch directions, suggesting the existence of a competition between anterograde and retrograde activities (Muresan et al., 1996). Indeed, vesicles attached to kinesins as well as dyneins have been identified. Moreover, direct interactions between KIF protein complexes and dynein associated proteins have also been observed; for example, the dynein binding protein p150Glued interacts with the kinesin associated protein KAP3 (Deacon et al., 2003). Thus, the net directionality of a cargo's movement is determined by a balance in anterograde versus retrograde activities, highlighting the importance of coordinated regulation of opposing motors.

The first kinesin molecule identified, also known as conventional kinesin/Kinesin-1/KIF5/KHC, is one of the most well studied kinesins that has important roles in anterograde transport to axons as well as dendrites (Hirokawa and Takemura, 2005). Biochemical studies with mammalian KIF5 demonstrate that KIF5 is involved in the axonal transport of many proteins including organelles containing presynaptic proteins SNAP-25, syntaxin, synaptotagmin, as well as as growth factor receptor TrkA (Arimura et al., 2009; Diefenbach et al., 2002; Su et al., 2004). KIF5 also interacts directly with an adapter protein GRIP, which may steer the kinesin towards dendrites to mediate the dendritic transport of AMPA receptor subunit GluR2, whereas overexpression of another adapter molecule JIP3 appears to antagonize the effect of GRIP (Setou et al., 2002). Thus, KIF5 can function towards axons and dendrites, and its activity appears to be regulated by adapter proteins such as GRIP and JIP3. Dyneins also exhibit axonal and dendritic functions: they are involved in the transport of TrkA-containing vesicles, BDNF-containing vesicles, as well as mitochondria from the axon towards the soma, whereas they interact with RAB5 and RAB7 endosomes as well as the gephryin adapter for glycine receptor transport in dendrites (Fuhrmann et al., 2002; Gauthier et al., 2004; Hollenbeck and Saxton, 2005; Satoh et al., 2008; Saxena et al., 2005). *C. elegans* and *Drosophila* mutants for conventional kinesin as well as cytoplasmic dynein confirm the importance of these motors in axonal transport, and further suggest roles in polarization of protein transport. Kinesin-1/Kif5/KHC mutants show reduced synaptic localization, and instead exhibit abnormal accumulation of synaptic vesicle proteins in *Drosophila* and *C. elegans* axons (Byrd et al., 2001; Hurd and Saxton, 1996; Saxton et al., 1991). Furthermore, C. elegans mutants in the *unc-116* gene that encode the conventional kinesins/Kinesin-1/Kif5,

show mislocalization of synaptic vesicle proteins to dendrites, indicating UNC-116/KIF5 is required for the asymmetric transport of axonal proteins (Byrd et al., 2001). Dynein mutants of *Drosophila* and *C. elegans* also show defects in axonal transport with abnormal accumulations in the axons (Bowman et al., 1999; Koushika et al., 2004; Martin et al., 1999). Interestingly, further analyses of fly mutants in the components of the dynein motor complex also revealed roles in dendritic arborization but not in axon morphogenesis, indicating asymmetric influence of dynein function (Satoh et al., 2008).

1.5.1.) UNC-104/KIF1A kinesin: Transporting synaptic vesicle precursors to axons

The kinesin-3 family member, UNC-104/KIF1A, is the primary motor responsible for the anterograde transport of synaptic vesicle precursors to axons (Hirokawa and Takemura, 2005). The significance of UNC-104/KIF1A was first recognized when *C. elegans unc-104* mutants was shown to have defects in transporting synaptic vesicles to axons (Hall and Hedgecock, 1991). Subsequently, UNC-104 homologs was found to be required for synaptic vesicle transport in flies and mice (Pack-Chung et al., 2007; Yonekawa et al., 1998). Immunocytochemistry and immunoprecipitation experiments in mice have identified RAB-3A, synaptophysin and synaptotagmin as components of vesicles associated with KIF1A(Okada et al., 1995), and presynaptic proteins such as RAB-3, SNB-1 (synaptobrevin), SNT-1 (synaptotagmin) and SAD-1 all require UNC-104/KIF1A function for their axonal localization in *C. elegans* neurons (Crump et al., 2001; Nonet et al., 1997; Patel et al., 2006; Sieburth et al., 2005).

Unlike most motors that function as dimers or tetramers, native polyacrylamide gel electrophoresis and light scattering analyses indicate that KIF1A acts a monomer (Okada

et al., 1995). However, dimeric KIF1A has also been reported, the contribution of which *in vivo* transport remains to be clarified (Tomishige et al., 2002). SYD-2/liprin-α, which has a scaffolding function in synapse development, interacts with UNC-104/KIF1A directly (Shin et al., 2003), clusters UNC-104 as well as promotes its motility (Wagner et al., 2009). This interaction may serve as a link between synaptic components and their axonal motors. Furthermore, the PH (pleckstrin homology) domain in KIF1A interacts specifically with PIP2 (phosphatidylinositol 4,5-bisphosphate), and mutations in this domain lead to defective transport (Klopfenstein et al., 2002). This lipid interaction may assist UNC-104/KIF1A recuirtment to the surface of its cargo vesicle.

1.5.2.) Kinase-dependent regulation of microtubule motors in neurons

The highly conserved neuronal kinase p35/CDK5, as well as cyclin CYY-1, and its partner kinase, PCT-1 (Pctaire kinase), act in parallel pathways to regulate the balance between kinesin-dependent anterograde traffic and the dynein-dependent retrograde traffic of axonal proteins in mature polarized neurons (Ou et al., 2010). *In vivo* imaging of synaptic vesicle traffic suggests that p35/CDK5 and CYY-1/PCT-1 reduce dynein activity, and that upregulated dynein function in the mutants results in dramatic mislocalization of presynaptic proteins from axons to dendrites. Indeed, double mutants disrupting both pathways exhibit almost complete misaccumulation of axonal proteins in dendrites, whereas defective dynein function rescues these dendritic mislocalization defects of *p35/cdk5* and *cyy-1/pct-1* mutants.

1.6.) Maintaining axon-dendrite polarity with diffusion barriers

Once axon-dendrite domains are specified, an important mechanism ensuring molecular segregation of axonal and dendritic proteins is the existence of diffusion barriers. Using optical tweezers to assess the lateral mobility of membrane proteins, Winckler et al. provided the first demonstration that the axon initial segment (AIS), which is a spatial and physiological landmark in the proximal region of the axon, acts as a diffuson barrier (Winckler et al., 1999). Furthermore, DMSO and Latruncalin B treatments showed that this barrier is dependent on the actin cytoskeleton, which interacts with ankyrin and spectrin proteins at the AIS. Single particle tracking of lipids has also shown that a diffusion barrier at the AIS impedes the mobility of lipids such as phosphatidylethanolamine (Nakada et al., 2003). Interestingly, this diffusion barrier for lipids is also actin-dependent. Furthermore, its emergence strongly correlates with the clustering of AnkyrinG at the AIS, and with the increasing localization of membrane proteins such as the voltage-gated sodium channels that interact with the cortial actin/spectrin cytoskeleton through AnkyrinG. Consistent with the significance of AnkyrinG in this model, siRNA-mediated knockdown of AnkyrinG disrupts the membrane barrier (Song et al., 2009).

An actin and AnkyrinG-dependent barrier for the diffusion of cytosolic proteins also exists in mammalian neurons. The dense actin/spectrin cytoskeleton and the network of AnkyrinG binding proteins contribute to a proposed meshwork that acts as a filter in impeding the diffusion of soluble proteins at the AIS (Song et al., 2009).

In addition to its involvement in diffusion barriers, the AIS also has a separate function in the regulation of neuronal excitability. Its function in excitability involves

membrane proteins including voltage-gated sodium channels, potassium channels and members of the L1 family of cell adhesion molecules, which are also anchored to the dense dense actin/spectrin cytoskeleton network, through the AnkyrinG adapter protein (Rasband, 2010).

The structure of the AIS is suggestive of a unique and highly differentiated function. The membrane of the AIS lies along a dense subcortical cytoskeleton composed of spectrin and actin (Bennett and Baines, 2001). In addition, specialized microtubules are evident within the AIS. Electron micrographs reveal clusters of parallel microtubules that are not present in other parts of the neuron (Palay et al., 1968; Sobotzik et al., 2009). The AIS has long been considered a static structure, but recently been demonstrated to be regulated by neuronal activity, which can shift its position relative to the cell body (Grubb and Burrone, 2010; Kuba et al., 2010).

In invertebrate neurons, axonal and dendritic specializations typically emerge from a single process, not from the cell body. Therefore, the diffusion barriers are likely to have a different location. Indeed, *Drosophila* axons have a diffusion barrier dividing a proximal and distal segment of the axon that impedes the diffusion of axon guidance receptors such as Derailed and Roundabout2 and Roundabout3 (Katsuki et al., 2009). The relationship between this barrier and ankyrin or the AIS is unknown.

1.6.1.) C. elegans UNC-44 and mammalian AnkyrinG

Ankyrins are cytoskeletal adapter molecules, first identified in erythrocytes, that link a variety of membrane proteins to the spectrin/actin cytoskeleton (Rasband, 2010). Three genes encode ankyrins in mammals: AnkyrinR (also referred to as AnkR or ANK1),

AnkyrinB (AnkB or ANK2) and AnkyrinG (AnkG or ANK3) (Bennett and Chen, 2001). Each gene has multiple splice forms. In most cases, all three ankyrin genes are expressed in a single ell type (Bennett and Chen, 2001). AnkyrinB and AnkyrinG, whose function is well studied in neurons, have unusually long isoforms encoding giant proteins of ~4400 or ~4800 amino acids. These long isoforms are efficiently localized to the axon, whereas the shorter isoforms are restricted to the cell body (Chan et al., 1993; Kunimoto, 1995). AnkyrinG is enriched at the AIS and at nodes of Ranvier, whereas AnkyrinB is present throughout the axon (Kordeli et al., 1995; Kunimoto et al., 1998).

AnkyrinG is the master organizer of the AIS, playing a critical role in its establishment and maintenance (Hedstrom et al., 2008). It localizes to the proximal region in the axon, which develops into the AIS of the cell, and induces the clustering of L1 cell adhesion molecules, voltage-gated sodium and potassium channels, and the spectrin proteins (Jenkins and Bennett, 2001; Zhou et al., 1998). The extracellular and intracellular mechanisms regulating AnkyrinG localization to the nascent AIS remain to be uncovered. AnkyrinG is also a master organizer at nodes of Ranvier, recruiting a similar set of proteins as it does at the AIS (Rasband, 2010). AnkyrinB, also able to bind L1 molecules, contributes to the organization of the paranodal membrane, situated adjacent to the nodes of Ranvier (Ogawa et al., 2006).

AnkyrinG also has a role in the maintenance of neuronal polarity. Knocking down AnkyrinG expression in cultured hippocampal neurons results in misaccumulation of dendritic cytoskeletal protein MAP2 and K^+/Cl^- cotransporter KCC2 to axons (Hedstrom et al., 2008). In cerebellum-specific AnkyrinG knockout mice, purkinje cells showed defects in the maintenance of polarity, developing postsynaptic spines containing dendritic

molecules such as PSD95 (Sobotzik et al., 2009). It will be interesting to see if AnkyrinG's regulation of neuronal polarity is associated with its role in establishing diffusion barriers for membrane and cytosolic factors. Microtubule fascicles associated with the AIS are also lost in AnkyrinG knockout mice (Sobotzik et al., 2009).

The *Drosophila* genome encodes two ankyrin genes, *Dank1* and *Dank2* (Bouley et al., 2000; Dubreuil and Yu, 1994). Like the mammalian ankyrins-B and -G, the fly *Dank2* gene encodes a giant ankyrin (*Dank2-L),* approximately 4000 amino acids long (Koch et al., 2008; Pielage et al., 2008). Short ankyrin isoforms in the fly are restricted to cell bodies, whereas the longer isoforms are present throughout the axon (Bouley et al., 2000; Koch et al., 2008; Pielage et al., 2008), and interact with the *Drosophila* L1 homolog, neuroglian (Bouley et al., 2000). Fly *Dank2-L* is required for the stabilization of synapses at the NMJ (Koch et al., 2008; Pielage et al., 2008).

C. elegans unc-44 was originally identified as a mutant with defective locomotion, and has since been identified in numerous screens as an important regulator of axon elongation and guidance in a variety of cell types (Brenner, 1974; Hedgecock et al., 1985; Siddiqui and Culotti, 1991). Analysis of transposon insertion alleles of *unc-44* and their revertants identified *unc-44* as the sole *C. elegans* homolog of mammalian ankyrins (Otsuka et al., 1995). *unc-44* encodes a large number of transcripts ranging from ~1 kb to ~22 kb, giving rise to smaller conventional ankyrin proteins, as well as medium and giant isoforms of ~2000 amino acids and ~7000 amino acids (Boontrakulpoontawee and Otsuka, 2002; Otsuka et al., 2002; Otsuka et al., 1995). Interestingly, examination of multiple alleles demonstrated that the larger splice forms are disrupted in all alleles, suggesting the giant proteins are required for proper axon elongation and guidance (Boontrakulpoontawee

and Otsuka, 2002; Otsuka et al., 1995). The smaller isoforms are expressed in many tissues including neurons, whereas the ~7000 amino acid long isoform appears specifically expressed in the nervous system (Otsuka et al., 2002). Reminiscent of the subcellular distribution of mammalian and fly giant ankyrins, the long *C. elegans* ankyrin is localized at the periphery of cell bodies and also all along neuronal processes (Otsuka et al., 2002).

2.) Steps and mechanisms regulating protein transport in neurons: A focus on GPCRs

Following neuronal polarization and the establishment of axonal and dendritic domains, neuronal proteins are accurately transported to specific subcellular destinations. The asymmetric transport of proteins has been studied in a wide variety of polarized cells. Here, we will briefly review the major steps in protein transport, with a particular emphasis on the traffic of GPCRs (G-protein coupled receptors).

GPCRs are a superfamily of seven transmembrane signaling receptors that modulate cellular functions through heterotrimeric G proteins and downstream effectors. This superfamily of cell surface receptors comprises the largest class of signaling receptors (Bargmann, 2006). The diverse set of GPCRs with vital roles in neuronal function includes neurotransmitter receptors, neuropeptide receptors, photoreceptors and chemoreceptors (odorant receptors and taste receptors) (Dong et al., 2007).

Both the biosynthesis of GPCRs and the endocytic regulation of GPCRs in response to ligand binding have been analyzed for multiple family members. The process of transporting and regulating the subcellular localization of GPCRs can be divided into

four main steps: 1.) Protein folding at the ER followed by ER exit 2.) Sorting into appropriate secretory vesicles 3.) Delivery to appropriate subcellular domain 4.) Maintenance or refinement of subcellular distribution by selective clustering or selective endocytosis.

2.1.) Protein folding and ER exit

Protein folding and ER exit are actively guided by general and dedicated accessory proteins (Dong et al., 2007). Proteins need to achieve their native conformation before they exit the ER, and this may be a particular challenge for GPCRs and other proteins with multiple transmembrane domains. Indeed, export of mature protein from the ER is the rate-limiting step in the biogenesis of δ-opioid receptor (DOR) and probably many other GPCRs (Petaja-Repo et al., 2000). Chaperones and chaperonins in the ER, such as BiP, calnexin and caltreticulin, aid in the protein folding process for GPCRs and many other proteins. By interacting with exposed hydrophobic surfaces, unpaired cysteines and immature glycans of unfolded proteins, they prevent the aggregation of immature proteins and promote sequential steps along the folding pathway (Ellgaard and Helenius, 2003).

To ensure that only mature, properly folded proteins reach their destinations, a quality control system in the ER monitors the conformations of newly synthesized proteins. The chaperones mentioned above act as conformational sensors and play a dual role in the ER: first, they assist in the folding process, and second, they identify proteins that are severely or irreversibly misfolded and target these for ubiquitin-mediated proteasomal destruction, as part of the ER-associated degradation (ERAD) pathway (Ellgaard and Helenius, 2003).

Elements within the GPCRs themselves also affect traffic. Heterodimerization plays an important role in the biogenesis of many GPCRs and can affect pharmacological and signaling properties of these proteins (Prinster et al., 2005). Indeed, α_{1D}-adrenergic receptors show poor surface expression on their own, however, heterodimerization with α_{1B} or β_2-adrenergic receptors significantly enhances their surface expression and function. Furthermore, cis-acting dileucine and phenylalanine-based sequences in the membrane proximal domain also play a role in promoting ER exit, as seen for the vasopressin V2R receptor and the dopamine D1R receptor (Bermak et al., 2001; Schulein et al., 1998). Conversely, cis-acting seqences such as the RxR motifs induce ER retention until masked by accessory proteins or heterodimers, as seen in the case of $GABA_BR2$ that masks the ER-retention sequence of its heterodimer $GABA_BR1$ to allow its ER exit (Margeta-Mitrovic et al., 2000; Pagano et al., 2001).

Aside from these molecular chaperones, a growing number of trans-acting factors or accessory proteins have been identified that are required for ER exit, or that promote the ER exit of specific GPCR proteins. These accessory proteins do not act on all GPCRs, and instead, show a high degree of substrate selectivity.

2.1.1.) ninaA

Studies of *Drosophila* and mammalian opsins first demonstrated the presence of GPCR-specific chaperones that promote folding and ER export. The *Drosophila ninaA* gene encodes a cyclophilin homolog that is required for rhodopsins Rh1 and Rh2, but not Rh3, to traffic to the rhabdomeres of fly photoreceptors (Colley et al., 1991). Cyclophilins

are peptidyl-prolyl *cis-trans* isomerases that catalyze the rate-limiting step to generate prolyl-peptide bonds conformations required for protein folding. In *ninaA* mutants, Rh1 and Rh2 rhodopsins are retained in the ER, presumably due to conformational abnormalities. Moreover, ninaA colocalizes with rhodopsin-positive vesicles, suggesting additional roles in later steps of rhodopsin transport (Baker et al., 1994). Similarly, a cyclophilin domain-containing protein, RanBP2, has been shown to promote surface expression of mammalian red/green rhodopsin in photoreceptor cells(Ferreira et al., 1996).

2.1.2.) ODR-4

C. elegans odr-4 gene encodes an accessory protein for a subset of chemoreceptors including ODR-10, a diacetyl odorant receptor (Dwyer et al., 1998). *odr-4* was identified in a screen for chemotaxis-defective mutants, and encodes a single-pass transmembrane protein, found on intracellular membranous organelles likely to be ER and transport vesicles. In absence of ODR-4 function, chemoreceptors like ODR-10 that are normally localized at sensory cilia at dendrite endings are instead retained in the cell body, probably in the ER. Thus, ODR-4 encodes a trans-acting factor that is likely to function at the ER, and perhaps later, to promote ER exit and further transport of ODR-10 to neuronal cilia.

As mentioned above, protein folding and ER exit is a rate-limiting step for many GPCRs, and also a cell-specific process for odorant receptors. Mammalian odorant receptors as well as *C.elegans* ODR-10 display poor surface expression and primarily ER retention when expressed in heterologous cells, suggesting a requirement of trans-acting accessory factors such as ODR-4 (Bush and Hall, 2008). ODR-4 co-expression promotes surface expression of ODR-10 as well as mammalian odorant receptor U131, suggesting

that the mechanism employed by ODR-4 is conserved (Gimelbrant et al., 2001), and consistent with the existence of mammalian ODR-4 homologs (Lehman et al., 2005).

2.2.) Sorting into secretory vesicles

After subsequent processing in the Golgi complex, including maturation of glycosylation as well as lipid modifications such as palmitoylation, GPCRs are sorted at the trans-Golgi network into secretory vesicles that traffic to the cell surface (Mellman and Nelson, 2008). Among the post-TGN vesicles are those destined for constitutive secretion, regulated secretion, endosomes or lysosomes. Sorting at the TGN has been most carefully analyzed in the epithelial MDCK (Madine-Darby canine kidney) cells, a well-established system for studying polarized trafficking. In MDCK cells, many proteins destined for the apical or basolateral domains are sorted into two distinct vesicle populations at the TGN (Wandinger-Ness et al., 1990). However, proteins can also take an indirect route to their final destination as exemplified by the polymeric Ig receptor in epithelial cells that reaches its destination through selective endocytosis followed by directional transport, termed transcytosis (Tuma and Hubbard, 2003).

Among the vesicles that bud off the TGN are clathrin-coated vesicles (CCVs). CCVs also bud off from the plasma membrane and endosome compartments. In each case, clathrin is recruited by distinct adaptor complexes, which in turn recognize cargo proteins that bear amio acid sequences such as YXXϕ and dileucine motifs. The assembly of CCVs from Golgi depends on the tetrameric AP-1 adaptor complex, whereas CCVs at the plasma membrane depend on a similar AP-2 complex or other adaptors (Traub and Kornfeld, 1997). A diversity of clathrin adaptors permits sorting to distinct compartments in

polarized cells. A specific AP-1 complex called AP-1B, consisting of an epithelia-specific μ1b subunit, is present in polarized epithelial cells, and is essential for basolateral sorting of membrane proteins (Folsch et al., 1999; Folsch et al., 2003).

2.2.1) UNC-101, the μ1 subunit of the C. elegans AP-1 complex

In *C. elegans*, the *unc-101* μ1 subunit of the AP-1 complex is required for membrane localization to cilia, suggesting CCVs are involved in cilia targeting (Bae et al., 2006; Dwyer et al., 2001). GPCRs including the diacetyl receptor ODR-10, require *unc-101* for specific sorting to cilia (Dwyer et al., 2001). In *unc-101* mutants, ODR-10 is present throughout the plasma membrane of the soma, axons and dendrites, suggesting that it is missorted to a "bulk" or constitutive secretion pathway. ciliary localization of ODR-10 (Dwyer et al., 2001). UNC-101 localizes at the Golgi and is required for ODR-10 positive dendritic vesicles, suggesting it functions at the Golgi to sort ODR-10 into specific targeting vesicles (Dwyer et al., 2001; Kaplan et al., 2010). A requirement of AP1 adaptors is thus characteristic of sorting both to cilia and the basolateral compartment.

2.3.) Delivering proteins to the appropriate subcellular destinations

Subsequent to sorting at the TGN, microtubule-dependent kinesin motors play a critical role in the delivery of axonal and dendritic cargoes (Goldstein and Yang, 2000). In neurons, kinesin-driven transport is guided by the established axon-dendrite polarity. Vesicles carrying dendritic proteins such as ODR-10 and the transferrin receptor (TfR) move specifically towards dendrites via kinesin motor activity (Burack et al., 2000; Dwyer et al., 2001; Setou et al., 2002). Similarly, vesicles carrying axonal proteins such as

VAMP2 move specifically towards axons (Nakata and Hirokawa, 2003). Asymmetry in microtubule-dependent transport could arise from "smart" kinesin motors that know where axons and dendrites are located, or from cargo molecules or adapters that recognize intracellular asymmetry and inform kinesins where to go, or a combination of the two factors (Goldstein and Yang, 2000). Elegant studies using full-length and chimeric kinesin constructs for KIF5 and KIF17 in cultured neurons have demonstrated that both kinesins as well as cargo molecules seem to contribute to the directionality of polarized transport (Jacobson et al., 2006; Nakata and Hirokawa, 2003). Kinesin-dependent anterograde delivery is supplemented in some cases by dynein and myosin motors, with dynein motors in particular being implicated in retrograde transport from processes towards (Arnold, 2009). The identities of kinesins and adapters that regulate directed delivery of GPCRs such as ODR-10 remain to be identified.

2.4.) Clustering or selective endocytosis to maintain or refine localization patterns

After the directed delivery of proteins to the target cell surface, membrane proteins can be clustered or stabilized by scaffold proteins. Examples of scaffold molecules include AnkyrinG and spectrin, which cluster voltage-gated sodium and potassium channels, and cell adhesion molecules at the AIS (Jenkins and Bennett, 2001; Zhou et al., 1998); Rapsyn, which clusters acetylcholine receptors at the neuromuscular junction (Fuhrer et al., 1999); and gephryn, which clusters glycine and $GABA_A$ receptors (Craig et al., 1996; Sassoe-Pognetto et al., 1999; Sassoe-Pognetto et al., 1995).

Some proteins are not delivered directly to the target membrane in polarized cells, but instead are delivered uniformly, then targeted by selective endocytosis followed by

directed delivery (transcytosis). Indeed, a majority of apical proteins follow the transcytotic pathway in hepatocytes, travelling initially to the basolateral surface followed by endocytosis and redirection to the apical domain (Tuma and Hubbard, 2003). The polymeric Ig receptor (pIG-R) that transports IgM and dimeric IgA molecules from the basolateral to apical surface in epithelial cells represents one of the best-understood cases of transcytosis. A basolateral-localization signal in the cytoplasmic tail promotes the initial delivery of pIg-R to the basolateral domain. Thereafter, pIg-R is endocytosed and delivered to the apical domain, and these events are stimulated by binding of immunoglobin molecules and by serine phosphorylation of the cytoplasmic tail (Tuma and Hubbard, 2003). Transcytosis has also been observed in neurons, particularly for axonal proteins. L1/NgCAM shows polarized axonal localization at steady state. However, temporal analysis of its transport, combined with manipulations of endocytic regulators, showed that NgCAM is initially delivered to both axonal and somatodendritic domains, followed by preferential endocytosis in dendrites and subsequent traffic towards the axon (Wisco et al., 2003). A similar transcytosis route has also been observed for presynaptic vesicle associated protein VAMP2 in mammalian neurons, although the mechanisms underlying its transcytotic transport are not as well understood (Yap et al., 2008a; Yap et al., 2008b).

In this thesis, I set out to explore the regulation of polarized protein transport to axons, dendrites and sensory cilia. I expressed two presynaptic molecules, SAD-1::GFP and mCherry::RAB-3, in a pair of PVD mechanosensory neurons that extend a single axon and two highly branched dendrites. A genetic screen using this system identified *unc-*

33/CRMP as a major regulator that establishes the restricted localization of axonal and dendritic molecules. Subsequently, in a candidate approach, I observed that *unc-44*/ankyrin mutants displayed similar phenotypes as *unc-33* mutants. Further characterization of these two mutants suggest that the *C. elegans* microtubule-binding protein UNC-33 and the ankyrin homolog UNC-44 act together to establish cytoskeletal substrates for asymmetric kinesin recruitment and polarized protein transport. Chapter 2 describes this work.

Next, to better understand the regulation of chemoreceptor transport in the context of axon-dendrite identities, I cloned *odr-8*. Based on genetic mapping and Solexa/Illumina whole genome sequencing, I identified *odr-8* as the *C. elegans* homolog of UfSP2, a cysteine-protease specific for the ubiquitin-like peptide UFM1. My results suggest that ODR-8/UfSP2 aids in the transport of chemoreceptors like ODR-10 from the ER to the cilia, whereas UFM1-conjugation limits receptor exit from the ER. This ongoing work has led to the model that UFM1-conjugation and ODR-8-mediated deconjugation antagonize each other to control the surface expression of chemoreceptors, as described in Chapter 3. In Chapter 4, I discuss directions for future studies examining axon-dendrite polarization, and asymmetric protein transport in neurons.

References

Adler, C.E., Fetter, R.D., and Bargmann, C.I. (2006). UNC-6/Netrin induces neuronal asymmetry and defines the site of axon formation. Nat Neurosci *9*, 511-518.

Arimura, N., and Kaibuchi, K. (2007). Neuronal polarity: from extracellular signals to intracellular mechanisms. Nat Rev Neurosci *8*, 194-205.

Arimura, N., Kimura, T., Nakamuta, S., Taya, S., Funahashi, Y., Hattori, A., Shimada, A., Menager, C., Kawabata, S., Fujii, K.*, et al.* (2009). Anterograde transport of TrkB in axons is mediated by direct interaction with Slp1 and Rab27. Dev Cell *16*, 675-686.

Arnold, D.B. (2009). Actin and microtubule-based cytoskeletal cues direct polarized targeting of proteins in neurons. Sci Signal *2*, pe49.

Baas, P.W., Black, M.M., and Banker, G.A. (1989). Changes in microtubule polarity orientation during the development of hippocampal neurons in culture. J Cell Biol *109*, 3085-3094.

Baas, P.W., Deitch, J.S., Black, M.M., and Banker, G.A. (1988). Polarity orientation of microtubules in hippocampal neurons: uniformity in the axon and nonuniformity in the dendrite. Proc Natl Acad Sci U S A *85*, 8335-8339.

Bae, Y.K., Qin, H., Knobel, K.M., Hu, J., Rosenbaum, J.L., and Barr, M.M. (2006). General and cell-type specific mechanisms target TRPP2/PKD-2 to cilia. Development *133*, 3859-3870.

Baker, E.K., Colley, N.J., and Zuker, C.S. (1994). The cyclophilin homolog NinaA functions as a chaperone, forming a stable complex in vivo with its protein target rhodopsin. EMBO J *13*, 4886-4895.

Bargmann, C.I. (2006). Comparative chemosensation from receptors to ecology. Nature *444*, 295-301.

Barnes, A.P., Lilley, B.N., Pan, Y.A., Plummer, L.J., Powell, A.W., Raines, A.N., Sanes, J.R., and Polleux, F. (2007). LKB1 and SAD kinases define a pathway required for the polarization of cortical neurons. Cell *129*, 549-563.

Barnes, A.P., and Polleux, F. (2009). Establishment of axon-dendrite polarity in developing neurons. Annu Rev Neurosci *32*, 347-381.

Bennett, V., and Baines, A.J. (2001). Spectrin and ankyrin-based pathways: metazoan inventions for integrating cells into tissues. Physiol Rev *81*, 1353-1392.

Bennett, V., and Chen, L. (2001). Ankyrins and cellular targeting of diverse membrane proteins to physiological sites. Curr Opin Cell Biol *13*, 61-67.

Bermak, J.C., Li, M., Bullock, C., and Zhou, Q.Y. (2001). Regulation of transport of the dopamine D1 receptor by a new membrane-associated ER protein. Nat Cell Biol *3*, 492-498.

Biernat, J., Wu, Y.Z., Timm, T., Zheng-Fischhofer, Q., Mandelkow, E., Meijer, L., and Mandelkow, E.M. (2002). Protein kinase MARK/PAR-1 is required for neurite outgrowth and establishment of neuronal polarity. Mol Biol Cell *13*, 4013-4028.

Binder, L.I., Frankfurter, A., and Rebhun, L.I. (1985). The distribution of tau in the mammalian central nervous system. J Cell Biol *101*, 1371-1378.

Boontrakulpoontawee, P., and Otsuka, A.J. (2002). Mutational analysis of the Caenorhabditis elegans ankyrin gene unc-44 demonstrates that the large spliceoform is critical for neural development. Mol Genet Genomics *267*, 291-302.

Bouley, M., Tian, M.Z., Paisley, K., Shen, Y.C., Malhotra, J.D., and Hortsch, M. (2000). The L1-type cell adhesion molecule neuroglian influences the stability of neural ankyrin in the Drosophila embryo but not its axonal localization. J Neurosci *20*, 4515-4523.

Bowman, A.B., Patel-King, R.S., Benashski, S.E., McCaffery, J.M., Goldstein, L.S., and King, S.M. (1999). Drosophila roadblock and Chlamydomonas LC7: a conserved family of dynein-associated proteins involved in axonal transport, flagellar motility, and mitosis. J Cell Biol *146*, 165-180.

Bradke, F., and Dotti, C.G. (1999). The role of local actin instability in axon formation. Science *283*, 1931-1934.

Bradke, F., and Dotti, C.G. (2000). Differentiated neurons retain the capacity to generate axons from dendrites. Curr Biol *10*, 1467-1470.

Brenner, S. (1974). The genetics of Caenorhabditis elegans. Genetics *77*, 71-94.

Burack, M.A., Silverman, M.A., and Banker, G. (2000). The role of selective transport in neuronal protein sorting. Neuron *26*, 465-472.

Burton, P.R., and Paige, J.L. (1981). Polarity of axoplasmic microtubules in the olfactory nerve of the frog. Proc Natl Acad Sci U S A *78*, 3269-3273.

Bush, C.F., and Hall, R.A. (2008). Olfactory receptor trafficking to the plasma membrane. Cell Mol Life Sci *65*, 2289-2295.

Byrd, D.T., Kawasaki, M., Walcoff, M., Hisamoto, N., Matsumoto, K., and Jin, Y. (2001). UNC-16, a JNK-signaling scaffold protein, regulates vesicle transport in C. elegans. Neuron *32*, 787-800.

Caceres, A., Banker, G., Steward, O., Binder, L., and Payne, M. (1984a). MAP2 is localized to the dendrites of hippocampal neurons which develop in culture. Brain Res *315*, 314-318.

Caceres, A., Binder, L.I., Payne, M.R., Bender, P., Rebhun, L., and Steward, O. (1984b). Differential subcellular localization of tubulin and the microtubule-associated protein MAP2 in brain tissue as revealed by immunocytochemistry with monoclonal hybridoma antibodies. J Neurosci *4*, 394-410.

Chan, W., Kordeli, E., and Bennett, V. (1993). 440-kD ankyrinB: structure of the major developmentally regulated domain and selective localization in unmyelinated axons. J Cell Biol *123*, 1463-1473.

Chang, C., Adler, C.E., Krause, M., Clark, S.G., Gertler, F.B., Tessier-Lavigne, M., and Bargmann, C.I. (2006). MIG-10/lamellipodin and AGE-1/PI3K promote axon guidance and outgrowth in response to slit and netrin. Curr Biol *16*, 854-862.

Chen, Y.M., Wang, Q.J., Hu, H.S., Yu, P.C., Zhu, J., Drewes, G., Piwnica-Worms, H., and Luo, Z.G. (2006). Microtubule affinity-regulating kinase 2 functions downstream of the PAR-3/PAR-6/atypical PKC complex in regulating hippocampal neuronal polarity. Proc Natl Acad Sci U S A *103*, 8534-8539.

Cole, A.R., Knebel, A., Morrice, N.A., Robertson, L.A., Irving, A.J., Connolly, C.N., and Sutherland, C. (2004). GSK-3 phosphorylation of the Alzheimer epitope within collapsin response mediator proteins regulates axon elongation in primary neurons. J Biol Chem *279*, 50176-50180.

Colley, N.J., Baker, E.K., Stamnes, M.A., and Zuker, C.S. (1991). The cyclophilin homolog ninaA is required in the secretory pathway. Cell *67*, 255-263.

Colon-Ramos, D.A., Margeta, M.A., and Shen, K. (2007). Glia promote local synaptogenesis through UNC-6 (netrin) signaling in C. elegans. Science *318*, 103-106.

Craig, A.M., Banker, G., Chang, W., McGrath, M.E., and Serpinskaya, A.S. (1996). Clustering of gephyrin at GABAergic but not glutamatergic synapses in cultured rat hippocampal neurons. J Neurosci *16*, 3166-3177.

Crump, J.G., Zhen, M., Jin, Y., and Bargmann, C.I. (2001). The SAD-1 kinase regulates presynaptic vesicle clustering and axon termination. Neuron *29*, 115-129.

Deacon, S.W., Serpinskaya, A.S., Vaughan, P.S., Lopez Fanarraga, M., Vernos, I., Vaughan, K.T., and Gelfand, V.I. (2003). Dynactin is required for bidirectional organelle transport. J Cell Biol *160*, 297-301.

Dent, E.W., Kwiatkowski, A.V., Mebane, L.M., Philippar, U., Barzik, M., Rubinson, D.A., Gupton, S., Van Veen, J.E., Furman, C., Zhang, J.*, et al.* (2007). Filopodia are required for cortical neurite initiation. Nat Cell Biol *9*, 1347-1359.

Deo, R.C., Schmidt, E.F., Elhabazi, A., Togashi, H., Burley, S.K., and Strittmatter, S.M. (2004). Structural bases for CRMP function in plexin-dependent semaphorin3A signaling. EMBO J *23*, 9-22.

Desai, C., Garriga, G., McIntire, S.L., and Horvitz, H.R. (1988). A genetic pathway for the development of the Caenorhabditis elegans HSN motor neurons. Nature *336*, 638-646.

Diefenbach, R.J., Diefenbach, E., Douglas, M.W., and Cunningham, A.L. (2002). The heavy chain of conventional kinesin interacts with the SNARE proteins SNAP25 and SNAP23. Biochemistry *41*, 14906-14915.

Dong, C., Filipeanu, C.M., Duvernay, M.T., and Wu, G. (2007). Regulation of G protein-coupled receptor export trafficking. Biochim Biophys Acta *1768*, 853-870.

Dotti, C.G., Banker, G.A., and Binder, L.I. (1987). The expression and distribution of the microtubule-associated proteins tau and microtubule-associated protein 2 in hippocampal neurons in the rat in situ and in cell culture. Neuroscience *23*, 121-130.

Dotti, C.G., Sullivan, C.A., and Banker, G.A. (1988). The establishment of polarity by hippocampal neurons in culture. J Neurosci *8*, 1454-1468.

Dubreuil, R.R., and Yu, J. (1994). Ankyrin and beta-spectrin accumulate independently of alpha-spectrin in Drosophila. Proc Natl Acad Sci U S A *91*, 10285-10289.

Dwyer, N.D., Adler, C.E., Crump, J.G., L'Etoile, N.D., and Bargmann, C.I. (2001). Polarized dendritic transport and the AP-1 mu1 clathrin adaptor UNC-101 localize odorant receptors to olfactory cilia. Neuron *31*, 277-287.

Dwyer, N.D., Troemel, E.R., Sengupta, P., and Bargmann, C.I. (1998). Odorant receptor localization to olfactory cilia is mediated by ODR-4, a novel membrane-associated protein. Cell *93*, 455-466.

Ellgaard, L., and Helenius, A. (2003). Quality control in the endoplasmic reticulum. Nat Rev Mol Cell Biol *4*, 181-191.

Esch, T., Lemmon, V., and Banker, G. (1999). Local presentation of substrate molecules directs axon specification by cultured hippocampal neurons. J Neurosci *19*, 6417-6426.

Ferreira, P.A., Nakayama, T.A., Pak, W.L., and Travis, G.H. (1996). Cyclophilin-related protein RanBP2 acts as chaperone for red/green opsin. Nature *383*, 637-640.

Folsch, H., Ohno, H., Bonifacino, J.S., and Mellman, I. (1999). A novel clathrin adaptor complex mediates basolateral targeting in polarized epithelial cells. Cell *99*, 189-198.

Folsch, H., Pypaert, M., Maday, S., Pelletier, L., and Mellman, I. (2003). The AP-1A and AP-1B clathrin adaptor complexes define biochemically and functionally distinct membrane domains. J Cell Biol *163*, 351-362.

Forscher, P., and Smith, S.J. (1988). Actions of cytochalasins on the organization of actin filaments and microtubules in a neuronal growth cone. J Cell Biol *107*, 1505-1516.

Fuhrer, C., Gautam, M., Sugiyama, J.E., and Hall, Z.W. (1999). Roles of rapsyn and agrin in interaction of postsynaptic proteins with acetylcholine receptors. J Neurosci *19*, 6405-6416.

Fuhrmann, J.C., Kins, S., Rostaing, P., El Far, O., Kirsch, J., Sheng, M., Triller, A., Betz, H., and Kneussel, M. (2002). Gephyrin interacts with Dynein light chains 1 and 2, components of motor protein complexes. J Neurosci *22*, 5393-5402.

Fukata, Y., Itoh, T.J., Kimura, T., Menager, C., Nishimura, T., Shiromizu, T., Watanabe, H., Inagaki, N., Iwamatsu, A., Hotani, H.*, et al.* (2002). CRMP-2 binds to tubulin heterodimers to promote microtubule assembly. Nat Cell Biol *4*, 583-591.

Gartner, A., Huang, X., and Hall, A. (2006). Neuronal polarity is regulated by glycogen synthase kinase-3 (GSK-3beta) independently of Akt/PKB serine phosphorylation. J Cell Sci *119*, 3927-3934.

Garvalov, B.K., Flynn, K.C., Neukirchen, D., Meyn, L., Teusch, N., Wu, X., Brakebusch, C., Bamburg, J.R., and Bradke, F. (2007). Cdc42 regulates cofilin during the establishment of neuronal polarity. J Neurosci *27*, 13117-13129.

Gauthier, L.R., Charrin, B.C., Borrell-Pages, M., Dompierre, J.P., Rangone, H., Cordelieres, F.P., De Mey, J., MacDonald, M.E., Lessmann, V., Humbert, S.*, et al.* (2004). Huntingtin controls neurotrophic support and survival of neurons by enhancing BDNF vesicular transport along microtubules. Cell *118*, 127-138.

Gimelbrant, A.A., Haley, S.L., and McClintock, T.S. (2001). Olfactory receptor trafficking involves conserved regulatory steps. J Biol Chem *276*, 7285-7290.

Goldstein, L.S., and Yang, Z. (2000). Microtubule-based transport systems in neurons: the roles of kinesins and dyneins. Annu Rev Neurosci *23*, 39-71.

Gomis-Ruth, S., Wierenga, C.J., and Bradke, F. (2008). Plasticity of polarization: changing dendrites into axons in neurons integrated in neuronal circuits. Curr Biol *18*, 992-1000.

Goshima, Y., Nakamura, F., Strittmatter, P., and Strittmatter, S.M. (1995). Collapsin-induced growth cone collapse mediated by an intracellular protein related to UNC-33. Nature *376*, 509-514.

Grubb, M.S., and Burrone, J. (2010). Activity-dependent relocation of the axon initial segment fine-tunes neuronal excitability. Nature *465*, 1070-1074.

Guo, S., and Kemphues, K.J. (1996). Molecular genetics of asymmetric cleavage in the early Caenorhabditis elegans embryo. Curr Opin Genet Dev *6*, 408-415.

Hall, D.H., and Hedgecock, E.M. (1991). Kinesin-related gene unc-104 is required for axonal transport of synaptic vesicles in C. elegans. Cell *65*, 837-847.

Hamajima, N., Matsuda, K., Sakata, S., Tamaki, N., Sasaki, M., and Nonaka, M. (1996). A novel gene family defined by human dihydropyrimidinase and three related proteins with differential tissue distribution. Gene *180*, 157-163.

Hedgecock, E.M., Culotti, J.G., Thomson, J.N., and Perkins, L.A. (1985). Axonal guidance mutants of Caenorhabditis elegans identified by filling sensory neurons with fluorescein dyes. Dev Biol *111*, 158-170.

Hedstrom, K.L., Ogawa, Y., and Rasband, M.N. (2008). AnkyrinG is required for maintenance of the axon initial segment and neuronal polarity. J Cell Biol *183*, 635-640.

Heidemann, S.R., Landers, J.M., and Hamborg, M.A. (1981). Polarity orientation of axonal microtubules. J Cell Biol *91*, 661-665.

Hilliard, M.A., and Bargmann, C.I. (2006). Wnt signals and frizzled activity orient anterior-posterior axon outgrowth in C. elegans. Dev Cell *10*, 379-390.

Hirokawa, N., and Noda, Y. (2008). Intracellular transport and kinesin superfamily proteins, KIFs: structure, function, and dynamics. Physiol Rev *88*, 1089-1118.

Hirokawa, N., and Takemura, R. (2005). Molecular motors and mechanisms of directional transport in neurons. Nat Rev Neurosci *6*, 201-214.

Hollenbeck, P.J., and Saxton, W.M. (2005). The axonal transport of mitochondria. J Cell Sci *118*, 5411-5419.

Horiguchi, K., Hanada, T., Fukui, Y., and Chishti, A.H. (2006). Transport of PIP3 by GAKIN, a kinesin-3 family protein, regulates neuronal cell polarity. J Cell Biol *174*, 425-436.

Hung, W., Hwang, C., Po, M.D., and Zhen, M. (2007). Neuronal polarity is regulated by a direct interaction between a scaffolding protein, Neurabin, and a presynaptic SAD-1 kinase in Caenorhabditis elegans. Development *134*, 237-249.

Hur, E.M., and Zhou, F.Q. (2010). GSK3 signalling in neural development. Nat Rev Neurosci *11*, 539-551.

Hurd, D.D., and Saxton, W.M. (1996). Kinesin mutations cause motor neuron disease phenotypes by disrupting fast axonal transport in Drosophila. Genetics *144*, 1075-1085.

Inagaki, N., Chihara, K., Arimura, N., Menager, C., Kawano, Y., Matsuo, N., Nishimura, T., Amano, M., and Kaibuchi, K. (2001). CRMP-2 induces axons in cultured hippocampal neurons. Nat Neurosci *4*, 781-782.

Jacobs, T., Causeret, F., Nishimura, Y.V., Terao, M., Norman, A., Hoshino, M., and Nikolic, M. (2007). Localized activation of p21-activated kinase controls neuronal polarity and morphology. J Neurosci *27*, 8604-8615.

Jacobson, C., Schnapp, B., and Banker, G.A. (2006). A change in the selective translocation of the Kinesin-1 motor domain marks the initial specification of the axon. Neuron *49*, 797-804.

Jenkins, S.M., and Bennett, V. (2001). Ankyrin-G coordinates assembly of the spectrin-based membrane skeleton, voltage-gated sodium channels, and L1 CAMs at Purkinje neuron initial segments. J Cell Biol *155*, 739-746.

Jiang, H., Guo, W., Liang, X., and Rao, Y. (2005). Both the establishment and the maintenance of neuronal polarity require active mechanisms: critical roles of GSK-3beta and its upstream regulators. Cell *120*, 123-135.

Jiang, H., and Rao, Y. (2005). Axon formation: fate versus growth. Nat Neurosci *8*, 544-546.

Kaplan, O.I., Molla-Herman, A., Cevik, S., Ghossoub, R., Kida, K., Kimura, Y., Jenkins, P., Martens, J.R., Setou, M., Benmerah, A.*, et al.* (2010). The AP-1 clathrin adaptor facilitates cilium formation and functions with RAB-8 in C. elegans ciliary membrane transport. J Cell Sci *123*, 3966-3977.

Kardon, J.R., and Vale, R.D. (2009). Regulators of the cytoplasmic dynein motor. Nat Rev Mol Cell Biol *10*, 854-865.

Katsuki, T., Ailani, D., Hiramoto, M., and Hiromi, Y. (2009). Intra-axonal patterning: intrinsic compartmentalization of the axonal membrane in Drosophila neurons. Neuron *64*, 188-199.

Kim, J.S., Hung, W., Narbonne, P., Roy, R., and Zhen, M. (2010). C. elegans STRADalpha and SAD cooperatively regulate neuronal polarity and synaptic organization. Development *137*, 93-102.

Kishi, M., Pan, Y.A., Crump, J.G., and Sanes, J.R. (2005). Mammalian SAD kinases are required for neuronal polarization. Science *307*, 929-932.

Klopfenstein, D.R., Tomishige, M., Stuurman, N., and Vale, R.D. (2002). Role of phosphatidylinositol(4,5)bisphosphate organization in membrane transport by the Unc104 kinesin motor. Cell *109*, 347-358.

Koch, I., Schwarz, H., Beuchle, D., Goellner, B., Langegger, M., and Aberle, H. (2008). Drosophila ankyrin 2 is required for synaptic stability. Neuron *58*, 210-222.

Kordeli, E., Lambert, S., and Bennett, V. (1995). AnkyrinG. A new ankyrin gene with neural-specific isoforms localized at the axonal initial segment and node of Ranvier. J Biol Chem *270*, 2352-2359.

Koushika, S.P., Schaefer, A.M., Vincent, R., Willis, J.H., Bowerman, B., and Nonet, M.L. (2004). Mutations in Caenorhabditis elegans cytoplasmic dynein components reveal specificity of neuronal retrograde cargo. J Neurosci *24*, 3907-3916.

Krause, M., Leslie, J.D., Stewart, M., Lafuente, E.M., Valderrama, F., Jagannathan, R., Strasser, G.A., Rubinson, D.A., Liu, H., Way, M.*, et al.* (2004). Lamellipodin, an Ena/VASP ligand, is implicated in the regulation of lamellipodial dynamics. Dev Cell *7*, 571-583.

Kuba, H., Oichi, Y., and Ohmori, H. (2010). Presynaptic activity regulates Na(+) channel distribution at the axon initial segment. Nature *465*, 1075-1078.

Kunimoto, M. (1995). A neuron-specific isoform of brain ankyrin, 440-kD ankyrinB, is targeted to the axons of rat cerebellar neurons. J Cell Biol *131*, 1821-1829.

Kunimoto, M., Adachi, T., and Ishido, M. (1998). Expression and localization of brain ankyrin isoforms and related proteins during early developmental stages of rat nervous system. J Neurochem *71*, 2585-2592.

Kwan, A.C., Dombeck, D.A., and Webb, W.W. (2008). Polarized microtubule arrays in apical dendrites and axons. Proc Natl Acad Sci U S A *105*, 11370-11375.

Kwiatkowski, A.V., Rubinson, D.A., Dent, E.W., Edward van Veen, J., Leslie, J.D., Zhang, J., Mebane, L.M., Philippar, U., Pinheiro, E.M., Burds, A.A.*, et al.* (2007). Ena/VASP Is Required for neuritogenesis in the developing cortex. Neuron *56*, 441-455.

Lasiecka, Z.M., Yap, C.C., Vakulenko, M., and Winckler, B. (2009). Compartmentalizing the neuronal plasma membrane from axon initial segments to synapses. Int Rev Cell Mol Biol *272*, 303-389.

Lehman, C.W., Lee, J.D., and Komives, C.F. (2005). Ubiquitously expressed GPCR membrane-trafficking orthologs. Genomics *85*, 386-391.

Li, W., Herman, R.K., and Shaw, J.E. (1992). Analysis of the Caenorhabditis elegans axonal guidance and outgrowth gene unc-33. Genetics *132*, 675-689.

Lizcano, J.M., Goransson, O., Toth, R., Deak, M., Morrice, N.A., Boudeau, J., Hawley, S.A., Udd, L., Makela, T.P., Hardie, D.G.*, et al.* (2004). LKB1 is a master kinase that activates 13 kinases of the AMPK subfamily, including MARK/PAR-1. EMBO J *23*, 833-843.

Margeta-Mitrovic, M., Jan, Y.N., and Jan, L.Y. (2000). A trafficking checkpoint controls GABA(B) receptor heterodimerization. Neuron *27*, 97-106.

Martin, M., Iyadurai, S.J., Gassman, A., Gindhart, J.G., Jr., Hays, T.S., and Saxton, W.M. (1999). Cytoplasmic dynein, the dynactin complex, and kinesin are interdependent and essential for fast axonal transport. Mol Biol Cell *10*, 3717-3728.

Mellman, I., and Nelson, W.J. (2008). Coordinated protein sorting, targeting and distribution in polarized cells. Nat Rev Mol Cell Biol *9*, 833-845.

Menager, C., Arimura, N., Fukata, Y., and Kaibuchi, K. (2004). PIP3 is involved in neuronal polarization and axon formation. J Neurochem *89*, 109-118.

Morfini, G., DiTella, M.C., Feiguin, F., Carri, N., and Caceres, A. (1994). Neurotrophin-3 enhances neurite outgrowth in cultured hippocampal pyramidal neurons. J Neurosci Res *39*, 219-232.

Muresan, V., Godek, C.P., Reese, T.S., and Schnapp, B.J. (1996). Plus-end motors override minus-end motors during transport of squid axon vesicles on microtubules. J Cell Biol *135*, 383-397.

Nakada, C., Ritchie, K., Oba, Y., Nakamura, M., Hotta, Y., Iino, R., Kasai, R.S., Yamaguchi, K., Fujiwara, T., and Kusumi, A. (2003). Accumulation of anchored proteins forms membrane diffusion barriers during neuronal polarization. Nat Cell Biol *5*, 626-632.

Nakata, T., and Hirokawa, N. (2003). Microtubules provide directional cues for polarized axonal transport through interaction with kinesin motor head. J Cell Biol *162*, 1045-1055.

Nance, J., and Zallen, J.A. (2011). Elaborating polarity: PAR proteins and the cytoskeleton. Development *138*, 799-809.

Nishimura, T., Fukata, Y., Kato, K., Yamaguchi, T., Matsuura, Y., Kamiguchi, H., and Kaibuchi, K. (2003). CRMP-2 regulates polarized Numb-mediated endocytosis for axon growth. Nat Cell Biol *5*, 819-826.

Nonet, M.L., Staunton, J.E., Kilgard, M.P., Fergestad, T., Hartwieg, E., Horvitz, H.R., Jorgensen, E.M., and Meyer, B.J. (1997). Caenorhabditis elegans rab-3 mutant synapses exhibit impaired function and are partially depleted of vesicles. J Neurosci *17*, 8061-8073.

Ogawa, Y., Schafer, D.P., Horresh, I., Bar, V., Hales, K., Yang, Y., Susuki, K., Peles, E., Stankewich, M.C., and Rasband, M.N. (2006). Spectrins and ankyrinB constitute a specialized paranodal cytoskeleton. J Neurosci *26*, 5230-5239.

Okada, Y., Yamazaki, H., Sekine-Aizawa, Y., and Hirokawa, N. (1995). The neuron-specific kinesin superfamily protein KIF1A is a unique monomeric motor for anterograde axonal transport of synaptic vesicle precursors. Cell *81*, 769-780.

Otsuka, A.J., Boontrakulpoontawee, P., Rebeiz, N., Domanus, M., Otsuka, D., Velamparampil, N., Chan, S., Vande Wyngaerde, M., Campagna, S., and Cox, A. (2002). Novel UNC-44 AO13 ankyrin is required for axonal guidance in C. elegans, contains six highly repetitive STEP blocks separated by seven potential transmembrane domains, and is localized to neuronal processes and the periphery of neural cell bodies. J Neurobiol *50*, 333-349.

Otsuka, A.J., Franco, R., Yang, B., Shim, K.H., Tang, L.Z., Zhang, Y.Y., Boontrakulpoontawee, P., Jeyaprakash, A., Hedgecock, E., Wheaton, V.I.*, et al.* (1995). An ankyrin-related gene (unc-44) is necessary for proper axonal guidance in Caenorhabditis elegans. J Cell Biol *129*, 1081-1092.

Ou, C.Y., Poon, V.Y., Maeder, C.I., Watanabe, S., Lehrman, E.K., Fu, A.K., Park, M., Fu, W.Y., Jorgensen, E.M., Ip, N.Y.*, et al.* (2010). Two cyclin-dependent kinase pathways are essential for polarized trafficking of presynaptic components. Cell *141*, 846-858.

Pack-Chung, E., Kurshan, P.T., Dickman, D.K., and Schwarz, T.L. (2007). A Drosophila kinesin required for synaptic bouton formation and synaptic vesicle transport. Nat Neurosci *10*, 980-989.

Pagano, A., Rovelli, G., Mosbacher, J., Lohmann, T., Duthey, B., Stauffer, D., Ristig, D., Schuler, V., Meigel, I., Lampert, C.*, et al.* (2001). C-terminal interaction is essential for surface trafficking but not for heteromeric assembly of GABA(b) receptors. J Neurosci *21*, 1189-1202.

Palay, S.L., Sotelo, C., Peters, A., and Orkand, P.M. (1968). The axon hillock and the initial segment. J Cell Biol *38*, 193-201.

Pan, C.L., Howell, J.E., Clark, S.G., Hilliard, M., Cordes, S., Bargmann, C.I., and Garriga, G. (2006). Multiple Wnts and frizzled receptors regulate anteriorly directed cell and growth cone migrations in Caenorhabditis elegans. Dev Cell *10*, 367-377.

Patel, M.R., Lehrman, E.K., Poon, V.Y., Crump, J.G., Zhen, M., Bargmann, C.I., and Shen, K. (2006). Hierarchical assembly of presynaptic components in defined C. elegans synapses. Nat Neurosci *9*, 1488-1498.

Petaja-Repo, U.E., Hogue, M., Laperriere, A., Walker, P., and Bouvier, M. (2000). Export from the endoplasmic reticulum represents the limiting step in the maturation and cell surface expression of the human delta opioid receptor. J Biol Chem *275*, 13727-13736.

Pielage, J., Cheng, L., Fetter, R.D., Carlton, P.M., Sedat, J.W., and Davis, G.W. (2008). A presynaptic giant ankyrin stabilizes the NMJ through regulation of presynaptic microtubules and transsynaptic cell adhesion. Neuron *58*, 195-209.

Polleux, F., Giger, R.J., Ginty, D.D., Kolodkin, A.L., and Ghosh, A. (1998). Patterning of cortical efferent projections by semaphorin-neuropilin interactions. Science *282*, 1904-1906.

Polleux, F., Morrow, T., and Ghosh, A. (2000). Semaphorin 3A is a chemoattractant for cortical apical dendrites. Nature *404*, 567-573.

Poon, V.Y., Klassen, M.P., and Shen, K. (2008). UNC-6/netrin and its receptor UNC-5 locally exclude presynaptic components from dendrites. Nature *455*, 669-673.

Prinster, S.C., Hague, C., and Hall, R.A. (2005). Heterodimerization of g protein-coupled receptors: specificity and functional significance. Pharmacol Rev *57*, 289-298.

Quinn, C.C., Chen, E., Kinjo, T.G., Kelly, G., Bell, A.W., Elliott, R.C., McPherson, P.S., and Hockfield, S. (2003). TUC-4b, a novel TUC family variant, regulates neurite outgrowth and associates with vesicles in the growth cone. J Neurosci *23*, 2815-2823.

Quinn, C.C., Gray, G.E., and Hockfield, S. (1999). A family of proteins implicated in axon guidance and outgrowth. J Neurobiol *41*, 158-164.

Rasband, M.N. (2010). The axon initial segment and the maintenance of neuronal polarity. Nat Rev Neurosci *11*, 552-562.

Rolls, M.M., Satoh, D., Clyne, P.J., Henner, A.L., Uemura, T., and Doe, C.Q. (2007). Polarity and intracellular compartmentalization of Drosophila neurons. Neural Dev *2*, 7.

Sassoe-Pognetto, M., Giustetto, M., Panzanelli, P., Cantino, D., Kirsch, J., and Fritschy, J.M. (1999). Postsynaptic colocalization of gephyrin and GABAA receptors. Ann N Y Acad Sci *868*, 693-696.

Sassoe-Pognetto, M., Kirsch, J., Grunert, U., Greferath, U., Fritschy, J.M., Mohler, H., Betz, H., and Wassle, H. (1995). Colocalization of gephyrin and GABAA-receptor subunits in the rat retina. J Comp Neurol *357*, 1-14.

Satoh, D., Sato, D., Tsuyama, T., Saito, M., Ohkura, H., Rolls, M.M., Ishikawa, F., and Uemura, T. (2008). Spatial control of branching within dendritic arbors by dynein-dependent transport of Rab5-endosomes. Nat Cell Biol *10*, 1164-1171.

Saxena, S., Bucci, C., Weis, J., and Kruttgen, A. (2005). The small GTPase Rab7 controls the endosomal trafficking and neuritogenic signaling of the nerve growth factor receptor TrkA. J Neurosci *25*, 10930-10940.

Saxton, W.M., Hicks, J., Goldstein, L.S., and Raff, E.C. (1991). Kinesin heavy chain is essential for viability and neuromuscular functions in Drosophila, but mutants show no defects in mitosis. Cell *64*, 1093-1102.

Schnapp, B.J., and Reese, T.S. (1989). Dynein is the motor for retrograde axonal transport of organelles. Proc Natl Acad Sci U S A *86*, 1548-1552.

Schulein, R., Hermosilla, R., Oksche, A., Dehe, M., Wiesner, B., Krause, G., and Rosenthal, W. (1998). A dileucine sequence and an upstream glutamate residue in the intracellular carboxyl terminus of the vasopressin V2 receptor are essential for cell surface transport in COS.M6 cells. Mol Pharmacol *54*, 525-535.

Setou, M., Seog, D.H., Tanaka, Y., Kanai, Y., Takei, Y., Kawagishi, M., and Hirokawa, N. (2002). Glutamate-receptor-interacting protein GRIP1 directly steers kinesin to dendrites. Nature *417*, 83-87.

Shelly, M., Cancedda, L., Heilshorn, S., Sumbre, G., and Poo, M.M. (2007). LKB1/STRAD promotes axon initiation during neuronal polarization. Cell *129*, 565-577.

Shelly, M., and Poo, M.M. (2011). Role of LKB1 - SAD/MARK pathway in neuronal polarization. Dev Neurobiol.

Shi, S.H., Cheng, T., Jan, L.Y., and Jan, Y.N. (2004). APC and GSK-3beta are involved in mPar3 targeting to the nascent axon and establishment of neuronal polarity. Curr Biol *14*, 2025-2032.

Shi, S.H., Jan, L.Y., and Jan, Y.N. (2003). Hippocampal neuronal polarity specified by spatially localized mPar3/mPar6 and PI 3-kinase activity. Cell *112*, 63-75.

Shin, H., Wyszynski, M., Huh, K.H., Valtschanoff, J.G., Lee, J.R., Ko, J., Streuli, M., Weinberg, R.J., Sheng, M., and Kim, E. (2003). Association of the kinesin motor KIF1A with the multimodular protein liprin-alpha. J Biol Chem *278*, 11393-11401.

Siddiqui, S.S., and Culotti, J.G. (1991). Examination of neurons in wild type and mutants of Caenorhabditis elegans using antibodies to horseradish peroxidase. J Neurogenet *7*, 193-211.

Sieburth, D., Ch'ng, Q., Dybbs, M., Tavazoie, M., Kennedy, S., Wang, D., Dupuy, D., Rual, J.F., Hill, D.E., Vidal, M.*, et al.* (2005). Systematic analysis of genes required for synapse structure and function. Nature *436*, 510-517.

Sobotzik, J.M., Sie, J.M., Politi, C., Del Turco, D., Bennett, V., Deller, T., and Schultz, C. (2009). AnkyrinG is required to maintain axo-dendritic polarity in vivo. Proc Natl Acad Sci U S A *106*, 17564-17569.

Song, A.H., Wang, D., Chen, G., Li, Y., Luo, J., Duan, S., and Poo, M.M. (2009). A selective filter for cytoplasmic transport at the axon initial segment. Cell *136*, 1148-1160.

Stenmark, P., Ogg, D., Flodin, S., Flores, A., Kotenyova, T., Nyman, T., Nordlund, P., and Kursula, P. (2007). The structure of human collapsin response mediator protein 2, a regulator of axonal growth. J Neurochem *101*, 906-917.

Su, Q., Cai, Q., Gerwin, C., Smith, C.L., and Sheng, Z.H. (2004). Syntabulin is a microtubule-associated protein implicated in syntaxin transport in neurons. Nat Cell Biol *6*, 941-953.

Swaney, K.F., Huang, C.H., and Devreotes, P.N. (2010). Eukaryotic chemotaxis: a network of signaling pathways controls motility, directional sensing, and polarity. Annu Rev Biophys *39*, 265-289.

Tahirovic, S., and Bradke, F. (2009). Neuronal polarity. Cold Spring Harb Perspect Biol *1*, a001644.

Tomishige, M., Klopfenstein, D.R., and Vale, R.D. (2002). Conversion of Unc104/KIF1A kinesin into a processive motor after dimerization. Science *297*, 2263-2267.

Traub, L.M., and Kornfeld, S. (1997). The trans-Golgi network: a late secretory sorting station. Curr Opin Cell Biol *9*, 527-533.

Tsuboi, D., Hikita, T., Qadota, H., Amano, M., and Kaibuchi, K. (2005). Regulatory machinery of UNC-33 Ce-CRMP localization in neurites during neuronal development in Caenorhabditis elegans. J Neurochem *95*, 1629-1641.

Tuma, P.L., and Hubbard, A.L. (2003). Transcytosis: crossing cellular barriers. Physiol Rev *83*, 871-932.

Wagner, O.I., Esposito, A., Kohler, B., Chen, C.W., Shen, C.P., Wu, G.H., Butkevich, E., Mandalapu, S., Wenzel, D., Wouters, F.S.*, et al.* (2009). Synaptic scaffolding protein SYD-2 clusters and activates kinesin-3 UNC-104 in C. elegans. Proc Natl Acad Sci U S A *106*, 19605-19610.

Wandinger-Ness, A., Bennett, M.K., Antony, C., and Simons, K. (1990). Distinct transport vesicles mediate the delivery of plasma membrane proteins to the apical and basolateral domains of MDCK cells. J Cell Biol *111*, 987-1000.

Wang, L.H., and Strittmatter, S.M. (1997). Brain CRMP forms heterotetramers similar to liver dihydropyrimidinase. J Neurochem *69*, 2261-2269.

Winckler, B., Forscher, P., and Mellman, I. (1999). A diffusion barrier maintains distribution of membrane proteins in polarized neurons. Nature *397*, 698-701.

Wisco, D., Anderson, E.D., Chang, M.C., Norden, C., Boiko, T., Folsch, H., and Winckler, B. (2003). Uncovering multiple axonal targeting pathways in hippocampal neurons. J Cell Biol *162*, 1317-1328.

Witte, H., Neukirchen, D., and Bradke, F. (2008). Microtubule stabilization specifies initial neuronal polarization. J Cell Biol *180*, 619-632.

Yap, C.C., Nokes, R.L., Wisco, D., Anderson, E., Folsch, H., and Winckler, B. (2008a). Pathway selection to the axon depends on multiple targeting signals in NgCAM. J Cell Sci *121*, 1514-1525.

Yap, C.C., Wisco, D., Kujala, P., Lasiecka, Z.M., Cannon, J.T., Chang, M.C., Hirling, H., Klumperman, J., and Winckler, B. (2008b). The somatodendritic endosomal regulator NEEP21 facilitates axonal targeting of L1/NgCAM. J Cell Biol *180*, 827-842.

Yi, J.J., Barnes, A.P., Hand, R., Polleux, F., and Ehlers, M.D. (2010). TGF-beta signaling specifies axons during brain development. Cell *142*, 144-157.

Yonekawa, Y., Harada, A., Okada, Y., Funakoshi, T., Kanai, Y., Takei, Y., Terada, S., Noda, T., and Hirokawa, N. (1998). Defect in synaptic vesicle precursor transport and neuronal cell death in KIF1A motor protein-deficient mice. J Cell Biol *141*, 431-441.

Yoshimura, T., Kawano, Y., Arimura, N., Kawabata, S., Kikuchi, A., and Kaibuchi, K. (2005). GSK-3beta regulates phosphorylation of CRMP-2 and neuronal polarity. Cell *120*, 137-149.

Zhou, D., Lambert, S., Malen, P.L., Carpenter, S., Boland, L.M., and Bennett, V. (1998). AnkyrinG is required for clustering of voltage-gated Na channels at axon initial segments and for normal action potential firing. J Cell Biol *143*, 1295-1304.

Chapter 2

unc-33/CRMP and *unc-44/*ankyrin organize neuronal microtubules and localize UNC-104/Kif1A kinesin to polarize axon-dendrite protein sorting

Abstract

Three proteins implicated in apparently distinct aspects of axon differentiation are the microtubule-binding protein CRMP, which promotes axon specification, the kinesin UNC-104/Kif1A, which directs axonal traffic, and ankyrinG, which prevents dendritic protein diffusion into axons. The relationships among these molecules are unknown. We show here that the *C. elegans* CRMP homolog UNC-33 and ankyrin homolog UNC-44 act together to establish asymmetric sorting signals for both axons and dendrites. UNC-33 is localized to axons by UNC-44, and enriched in an axon segment near the cell body that suggests analogies with the vertebrate axon initial segment. In *unc-33* and *unc-44* mutants, axonal proteins are distributed randomly between axons and dendrites, dendritic proteins are partly localized to axons, and the distinctive organization of axonal and dendritic microtubules is disrupted. Dendrite integrity is corrupted by misregulated UNC-104/KIF1A, which actively transports axonal proteins to dendrites. Although homologs of UNC-33 and UNC-44 are known to affect axons, the unexpected effects on dendrites suggest a broader function on asymmetric traffic. We propose that microtubules organized by UNC-33 capture the axonal motor UNC-104 to segregate axonal and dendritic sorting pathways.

Introduction

The asymmetric microtubule cytoskeleton is essential for axon-dendrite specification early in development and for polarized protein sorting in mature neurons. The role of microtubules in axon specification, the developmental process that establishes a single unique axon in each cell, has been characterized extensively in cultured hippocampal neurons and to a lesser extent *in vivo* (Arimura and Kaibuchi, 2007; Barnes and Polleux, 2009). Pharmacological manipulations that affect microtubule stability affect the number of axons per neuron and bias the selection of one process as the future axon (Witte et al., 2008), and many molecules that affect axon specification regulate microtubules. Among these are the microtubule-binding CRMP proteins, also called UNC-33, TOAD-64, Ulip, DRP, or TUC, which are linked to early events in axonal development *in vivo* and *in vitro* (Arimura and Kaibuchi, 2007). The founding CRMP protein, UNC-33, affects axon guidance and elongation in *C. elegans* (Li et al., 1992). The best-characterized vertebrate CRMP, now known as CRMP2, promotes axonal specification in cultured mammalian neurons: overexpression of CRMP2 causes neurons to form multiple axons at the expense of dendrites, and dominant-negative fragments or siRNAs targeted against CRMP2 result in the selective loss of axons (Fukata et al., 2002; Inagaki et al., 2001; Kimura et al., 2005; Yoshimura et al., 2005). CRMP proteins interact with tubulin heterodimers and microtubules, and promote microtubule assembly *in vitro* (Arimura et al., 2005; Fukata et al., 2002). CRMP2 also binds the kinesin light chain (KLC) subunit of Kinesin-1, and acts as an adapter for the transport of tubulin dimers, the actin regulators Sra-1/WAVE, and the neurotrophin receptor TrkB into axonal growth cones (Arimura et al., 2005; Kawano et al., 2005; Kimura et al., 2005). The relationship

between these developmental activities and the properties of differentiated axons is unknown.

In mature neurons, asymmetric microtubules regulate polarized protein sorting (Arnold, 2009). Specialized aspects of axonal microtubules, such as their ability to support transport by the axonal Kinesin-3/Kif1A/UNC-104 family, define functional properties of axons (Goldstein and Yang, 2000; Hirokawa and Takemura, 2005). Both kinesins and their cargo recognize features of axonal and dendritic microtubules that contribute to directional transport, although the complete nature of the sorting code has not been determined (Jacobson et al., 2006; Nakata and Hirokawa, 2003; Setou et al., 2002). Axonal microtubules are generally oriented with their plus ends away from the cell body (Burton and Paige, 1981; Heidemann et al., 1981), whereas dendritic microtubules can have the same orientation, the opposite orientation, or mixed polarity, depending on the cell type and distance from the cell body (Baas et al., 1988; Burton, 1985; Kwan et al., 2008). Axonal microtubules are also more stable than those in dendrites, associate with different microtubule-associated proteins (Conde and Caceres, 2009), and carry different post-translational modifications (Witte et al., 2008). Axonal protein sorting is reinforced by the axon initial segment (AIS), a spatial and physiological landmark near the cell body that acts as a membrane diffusion barrier and the action potential initiation zone (Grubb and Burrone, 2010; Winckler et al., 1999). In mammals, the giant actin-binding protein ankyrinG resides at the AIS and is required to maintain its integrity (Hedstrom et al., 2008; Jenkins and Bennett, 2001; Zhou et al., 1998). AnkyrinG supports axon functions by preventing dendritic kinesins and their cargo from entering axons, but appears not to affect the properties of dendrites (Hedstrom et al., 2008; Sobotzik et al., 2009; Song et al., 2009).

Although they are all important in axon development or function, relationships between CRMP, Kif1A, and ankyrinG have not been examined *in vivo* or *in vitro*. The biological significance of mammalian CRMPs, ankyrins, and kinesin3/Kif1A seem to be distinct, but are obscured by the fact that they belong to multigene families, with members that can have overlapping or antagonistic functions (Brot et al.; Ogawa et al., 2006; Quinn et al., 2003). *C. elegans* mutants in *unc-33,* its sole CRMP homolog, and *unc-44,* its sole ankyrin homolog, share defects in locomotion, axon elongation, and axon guidance (Brenner, 1974; Desai et al., 1988; Hedgecock et al., 1985; Li et al., 1992; Tsuboi et al., 2005). We show here that *C. elegans unc-33* acts with *unc-44* to generate essential cytoskeletal signals for polarized sorting of a wide array of neuronal proteins. Contrary to expectations, *unc-33* and *unc-44* mutants affect the microtubule cytoskeleton and protein sorting in dendrites as well as axons, in part by regulating the localization and activity of the conserved kinesin-3/KIF1A protein UNC-104. The profound requirement for *unc-33* and *unc-44* in differential transport to axons and dendrites suggests that they act as the source of the microtubule signals that polarize neuronal transport.

Results

Presynaptic proteins are mislocalized to PVD dendrites in *unc-33* (CRMP) mutants

The *C. elegans* PVD neurons, a pair of harsh touch sensors in the lateral body, have well-defined axons and dendrites that allow the straightforward visualization of polarized protein localization (Fig. 2.1a,b) (Oren-Suissa et al., 2010). Each PVD has an axon that grows ventrally and then anteriorly into the ventral nerve cord, and two major dendrite processes that grow laterally and then branch elaborately into “menorahs” that circle the

body (Oren-Suissa et al., 2010; Tsalik et al., 2003). Presynaptic specializations in PVD are restricted to the axon, and specifically to the ventral nerve cord (White et al., 1986). To generate axonal markers in PVD, a *des-2* promoter fragment (Treinin et al., 1998) was used to express two fluorescently tagged presynaptic molecules, RAB-3:: mCherry and SAD-1::GFP. RAB-3 is a Rab GTPase that labels a subset of synaptic vesicles (Nonet et al., 1997), and SAD-1 is a presynaptically localized serine/threonine kinase that affects presynaptic differentiation and neuronal polarity (Crump et al., 2001; Kishi et al., 2005). Both markers were localized to axonal PVD puncta in the ventral nerve cord, and were either faintly visible or undetectable in the PVD dendrites (Fig. 2.1c-f).

Several screens for altered localization of presynaptic proteins yielded two *unc-33* alleles, identified based on map position, visible phenotypes, and failure to complement existing *unc-33* alleles (see Methods). The two new *unc-33* alleles and three existing *unc-33* alleles all disrupted the distribution of the presynaptic markers RAB-3::mCherry and SAD-1::GFP in PVD, reducing fluorescence in axons and increasing it in dendrites to result in a nearly random distribution of presynaptic proteins (Fig. 2.1g-l; further quantification in Supplementary Fig. 2.1). Based on the fraction of defective animals and on fluorescence quantification, the mutants followed the allelic series: *wild type* > *e204* > *ky880* > *ky869* ≥ *e1193* = *mn407* (Fig. 2.1k,l; Supplementary Fig. 2.1). In strong alleles, all animals showed significant redistribution of axonal proteins into PVD dendrites.

A broader survey of axonal markers demonstrated that *unc-33* is a general regulator of axon-dendrite sorting, affecting diverse axonal proteins in multiple neuron types. The tagged axonally-enriched proteins SNN-1/synapsin, APT-4/α-adaptin, and SYD-2/Liprin-α were all mislocalized to PVD dendrites in *unc-33* mutants (Supplementary Fig. 2.1 and

Figure 2.1. *unc-33* mutants mislocalize presynaptic proteins to dendrites.

(a,b) PVD neuron morphology in an L4 animal. (a) *des-2*::myristoyl::GFP marker (b) Diagrams of PVD morphology and PVD position within the animal.

(c-j) Representative images of RAB-3::mCherry and SAD-1::GFP in PVD neurons of wild type (c-f) and *unc-33(mn407)* (g-j) animals, with schematics. For each set of fluorescence micrographs, the top panel is the maximum intensity projection of dendritic focal planes and the bottom panel is the maximum intensity projection for axonal focal planes. White and yellow arrowheads indicate axonal and dendritic puncta, respectively; 'cb' labels the PVD cell body, and asterisks mark gut autofluorescence. Anterior is at left and dorsal is up in all panels. Scale bars, 10 μm.

(k,l) Quantification of axonal localization defects (k) and dendritic mislocalization defects (l) of RAB-3::mCherry and SAD-1::GFP (n>30 animals/genotype). The fraction of animals with qualitative defects is shown; alternative quantification of fluorescence intensity per animal is provided in Supplementary Fig. 2.1.

(m) *unc-33* gene structure showing exons (black boxes), introns (lines), and untranslated regions (gray boxes), along with the positions and lesions of *unc-33* alleles. Arrows denote the positions of start codons for alternative transcripts of *unc-33*. The three UNC-33 protein isoforms (long, medium and short) are depicted with predicted microtubule-assembling domains shown in blue.

(n) Predicted microtubule-assembling regions of UNC-33 and rat CRMP-2. Gray regions highlight conserved residues; asterisk denotes the conserved glutamate mutated to a lysine in *unc-33(ky880)*.

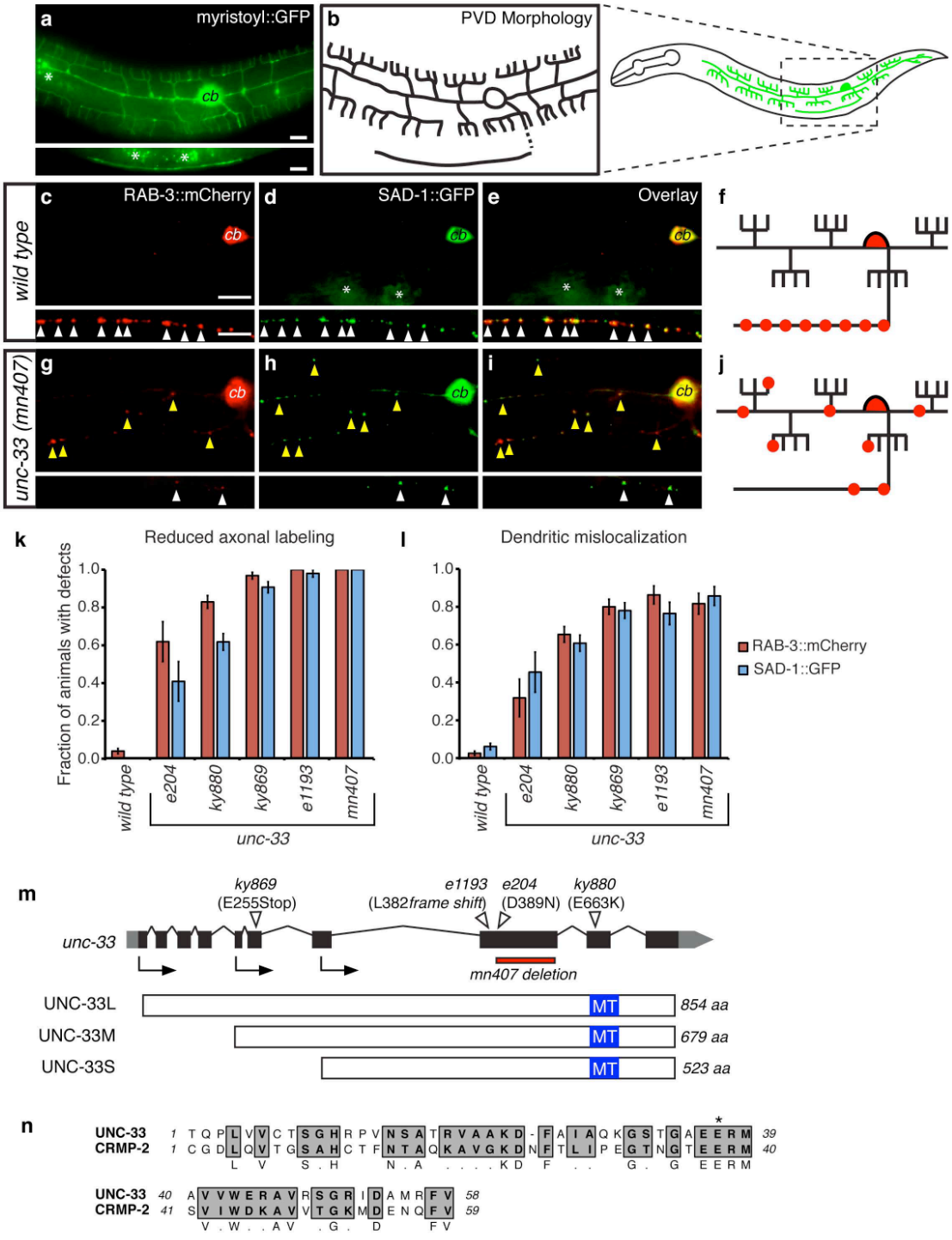
a
myristoyl::GFP
cb
b
PVD Morphology
wild type
c
RAB-3::mCherry
d
SAD-1::GFP
e
Overlay
f
unc-33 (mn407)
g
h
i
j
k
Reduced axonal labeling
Fraction of animals with defects
1.0
0.8
0.6
0.4
0.2
0.0
wild type
e204
ky880
ky869
e1193
mn407
unc-33
l
Dendritic mislocalization
RAB-3::mCherry
SAD-1::GFP
m
ky869
(E255Stop)
e1193
(L382frame shift)
e204
(D389N)
ky880
(E663K)
unc-33
mn407 deletion
UNC-33L
UNC-33M
UNC-33S
MT
854 aa
679 aa
523 aa
n
UNC-33
CRMP-2

Figure 2.1

Supplementary Figure 2.1. *unc-33* mutants mislocalize RAB-3::mCherry, SAD-1::GFP, and the active zone component SYD-2::GFP (*liprin-α*) to PVD dendrites

(a-d) Alternative quantification of axonal localization defects (a, c) and dendritic mislocalization defects (b, d) of RAB-3::mCherry (a-b) and SAD-1::GFP (c-d) in PVDs of *unc-33* mutants, scored as total average fluorescence intensity per cell (n=10-17 animals/genotype).

(e-f) Rescue of axonal marker localization defects of *unc-33(ky880)* mutant through pan-neuronal and PVD-specific expression of UNC-33L.

(g-h) SYD-2::GFP localization in PVD neurons of wild type and *unc-33(mn407)* animals, with schematics. For each set of fluorescence micrographs, the top panel is the maximum intensity projection of dendritic focal planes and the bottom panel is the maximum intensity projection for axonal focal planes. Yellow and white arrowheads indicate axonal and dendritic puncta, respectively; 'cb' denotes the PVD cell body and asterisks indicate gut autofluorescence. Anterior is at left and dorsal is up in all panels. Scale bar, 10 μm.

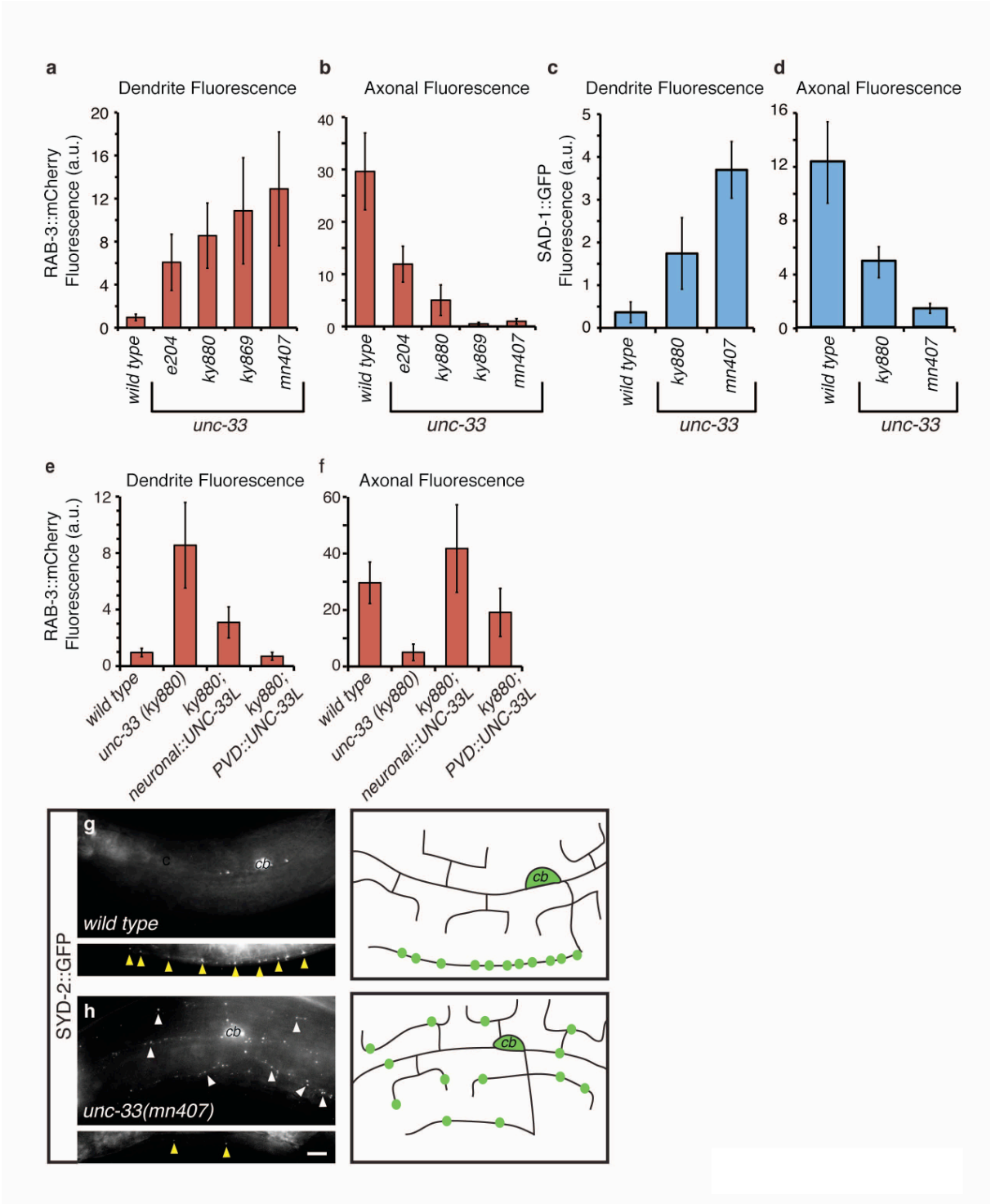

Supplementary Figure 2.1

data not shown). The full set of mislocalized proteins included synaptic vesicle proteins, plasma membrane proteins, and cytoplasmic proteins. Axonal markers were also mislocalized to dendrites in FLP mechanosensory neurons, AVE interneurons, and AWC and ASI chemosensory neurons (Supplementary Fig. 2.2 and data not shown).

unc-33 mutants have defects in axon guidance and elongation (Desai et al., 1988; Hedgecock et al., 1985; Siddiqui and Culotti, 1991), raising a question as to whether the protein localization defects could be a nonspecific side effect of misguided or shortened axons. PVD axons grew successfully to the ventral nerve cord in most *unc-33(mn407)* (80%, n=52) and *unc-33(ky880)* (100%, n=37) animals, but then terminated prematurely with a length around half that of wild-type PVD axons (Supplementary Fig. 2.3g). The axons of FLP neurons in the head also terminated prematurely (Supplementary Fig. 2.3a). To assess the possible effects of guidance and termination defects on protein sorting, we examined *unc-34* (Ena/VASP) mutants, which had similar axon guidance and premature termination defects in PVD and FLP (Supplementary Fig. 2.3a-c, g). In contrast with *unc-33, unc-34* mutants were nearly normal in the localization of RAB-3::mCherry and SAD-1::GFP in PVD and FLP (Supplementary Fig. 2.3d-f, h-i). These results argue that defects in axon guidance and elongation are not sufficient to explain the mistargeting of axonal proteins in *unc-33* mutants.

UNC-33L acts cell autonomously in PVD to establish axonal polarity

unc-33 encodes three distinct protein isoforms with alternative N-termini and a common 523 amino acid C-terminal sequence: UNC-33L (long), UNC-33M (medium), and UNC-33S (short) (Li et al., 1992; Tsuboi et al., 2005). The canonical allele *unc-*

Supplementary Figure 2.2. *unc-33* mutants mislocalize presynaptic proteins in multiple neuronal cell types

(a-b) SAD-1::GFP distribution in FLP neurons of wild type and *unc-33(mn407)* animals, with schematics. 'cb' indicates FLP cell bodies; yellow arrowheads point to SAD-1::GFP puncta mislocalized to FLP dendrites. Asterisks denote labeling of AWC neuron cell bodies with an *odr-1::dsRed* marker. Anterior is at left and dorsal is up in all panels.

(c) Dendritic mislocalization defects of RAB-3::mCherry and SAD-1::GFP in FLPs of *unc-33* mutants, and rescue of *unc-33* mutants through pan-neuronal and FLP-specific expression of UNC-33L. The fraction of animals with qualitative defects is shown (n>30 animals/genotype). *tag-168p*, pan-neuronal promoter; *mec-3p*, promoter expressed in PVD, FLP, and six mechanosensory neurons; *des-2p*, promoter expressed in PVD and FLP.

(d-e) Distribution of UNC-2::GFP (Saheki et al., 2009), an α-subunit of a presynaptic voltage-gated calcium channel, in AWC and AWB chemosensory neurons of wild type (d) and *unc-33(ky869)* (e) animals, with schematics. Yellow arrowheads indicate mistargeting of UNC-2::GFP to dendrites. Scale bar, 10 μm.

(f-h) Distribution of GFP::RAB-3 in AVE interneurons of wild type (f), *unc-33(e204)* (g) and *unc-44(e362)* (h) animals, with corresponding diagrams. Yellow arrowheads indicate mistargeting of GFP::RAB-3 to dendrites, observed in 65% (*unc-33,* n=222*)* or 23% *(unc-44,* n=92*)* of animals. Scale bar, 10 μm.

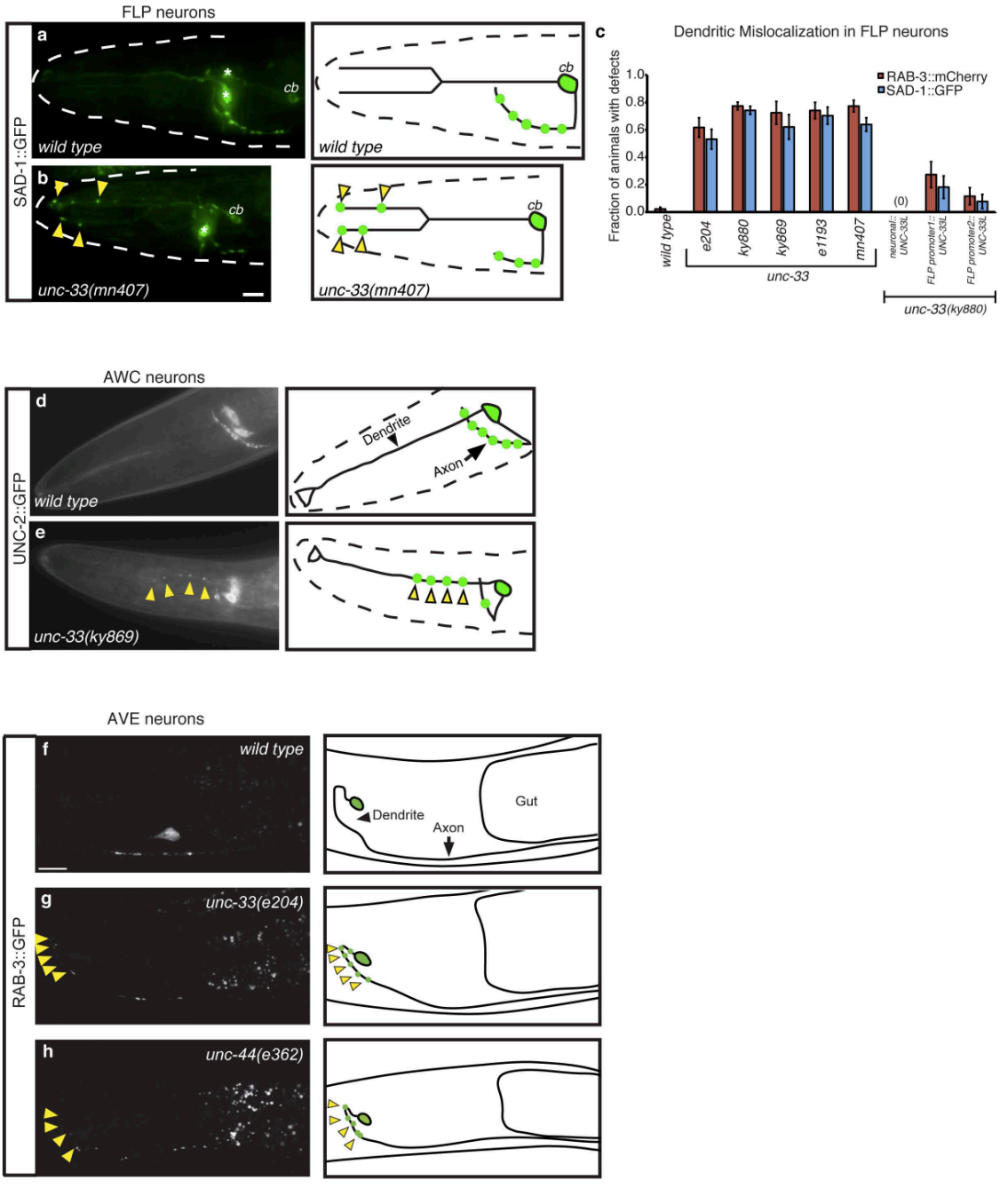

Supplementary Figure 2.2

Supplementary Figure 2.3. *unc-33* and *unc-34/Enabled* mutants have short FLP and PVD axons, but *unc-34* mutants do not mislocalize axonal markers

(a) Premature termination of FLP axons in wild type, *unc-33(ky880)* and *unc-34(e315)*.

(b-c) Representative maximum projection fluorescence images of *des-2*::myristoyl::GFP showing FLP axon in a wild type animal (b), and a prematurely terminated FLP axon in an *unc-34(e315)* mutant (c). 'cb' indicates the FLP cell body; white brackets indicate axons. Anterior is at left and dorsal is up in all panels.

(d) Dendritic mislocalization of RAB-3::mCherry and SAD-1::GFP in FLPs of wild type and *unc-34(e315)* animals. Compare *unc-33,* Supplementary Fig. 2.2c.

(e-f) Representative maximum projection fluorescence images showing SAD-1::GFP localization in a wild type FLP (e) and in a FLP with a prematurely terminated axon in an *unc-34 (e315)* animal (f). White arrowheads point to SAD-1::GFP axonal puncta. Asterisks denote AWC cell bodies labeled with an *odr-1::dsRed* marker. Scale bars, 10 μm.

(g) Quantification of animals with PVD axons shorter than the vulva spatial landmark.

(h-i) Axonal localization defects (H) and dendritic mislocalization defects (I) of RAB-3::mCherry and SAD-1::GFP in PVDs of wild type and *unc-34(e315)* animals (n>30 animals/genotype). Compare *unc-33,* Fig. 2.1k,l.

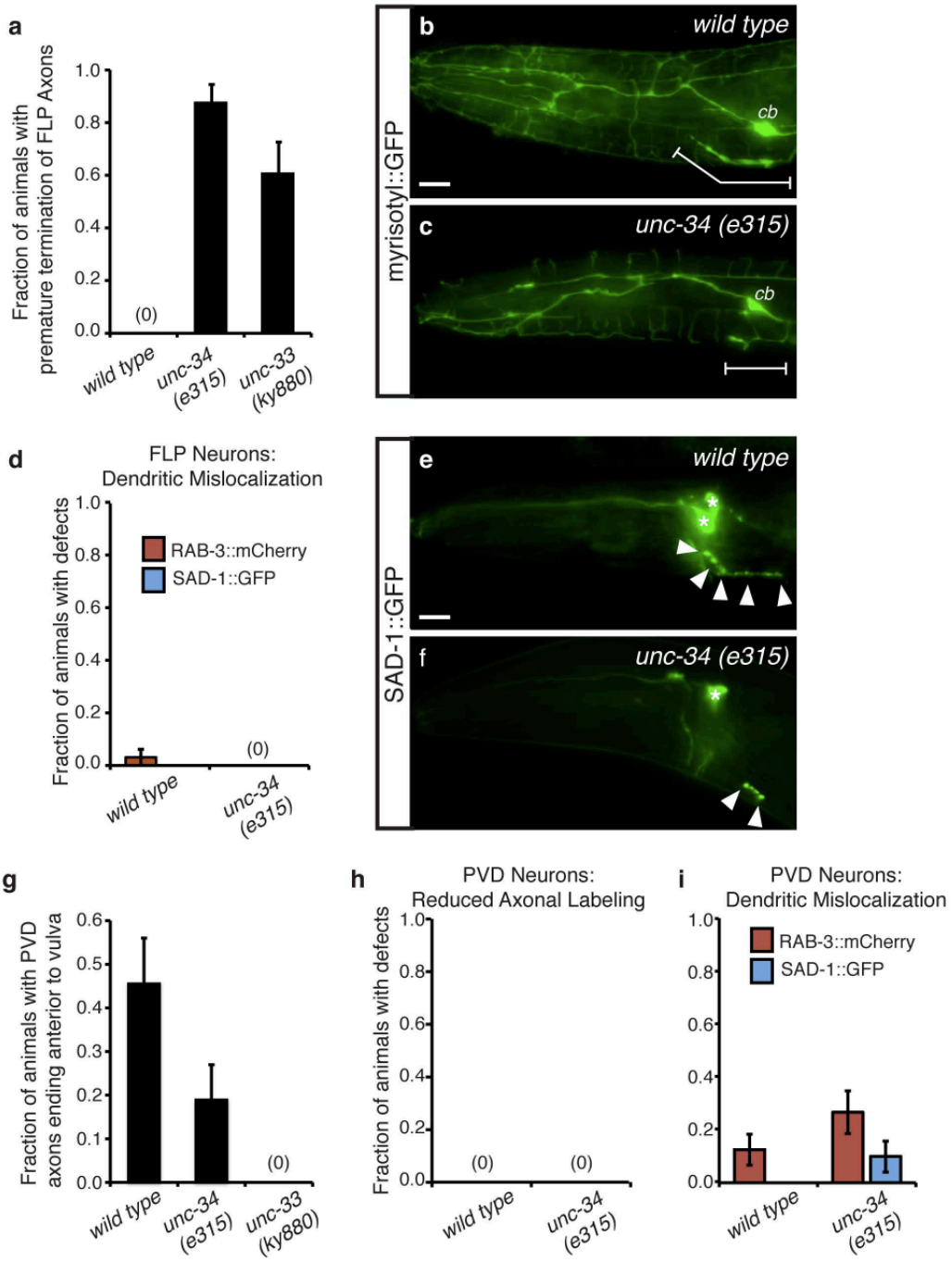

Supplementary Figure 2.3

33(e204) is a missense mutation that affects all isoforms, and two likely null alleles disrupting all isoforms are *unc-33(e1193*), a frameshift mutation, and *unc-33(mn407)*, a 500 base pair deletion (Tsuboi et al., 2005). Sequencing of the new alleles revealed that *unc-33(ky869)* generates a nonsense codon in the long and medium forms of *unc-33* (Fig. 2.1m), and *unc-33(ky880)* is a glutamate to lysine missense mutation affecting all isoforms in the region corresponding to the microtubule (MT)-stabilizing domain of CRMP-2 (E663 in UNC-33L) (Fukata et al., 2002) (Fig. 2.1n).

To establish the molecular requirements for appropriate axonal protein sorting, we asked which of the three UNC-33 isoforms was involved, and identified the site and time of *unc-33* action. Most known *unc-33* alleles affect all three predicted *unc-33* isoforms, any of which might be important for axonal protein localization. However, the strong mutant phenotype of *unc-33(ky869),* which should spare the short form of *unc-33* (Fig. 2.1k-m), suggested that the long or medium isoform was required for activity. To test these isoforms individually, full-length untagged cDNAs encoding either the UNC-33L protein or the UNC-33M protein were expressed from pan-neuronal promoters and introduced into *unc-33(mn407)* null mutants. UNC-33L, but not UNC-33M, fully rescued *unc-33* locomotion, egg-laying, and polarized localization of RAB-3::mCherry and SAD-1::GFP in PVD (Fig. 2.2a-b, Supplementary Fig. 2.1, and data not shown). The combined results from isoform-specific rescue and the *unc-33(ky869)* mutant allele suggest that UNC-33L is sufficient and probably essential for *unc-33* activity.

unc-33 reporters and UNC-33 proteins are expressed in many or all neurons, but generally not expressed in non-neuronal cells (Altun-Gultekin et al., 2001; Li et al., 1992; Tsuboi et al., 2005). An UNC-33L cDNA under a pan-neuronal promoter fully rescued the *unc-33* phenotype (Fig. 2.2a,b). More selective rescue was accomplished by expressing the UNC-33L cDNA from a *des-2* promoter fragment that is expressed only in PVD and FLP neurons. This transgene resulted in near-complete rescue of the axonal sorting defects in PVD and FLP, consistent with cell-autonomous action of *unc-33* (Fig. 2.2a,b; Supplementary Fig. 2.1, 2.2).

We identified the developmental stage at which *unc-33* acts by first characterizing wild-type PVD development, then restoring *unc-33* function at different times using a heat shock promoter from *hsp16-41*. The PVD neurons are born during the early L2 larval stage (Sulston and Horvitz, 1977), extend a primary axon and two primary dendrites during L2 and early L3 stages, and elaborate dendritic branches during the late L3 stage and L4 stages (Fig. 2.2c-e) (Oren-Suissa et al., 2010). Localized axonal expression of RAB-3::mCherry and SAD-1::GFP was first detectable in the late L3 stage (Supplementary Fig. 2.4). *hsp16-41::unc-33L* rescued adult *unc-33* defects after heat shock during L2 and L3 larval stages, but little rescue was observed after heat shock during the L1 stage, the L4 stage, or the young adult stage (Fig. 2.2f). These results suggest that *unc-33* acts in PVD neurons near the time when axon-dendrite polarity is established, and cannot restore polarized protein transport at later developmental times.

UNC-33L has previously been reported to be enriched in nerve ring axons (Tsuboi et al., 2005); a new polyclonal antibody generated against UNC-33L confirmed its axonal localization in nerve ring and ventral cord axons, and absence from amphid dendrites (Fig.

Figure 2.2. UNC-33L functions in PVD during the establishment of polarity

(a,b) Isoform-specific and cell autonomous rescue of axonal protein localization in PVDs of *unc-33* mutants. Quantification of axonal localization defects (a) and dendritic mislocalization defects (b) of RAB-3::mCherry and SAD-1::GFP were as in Fig. 2.1; n>25 animals per genotype.

(c-e) Developmental progression of PVD neurons, visualized with *des-2*::myrisotyl::GFP marker, with schematic diagrams at right. In c, two focal planes are shown for the late L2/early L3 stage animal to show the two neurites being elaborated. White arrowheads in (c) and (d) indicate the primary processes of PVD, 'cb' marks the PVD cell body, and asterisks mark gut autofluorescence. Anterior is at left and dorsal is up in all panels. Scale bar, 10 μm.

(f) Quantification of axonal protein localization in PVD after heat shock-driven UNC-33L expression in *unc-33(mn407)* mutant animals (n>25 animals/condition). A corresponding time line of PVD and larval development is shown below. Rescue was defined as correct localization of RAB-3::mCherry in adult PVD neurons.

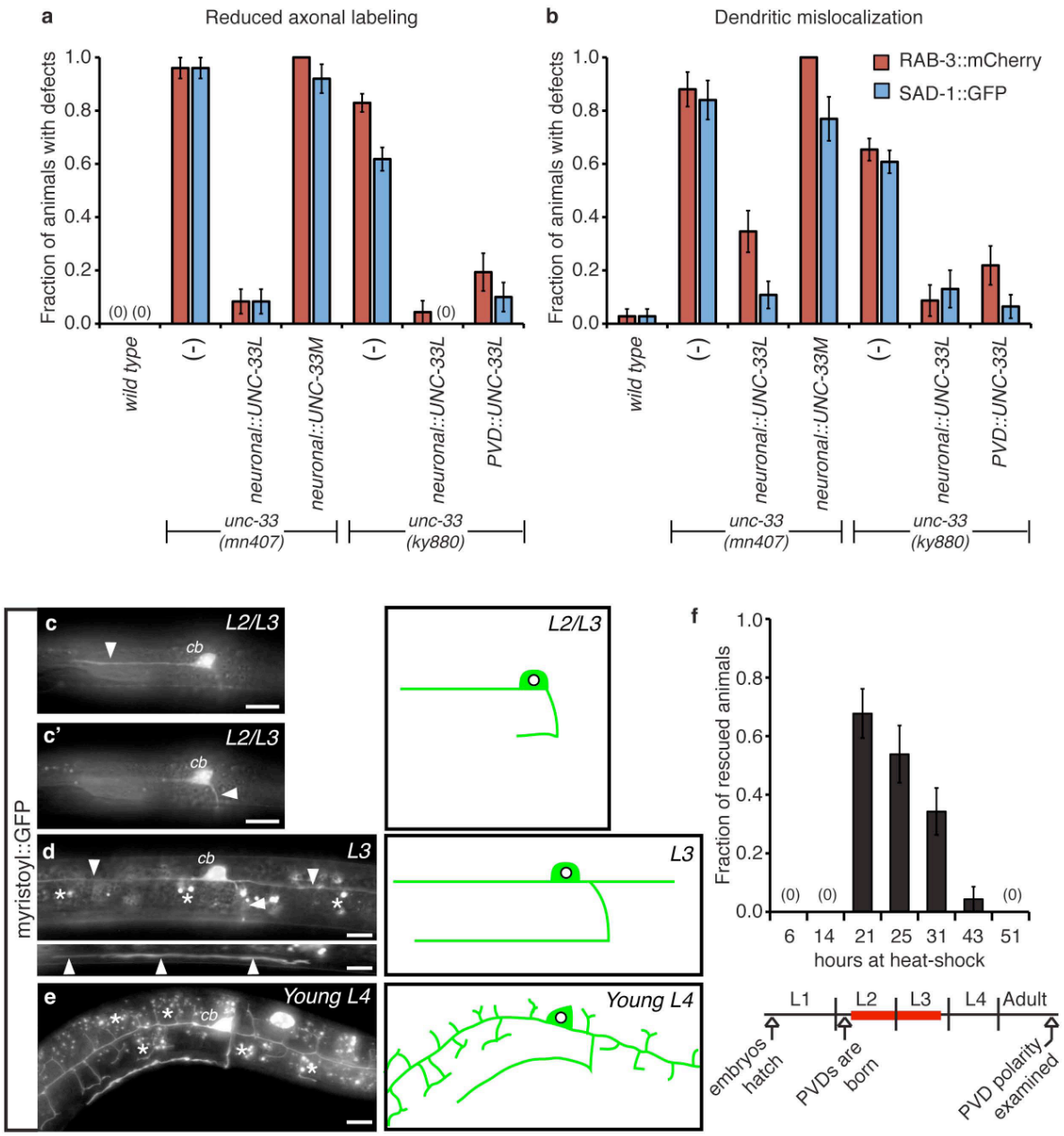
a
Reduced axonal labeling
Fraction of animals with defects
1.0
0.8
0.6
0.4
0.2
0.0
(0) (0)
(0)
wild type
(-)
neuronal::UNC-33L
neuronal::UNC-33M
(-)
neuronal::UNC-33L
PVD::UNC-33L
unc-33 (mn407)
unc-33 (ky880)
b
Dendritic mislocalization
RAB-3::mCherry
SAD-1::GFP
myristoyl::GFP
c
L2/L3
cb
c'
L2/L3
d
L3
e
Young L4
f
Fraction of rescued animals
(0)
(0)
(0)
6
14
21
25
31
43
51
hours at heat-shock
L1
L2
L3
L4
Adult
embryos hatch
PVDs are born
PVD polarity examined

Figure 2.2

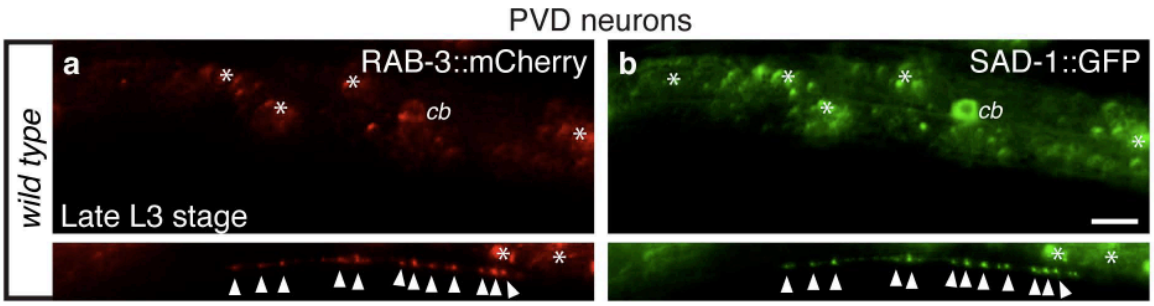

Supplementary Figure 2.4

Supplementary Figure 2.4. Polarized localization of presynaptic proteins RAB-3::mCherry and SAD-1::GFP can be detected in PVD neurons in late L3 larval stage (a-b) Representative images demonstrating the distribution of RAB-3::mCherry (a) and SAD-1::GFP (b) in PVD neurons of late L3 stage wild-type animals. For each set of fluorescence micrographs, the top panel is the maximum intensity projection of dendritic focal planes and the bottom panel is the maximum intensity projection for axonal focal planes. White arrowheads indicate axonal puncta, 'cb' marks the PVD cell body, and asterisks mark gut autofluorescence. Anterior is at left and dorsal is up in all panels. Scale bar, 10 μm.

2.3a). After testing several fusion proteins, we generated an internally-tagged UNC-33L::GFP protein that rescued locomotion and RAB-3::mCherry axonal localization defects of *unc-33* mutants. UNC-33L::GFP expressed under a pan-neuronal promoter was enriched in axons compared to dendrites, a pattern that resembled endogenous UNC-33L immunoreactivity (Fig. 2.3b). UNC-33L::GFP expressed under the *des-2* promoter labeled PVD axons consistently, but was minimally expressed in primary dendrite processes and was undetectable in dendrite branches (Fig. 2.3c). These results suggest a primary site of action in axons. Within the PVD axon, UNC-33L::GFP was enriched in a segment of the axon near, but not adjacent to, the PVD cell body, but the inactive UNC-33S::GFP isoform was not (Fig. 2.3c-e). Enrichment of UNC-33L::GFP in analogous axonal segments near the cell body was also observed in FLP and AWC neurons (data not shown).

UNC-104/KIF1A kinesin traffics axonal proteins to dendrites in *unc-33* mutants

The appearance of axonal proteins in dendrites in *unc-33* mutants could result either from a passive randomization of protein localization through diffusion, or from active defects in polarized protein traffic. To distinguish between these mechanisms, we combined *unc-33* mutations with mutations in *unc-104*/KIF1A, a conserved Kinesin-3 family member that mediates the axonal transport of presynaptic vesicles and a variety of presynaptic proteins (Hall and Hedgecock, 1991; Pack-Chung et al., 2007; Yonekawa et al., 1998). In *unc-104* mutants, axonal proteins are trapped in the cell body, but dendritic proteins are localized normally (Dwyer et al., 2001; Hirokawa and Takemura, 2005).

Figure 2.3. UNC-33L is enriched in PVD axons

(a) UNC-33L immunoreactivity in nerve ring of wild-type animal.

(b) Biologically active UNC-33L::GFP protein expressed from a pan-neuronal promoter in wild type animal, showing localization in nerve ring axons and absence from sensory dendrites. nr, nerve ring.

(c-d) Representative images of UNC-33L::GFP and UNC-33S::GFP proteins in wild type PVD neurons, with schematic diagrams at right. Red brackets indicate region of UNC-33L enrichment in axon, and arrowheads show expression in ventral nerve cord. Black brackets indicate proximal segment of PVD axon used for comparing fluorescence intensities in (e).

(e) Quantification of GFP (n=9), UNC-33L::GFP (n=11) and UNC-33S::GFP (n=10) fluorescence intensities, expressed as ratio of 'axon initial' domain to 'axon proximal' domain. *** $p < 0.001$ according to the Bonferroni t-test, ns, not significant. Anterior is at left and dorsal is up in all panels. Scale bars, 10 μm.

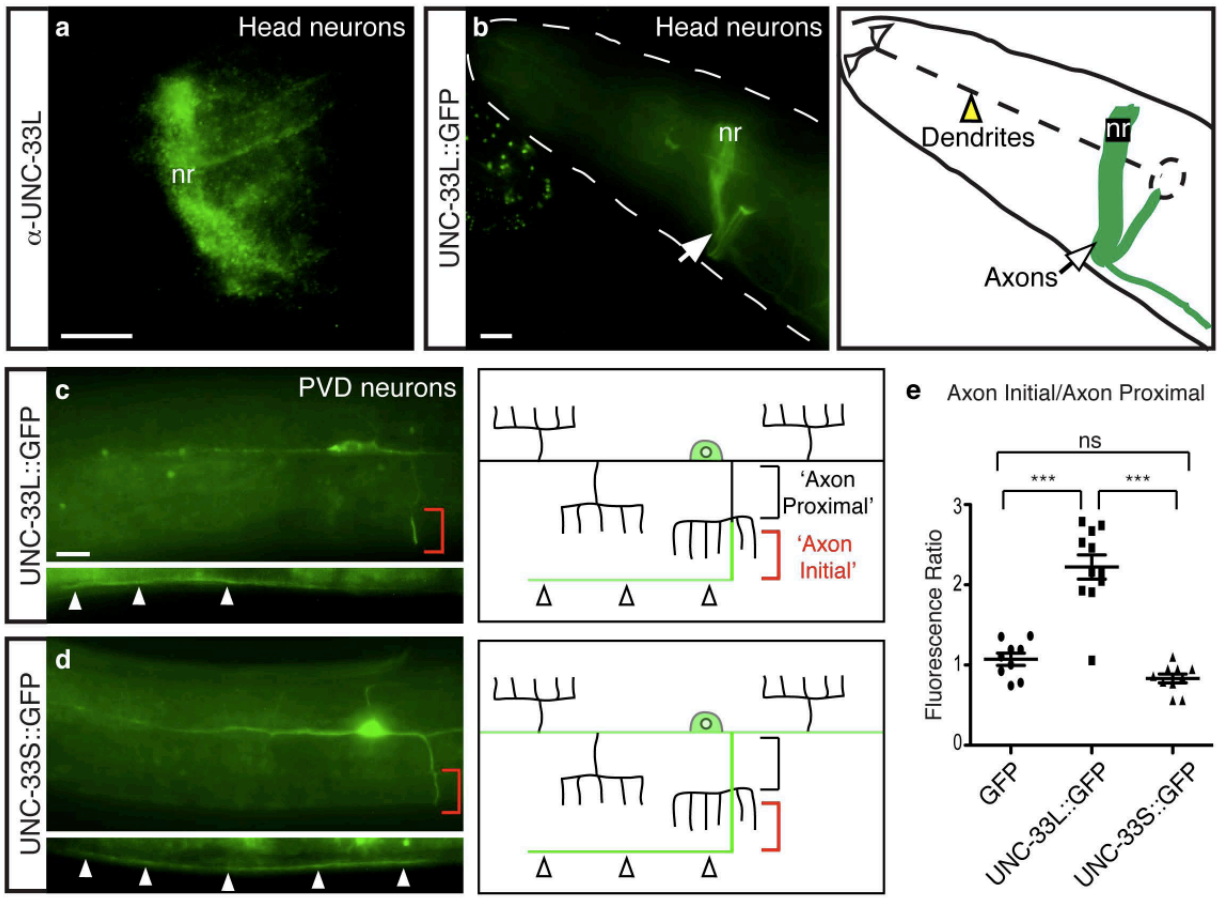
a
Head neurons
α-UNC-33L
nr
b
Head neurons
UNC-33L::GFP
nr
Dendrites
nr
Axons
c
PVD neurons
UNC-33L::GFP
'Axon Proximal'
'Axon Initial'
d
UNC-33S::GFP
e
Axon Initial/Axon Proximal
ns
***
***
Fluorescence Ratio
0
1
2
3
GFP
UNC-33L::GFP
UNC-33S::GFP

Figure 2.3

As expected from previous studies, RAB-3::mCherry and SAD-1::GFP markers were restricted to the PVD cell bodies in *unc-104* mutants (Fig. 2.4a-h), a pattern distinct from wild-type and *unc-33* patterns (Fig. 2.4i-l). An *unc-33 unc-104* double mutant resembled *unc-104*, with RAB-3::mCherry and SAD-1::GFP entirely restricted to the PVD cell body (Fig. 2.4m-p). Therefore, both the residual axonal localization and the inappropriate dendrite localization of synaptic proteins in *unc-33* mutants require UNC-104, suggesting that the axonal UNC-104 kinesin gains access to the dendrite in *unc-33* mutants.

To test this hypothesis, a monoclonal antibody that recognizes endogenous UNC-104 protein was used to examine its subcellular localization. In wild-type animals, UNC-104 immunoreactivity was strong in regions enriched in axonal processes, such as the nerve ring, the amphid commissure, and the ventral nerve cord, but staining was not observed in the amphid dendrite bundles (Fig. 2.5a). Similarly, the axon-rich regions in and near the ventral nerve cord were labeled in the tail, but sensory dendrites were not (Supplementary Fig. 2.5). These results suggest that endogenous UNC-104 protein is preferentially localized to axons.

By contrast, *unc-33* mutants had substantial UNC-104 immunoreactivity in the amphid dendrites and the tail dendrites, in addition to the expected UNC-104 immunoreactivity in nerve ring and ventral cord axons (Fig. 2.5b, Supplementary Fig. 2.5). To confirm this observation at the single-neuron level, a functional UNC-104::GFP fusion protein (Zhou et al., 2001) was expressed at low levels in PVD and FLP neurons using the *des-2* promoter. In agreement with the axonal localization observed via immunostaining,

Figure 2.4. *unc-104/KIF1A* kinesin mislocalizes presynaptic proteins to dendrites in *unc-33* mutants

(a-p) Representative images of RAB-3::mCherry and SAD-1::GFP in PVD neurons of wild type (a-d), *unc-104(e1265)* (e-h)*, unc-33(ky880)* (i-l), and *unc-104 unc-33* (m-p) animals, with corresponding diagrams. For each set of fluorescence micrographs, the top panel is the maximum intensity projection of dendritic focal planes and the bottom panel is the maximum intensity projection for axonal focal planes. White and yellow arrowheads indicate axonal and dendritic puncta, respectively; 'cb' marks the PVD cell body, and asterisks mark gut autofluorescence. Anterior is at left and dorsal is up in all panels. Scale bar, 10 μm.

(q,r) Quantification of axonal localization defects (q) and dendritic mislocalization defects (r) of RAB-3::mCherry and SAD-1::GFP, as in Fig. 2.1; n>30 animals/genotype.

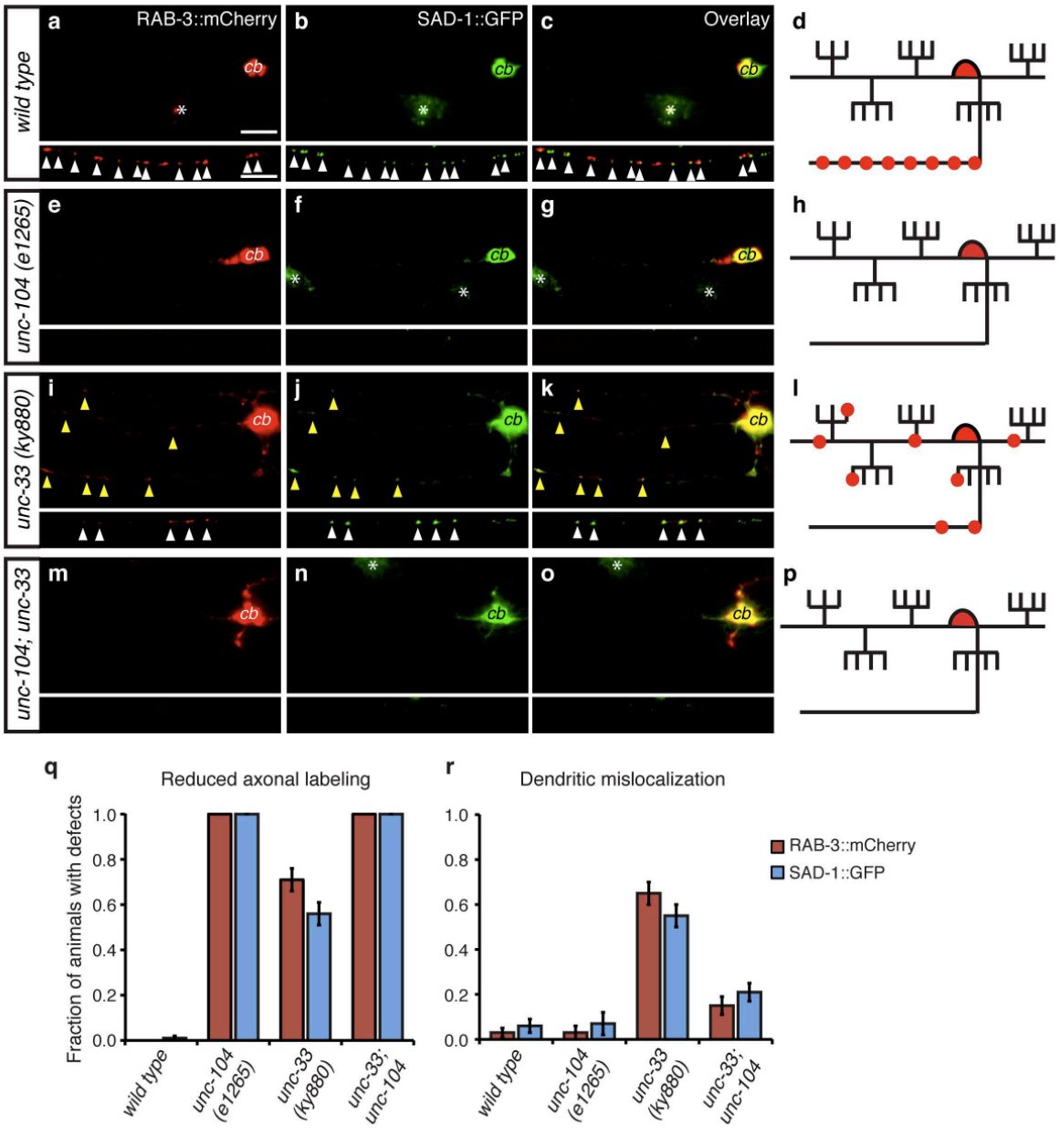
wild type
unc-104 (e1265)
unc-33 (ky880)
unc-104; unc-33
a
RAB-3::mCherry
b
SAD-1::GFP
c
Overlay
d
e
f
g
h
i
j
k
l
m
n
o
p
cb
q
Reduced axonal labeling
Fraction of animals with defects
1.0
0.8
0.6
0.4
0.2
0.0
wild type
unc-104 (e1265)
unc-33 (ky880)
unc-33; unc-104
r
Dendritic mislocalization
RAB-3::mCherry
SAD-1::GFP

Figure 2.4

Figure 2.5. UNC-104 is mislocalized to dendrites in *unc-33* mutants

(a,b) Immunostaining of endogenous UNC-104 in wild-type (a) and *unc-33(mn407)* (b) animals, with corresponding schematic diagrams. Yellow arrowheads indicate UNC-104 immunoreactivity in sensory dendrite regions. nr, nerve ring; vnc, ventral nerve cord.

(c,d) Localization of UNC-104::GFP in PVD neurons of wild-type (c) and *unc-33 (mn407)* (d) animals, with schematic diagrams. White arrowheads indicate UNC-104::GFP enrichment in PVD axons; yellow arrowheads indicate UNC-104::GFP in PVD dendrites.

(e) Quantification of animals with detectable UNC-104::GFP fluorescence in PVD dendrites (n>25 animals/genotype).

(f,g) Inferred UNC-104/KIF1A activity in neurons of wild-type animals (f) and *unc-33* mutants (g). Anterior is at left and dorsal is up in all panels. Scale bars, 10 μm.

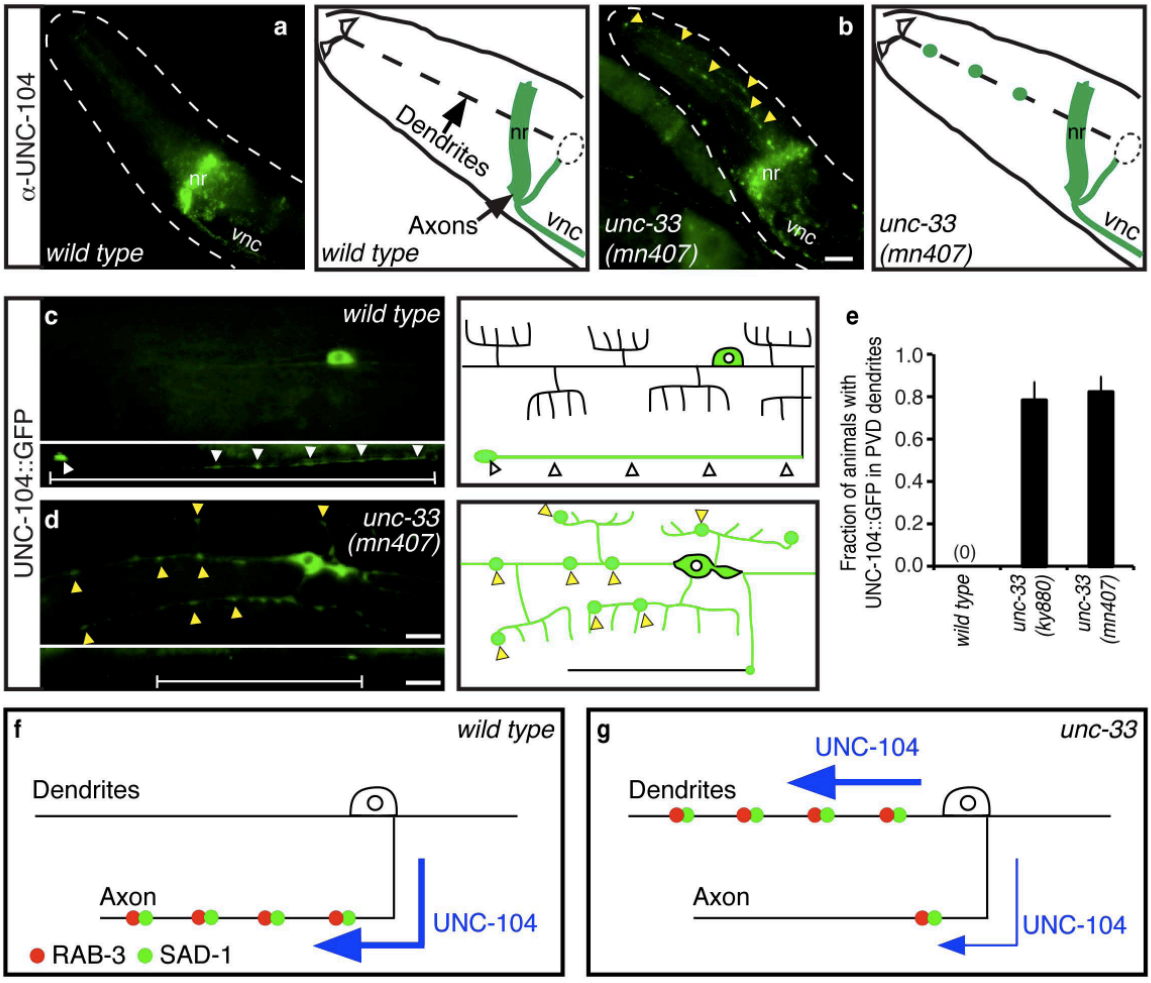
α-UNC-104
a
nr
vnc
wild type
Dendrites
Axons
nr
vnc
wild type
b
nr
vnc
unc-33
(mn407)
nr
vnc
unc-33
(mn407)
UNC-104::GFP
c
wild type
d
unc-33
(mn407)
e
Fraction of animals with
UNC-104::GFP in PVD dendrites
1.0
0.8
0.6
0.4
0.2
0.0
(0)
wild type
unc-33
(ky880)
unc-33
(mn407)
f
wild type
Dendrites
Axon
UNC-104
RAB-3
SAD-1
g
unc-33
UNC-104
Dendrites
Axon
UNC-104

Figure 2.5

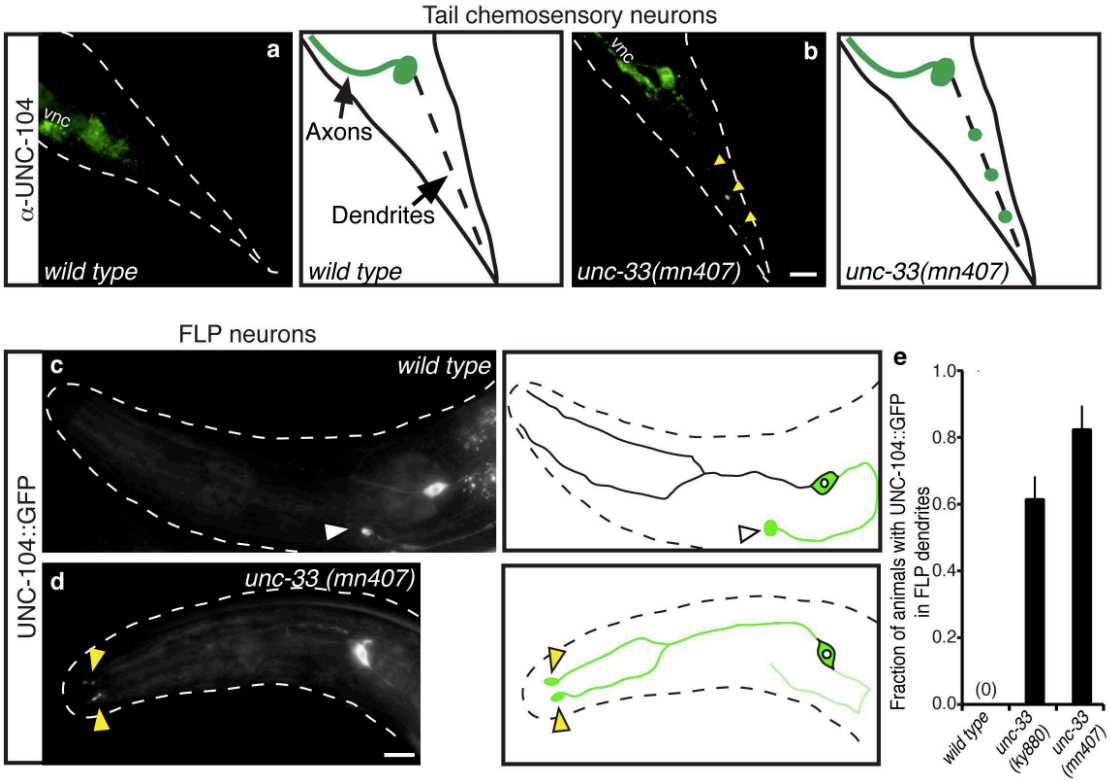

Supplementary Figure 2.5. Kinesin UNC-104 mislocalization to dendrites in multiple neurons in *unc-33* mutants

(a-b) Immunostaining against UNC-104 in the tail regions of wild type (a) and *unc-33(mn407)* animals, with corresponding schematic diagrams. Yellow arrowheads point to UNC-104 immunoreactivity in tail dendrite regions. vnc, ventral nerve cord.

(c-d) Localization of UNC-104::GFP in FLP neurons of wild type (c) and *unc-33(mn407)* (d) animals, with schematic diagrams. White arrowheads indicate UNC-104::GFP enrichment in FLP axons; yellow arrowheads indicate UNC-104::GFP mislocalized to FLP dendrite endings.

(e) Quantification of animals with detectable UNC-104::GFP fluorescence in FLP dendrites (n>25 animals/genotype). Scale bars, 10 μm.

UNC-104::GFP was present in wild-type PVD and FLP axons and cell bodies, weak in primary dendrites, and absent from dendrite branches (Fig. 2.5c, Supplementary Fig. 2.5c). In *unc-33* mutants, however, UNC-104::GFP fluorescence was reduced in axons and increased in dendrites and dendrite branches (Fig. 2.5d,e). The combined genetic and cell biological results suggest that the mislocalization of axonal proteins in *unc-33* mutants results from a failure to restrict UNC-104 kinesin to axons (Fig. 2.5f,g).

The cilia chemoreceptor ODR-10 is mislocalized to axons in *unc-33* mutants

To ask whether *unc-33* affected sorting of dendritic proteins as well as axonal proteins, we examined the well-characterized AWB chemosensory neurons. Each AWB has one dendrite that terminates in a sensory cilium at the tip of the nose, and one axon that grows into the nerve ring (Fig. 2.6a). ODR-10::GFP, a chemosensory G protein-coupled receptor, is enriched in AWB cilia and excluded from axons of wild-type animals (Dwyer et al., 1998; Sengupta et al., 1996)(Fig. 2.6b). In *unc-33* mutants, however, ODR-10::GFP was present in AWB axons as well as AWB cilia (Fig. 2.6c).

The defect in ODR-10::GFP localization in *unc-33* mutants was not as severe as the defect in axon protein localization, but it was consistently observed in multiple *unc-33* alleles at both early and late larval stages (Fig. 2.6f). The ODR-10::GFP defect appeared genetically distinct from the sorting defect affecting presynaptic proteins, based on double mutant interactions with *unc-104*. *unc-104* axonal kinesin mutants do not normally affect ODR-10::GFP localization (Fig. 2.6d,g)(Dwyer et al., 2001), and *unc-33; unc-104* double

Figure 2.6. A sensory chemoreceptor is mislocalized to axons in *unc-33* mutants

(a) Schematic diagram of AWB chemosensory neurons in the head.

(b-e) Representative maximum projection fluorescence images showing ODR-10::GFP localization in AWB neurons of wild type (b), *unc-33* (c)*, unc-104* (d)*, and unc-104; unc-33* double mutant (e) animals. Yellow arrowheads indicate ODR-10::GFP in axons. Anterior is at left and dorsal is up in all images. Scale bar, 10 μm. (f,g) Quantification of animals with ODR-10::GFP fluorescence in axons (n>40 animals per genotype).

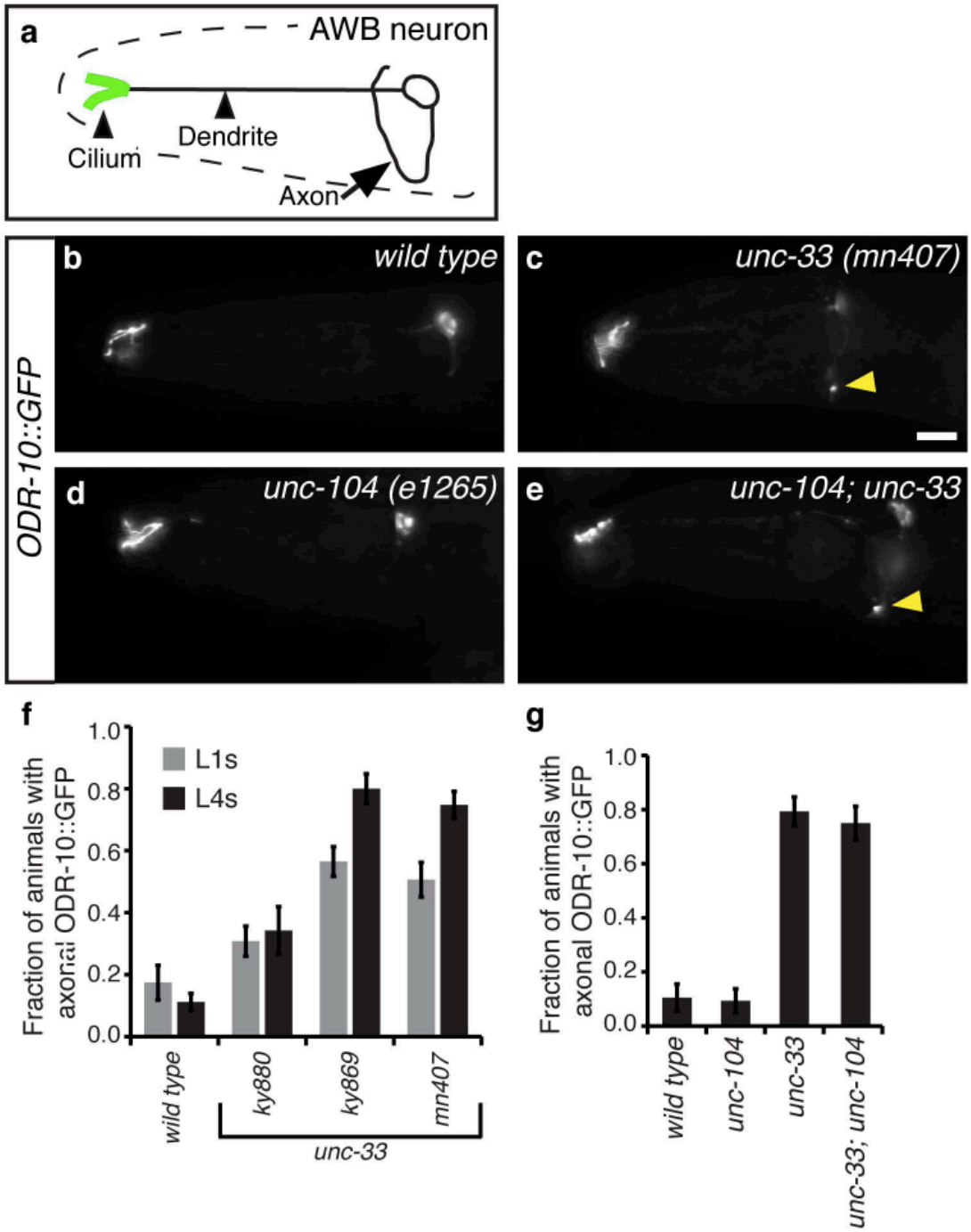
a
AWB neuron
Cilium
Dendrite
Axon
ODR-10::GFP
b
wild type
c
unc-33 (mn407)
d
unc-104 (e1265)
e
unc-104; unc-33
f
Fraction of animals with axonal ODR-10::GFP
1.0
0.8
0.6
0.4
0.2
0.0
L1s
L4s
wild type
ky880
ky869
mn407
unc-33
g
Fraction of animals with axonal ODR-10::GFP
1.0
0.8
0.6
0.4
0.2
0.0
wild type
unc-104
unc-33
unc-33; unc-104

Figure 2.6

mutants resembled *unc-33* single mutants, with ODR-10::GFP in both axons and cilia (Fig. 2.6e,g). Thus ODR-10 mislocalization in *unc-33* mutants was not caused by dysregulated UNC-104. The altered localization of ODR-10::GFP did, however, require *odr-4,* a gene that is normally required for ODR-10 exit from the endoplasmic reticulum and localization to cilia (Dwyer et al., 1998)(Supplementary Fig. 2.6). *unc-101*, an AP1 μ1-adaptin subunit that restricts ODR-10::GFP to cilia (Dwyer et al., 2001), overshadowed the effect of *unc-33* in *unc-101; unc-33* double mutants (Supplementary Fig. 2.6). These results suggest that cilia proteins in *unc-33* mutants are mislocalized, but still interact with the normal cilia sorting machinery.

unc-33 organizes the neuronal microtubule cytoskeleton

The widespread defects in axons and dendrites prompted an examination of the cytoskeleton in *unc-33* mutants. *C. elegans* neurons are rich in microtubules, and a monoclonal antibody against α-tubulin (DM1A) preferentially labeled the *C. elegans* nervous system, revealing axonal processes in the nerve ring and ventral nerve cord, as well as amphid dendrites and cilia (Fig. 2.7a, Supplementary Fig. 2.7). This staining pattern was strikingly altered in *unc-33* mutants. First, tubulin immunoreactivity was enriched in the distal segments of dendrites, consistent with an increase in dendrite microtubules previously observed in electron micrographs of *unc-33* mutants (Hedgecock et al., 1985). Second, axonal anti-tubulin staining in the nerve ring was strongly reduced (Fig. 2.7b, Supplementary Fig. 2.7). These results suggest that the overall organization of neuronal microtubules is altered in *unc-33* mutants.

Supplementary Figure 2.6. *odr-4* and *unc-101* regulate the distribution of ODR-10::GFP in wild type and *unc-33* animals

(a-d) Representative maximum projection fluorescence images showing ODR-10::GFP localization in AWB neurons of *odr-4* (a)*, unc-101* (c)*, odr-4; unc-33* (b) and *unc-101; unc-33* (d) animals. Anterior is at left and dorsal is up in all images. Scale bar, 10 μm. Comparisons with Fig 2.5a-c show that the double mutants *odr-4; unc-33* and *unc-101; unc-33* resemble *odr-4* and *unc-101* single mutants, respectively.

(e) Quantification of animals with axonal ODR-10::GFP fluorescence, demonstrating that both the normal cilia localization as well as the axonal mislocalization of ODR-10::GFP in *unc-33* mutants are *odr-4*-dependent (n>30 animals per genotype). Since *odr-4* is required for the exit of ODR-10::GFP from the ER, the observation that axonal ODR-10::GFP in *unc-33* mutants also requires *odr-4* function implies that the axonal mislocalization is due to the misregulation of a post-ER step in trafficking.

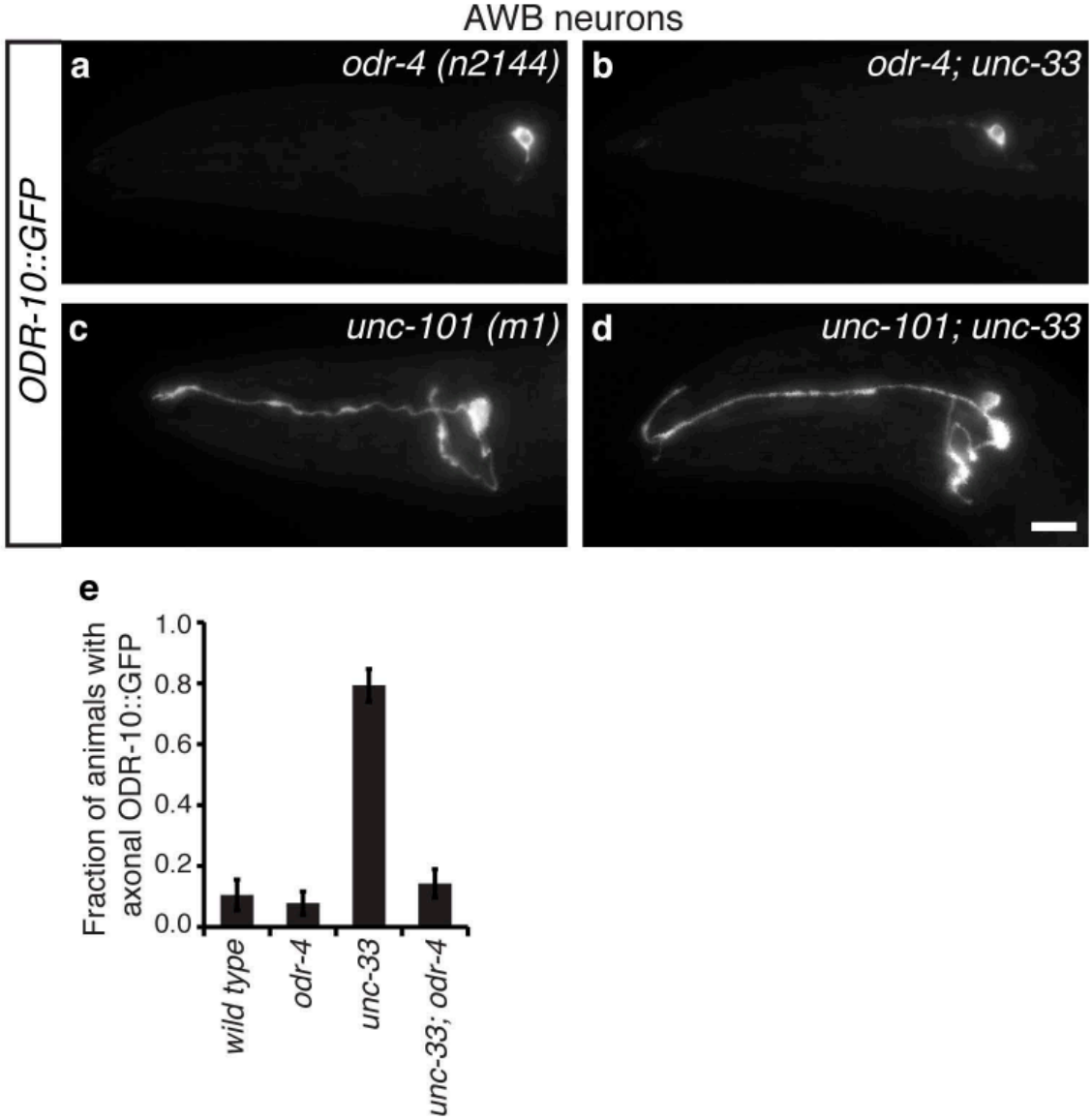

Supplementary Figure 2.6

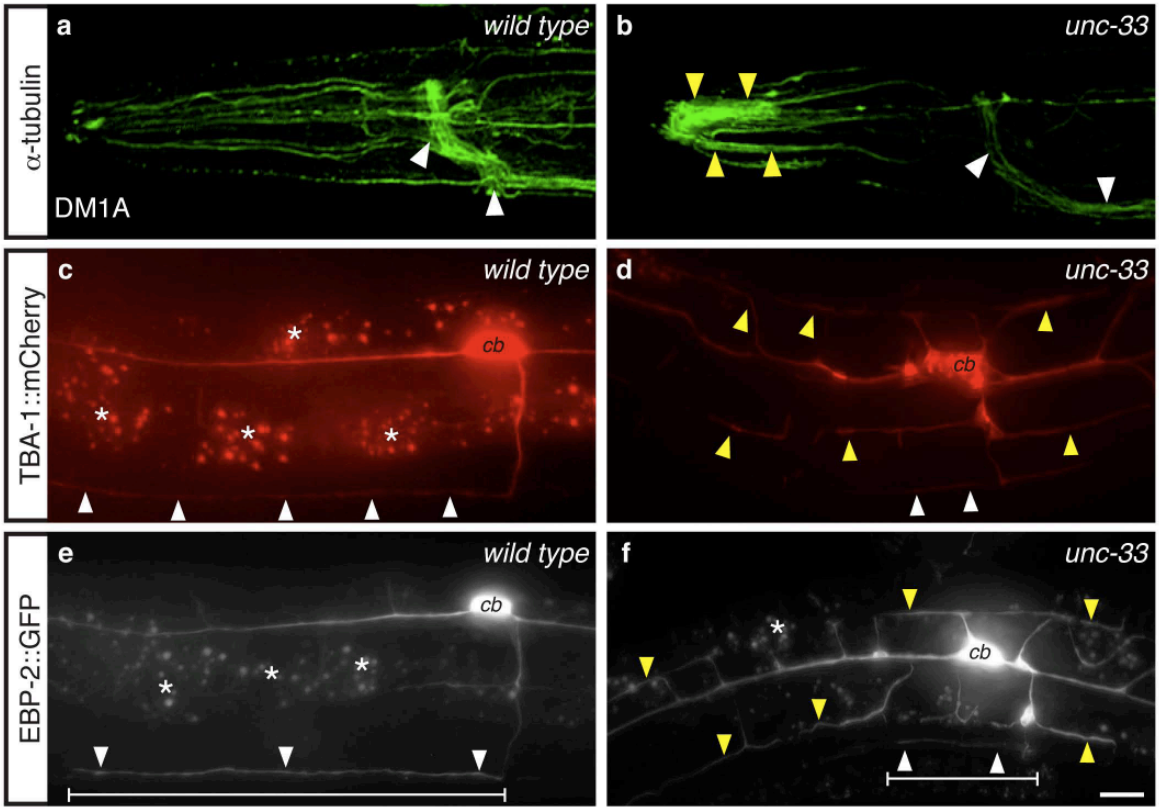

Figure 2.7. Neuronal microtubule defects in *unc-33* mutants

(a,b) Representative maximum intensity projections of confocal images of α-tubulin immunoreactivity in head neurons of wild type and *unc-33(ky880)* animals (*unc-33(mn407)* in Supplementary Fig. 2.7). White arrowheads indicate axon-rich nerve ring and ventral nerve cord regions, yellow arrowheads indicate distal sensory dendrites.

(c,d) TBA-1::mCherry (α-tubulin) fluorescence in PVD neurons of representative wild type (c) and *unc-33(mn407)* (d) animals.

(e,f) Distribution of EBP-2::GFP (EB1) in PVD neurons of representative wild-type (e) and *unc-33(ky880)* (f) animals. In (c-f), white arrowheads indicate fluorescence in PVD axons, yellow arrowheads indicate fluorescence in PVD dendrites; 'cb' denotes the PVD cell body, and asterisks indicate gut autofluorescence.

Supplementary Figure 2.7. Distribution of tubulin post-translational modifications in *unc-33* null mutants

(a,b) Maximum intensity projections of α-tubulin immunoreactivity in head neurons of wild-type and *unc-33(mn407)* animals. White arrowheads indicate axon-rich nerve ring and ventral nerve cord regions; yellow arrowheads indicate distal sensory dendrites. (c-d) Immunostaining of glutamylated tubulin detects neuronal cilia in wild type (a) and *unc-33* (b) animals.

(e-h) Immunostaining of acetylated α-tubulin (e-f) and detyrosinated α-tubulin (g-h) in the PLM mechanosensory neurons of wild type (e,g) and *unc-33(mn407)* (f,h) animals. Scale bars, 10 μm.

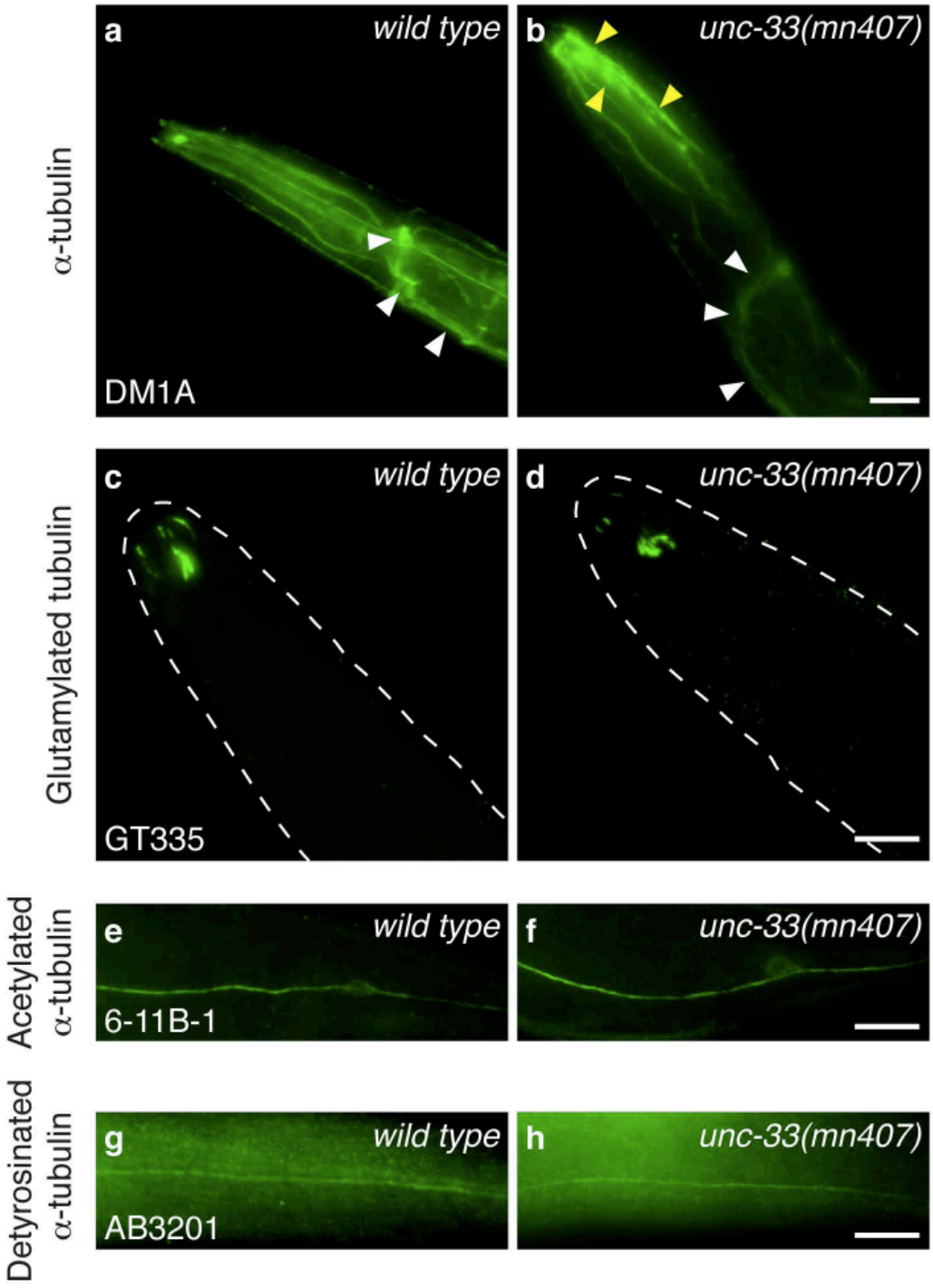

Supplementary Figure 2.7

Antibodies to different post-translationally modified forms of tubulin can serve as indirect probes of microtubule stability that label different pools of microtubules within a single cell. Staining of *unc-33* mutants with these antisera indicated that their abnormalities were restricted to certain microtubule populations. Microtubules in sensory cilia were labeled similarly in wild-type and *unc-33* animals with GT335, an anti-glutamylated tubulin antibody (Wolff et al., 1992), suggesting that this subset of microtubules was correctly localized in *unc-33* mutants (Supplementary Fig. 2.7c,d). Antibodies against acetylated α-tubulin and detyrosinated α-tubulin, two modifications associated with stable microtubules, shower similar strong staining of mechanosensory neurons of wild type (Siddiqui et al., 1989) and *unc-33* animals, again suggesting a normal localization of this microtubule subset (Supplementary Fig. 2.7e-h).

To examine tubulin distribution at the single cell level and bypass the fixation step associated with antibody staining, tagged reporters of microtubule structure were expressed in PVD neurons. In wild type animals, an mCherry-tagged α-tubulin protein was consistently detected in axons and primary dendrites of PVD neurons, but not in dendrite branches (Fig. 2.7c). In *unc-33* mutants, α-tubulin::mCherry fluorescence was significantly reduced in PVD axons, and brighter in dendrites and dendrite branches, matching the whole-animal results with anti-tubulin antibodies (Fig. 2.7d). A marker that should detect polymerized microtubules was generated by tagging the microtubule end-binding protein EBP-2 (EB1) (Srayko et al., 2005) with GFP. In wild-type animals, EBP-2::GFP labeled the soma, axon, and primary dendrites of PVD, but not dendritic branches; in *unc-33* mutants, EBP-2::GFP labeled dendritic branches as well, suggesting aberrant invasion of these structures by microtubules (Fig. 2.7e,f).

UNC-44/Ankyrin is required for UNC-33L axonal localization, neuronal microtubule organization and polarized protein trafficking

The *C. elegans unc-44* gene encodes its sole ankyrin homolog (Otsuka et al., 1995), and shares many functions with *unc-33*, including roles in axon growth and guidance (Hedgecock et al., 1985; Siddiqui and Culotti, 1991; Troemel et al., 1999). We identified *unc-44* mutants in several genetic screens for altered localization of axonal and dendritic proteins, suggesting that it might have functions related to those of *unc-33.* Indeed, examination of two *unc-44* alleles with the markers described above revealed a close correspondence between the defects in *unc-44* and *unc-33* mutants. *unc-44* mutants had reduced SAD-1::GFP and RAB-3::mCherry expression in PVD axons, and significant expression in dendrites (Fig. 2.8a,b). Similarly, UNC-104 kinesin was present in dendrites as well as axons of *unc-44* mutants, anti-tubulin immunoreactivity was reduced in axons and increased in dendrites, and the cilia protein ODR-10::GFP was partly localized to axons in AWB neurons (Fig. 2.8c-e). *unc-44* encodes at least ten proteins, of which two isoforms of >5000 amino acids are implicated in neuronal function (Otsuka et al., 1995); the mutants we examined are typical, but it is not known whether they are null alleles that affect all isoforms. Therefore, these experiments suggest common functions for *unc-44* and *unc-33,* but may not detect all functions of *unc-44*.

The suggestion that *unc-44* and *unc-33* have related functions was supported by an examination of UNC-33L protein: in *unc-44* PVD neurons, UNC-33L::GFP was depleted from axons, and instead accumulated in neuronal cell bodies and dendrite branches (Fig. 2.8f-h). Immunostaining of endogenous UNC-33L confirmed that immunoreactivity was

Figure 2.8. *unc-44/ankyrin* mutants disrupt axonal protein sorting and UNC-33L localization

(a,b) Quantification of *unc-44* axonal localization defects (a) and dendritic mislocalization defects (b) of RAB-3::mCherry and SAD-1::GFP in PVD neurons, as in Fig. 2.1; n>25 animals/genotype.
(c) Immunostaining of endogenous UNC-104 in *unc-44(ky110)* animal; yellow arrowheads indicate UNC-104 immunoreactivity in sensory dendrite regions. nr, nerve ring; vnc, ventral nerve cord. Compare Fig. 2.5a,b.
(d) Representative maximum projection fluorescence image showing ODR-10::GFP localization in AWB neurons of *unc-44(ky110)* animal. Yellow arrowhead indicates ODR-10::GFP in axons. Compare Fig. 2.6b,c.
(e) α-tubulin immunoreactivity in the head region of an *unc-44 (ky110)* animal. White arrowheads indicate axon-rich nerve ring and ventral nerve cord regions; yellow arrowheads indicate distal sensory dendrites. Compare Fig. 2.7a,b.
(f,g) UNC-33L::GFP protein in PVD neurons of wild-type (f) and *unc-44(ky110)* (g) animals, with corresponding schematic diagrams at right. Red brackets indicate region of UNC-33L enrichment in proximal axon, white arrowheads indicate axonal UNC-33L::GFP, and yellow arrowheads indicate UNC-33L::GFP foci in dendrites and dendrite branches. Asterisks indicate gut autofluorescence.
(h) Quantification of animals with detectable UNC-33L::GFP expression in PVD axons and dendrite branches (n>25 animals/genotype).
(i-k) Endogenous UNC-33L immunoreactivity in wild-type (i), *unc-33(ky880)* (j) and *unc-44(ky110)* (k) animals. Nerve ring (nr, top panels) and ventral nerve cord (vnc, bottom panels) are shown. Arrowheads indicate UNC-33L retained in neuronal cell bodies in *unc-44* mutants. Anterior is at left and dorsal is up in all panels. Scale bars, 10 μm.

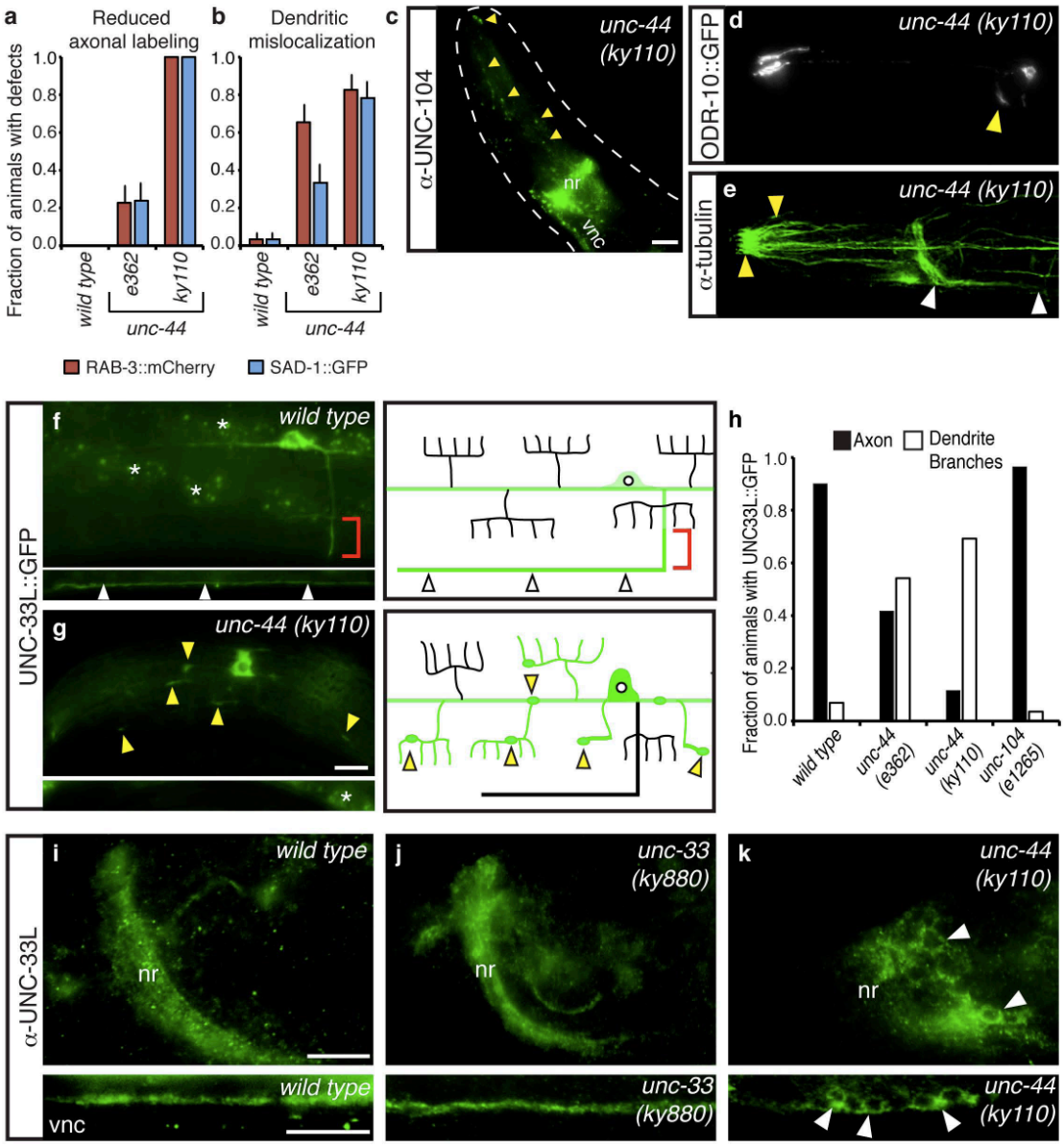
a
Reduced axonal labeling
Fraction of animals with defects
1.0
0.8
0.6
0.4
0.2
0.0
wild type
e362
ky110
unc-44
b
Dendritic mislocalization
c
α-UNC-104
unc-44 (ky110)
nr
vnc
d
ODR-10::GFP
unc-44 (ky110)
e
α-tubulin
unc-44 (ky110)
RAB-3::mCherry
SAD-1::GFP
UNC-33L::GFP
f
wild type
g
unc-44 (ky110)
h
Axon
Dendrite Branches
Fraction of animals with UNC33L::GFP
wild type
unc-44 (e362)
unc-44 (ky110)
unc-104 (e1265)
α-UNC-33L
i
wild type
nr
vnc
j
unc-33 (ky880)
k
unc-44 (ky110)

Figure 2.8

lost from the nerve ring and nerve cords, and enriched in cell bodies, throughout the nervous system of *unc-44* mutants (Fig. 2.8i,k). These results indicate that *unc-44* has an important role in UNC-33 axonal recruitment, and provide a molecular basis for the protein sorting defects of *unc-44* mutants.

UNC-33L localization was normal in *unc-33(ky880)* mutants, which have a mutation in the predicted tubulin-binding domain (Fig. 2.8j). Notably, this mutant UNC-33L protein is correctly localized to axons although tubulin, UNC-104, and synaptic proteins are mislocalized in *unc-33(ky880)* mutants. UNC-33L axonal localization was also normal in *unc-104(e1265)* kinesin mutants (Fig. 2.8h). These results indicate that the microtubule-binding function of UNC-33L is important for its activity, and reveal a hierarchy in polarized protein traffic in which UNC-33L localization is preserved even when other axonal and dendritic proteins are misdirected by altered microtubules and UNC-104.

Discussion

unc-33/CRMP and *unc-44*/ankyrin are essential for polarized neuronal sorting to both axons and dendrites in *C. elegans*. In *unc-33* and *unc-44* mutants, axonal transmembrane proteins (UNC-2), cytoplasmic proteins (SAD-1, SYD-2, SNN-1), and synaptic vesicle proteins (RAB-3, SNB-1) are randomized between axons and dendrites, and some dendritic proteins are altered as well. By examining the localization of multiple proteins in wild-type and mutant backgrounds, we found that UNC-44 localizes UNC-33 to the axon, where UNC-33 increases the steady-state level of axonal microtubules and alters

their organization, providing an asymmetric influence on the neuronal cytoskeleton. A requirement for UNC-33 at early developmental times suggests that this asymmetry establishes the lasting axon-dendrite polarity of the cell. Either UNC-33 itself or the *unc-33*-dependent asymmetric organization of microtubules directs the polarized recruitment of the kinesin UNC-104/KIF1A, which recruits and delivers axonal cargo proteins. A loss of this polarized information in *unc-33* and *unc-44* mutants leads to a large-scale disruption of protein sorting, microtubule distribution, and kinesin activity in both axons and dendrites.

Although *unc-33, unc-44* and their vertebrate homologs have been implicated in axon specification and elongation, most functions of *unc-33* and *unc-44* were not predicted by previous studies (Desai et al., 1988; Hedgecock et al., 1985; Tsuboi et al., 2005). CRMP2, the best-characterized CRMP protein, affects the number of axons per cell (the classical definition of "neuronal polarity" *in vitro*), and CRMP2 manipulations appear not to affect dendrites. We did not observe a reduction in axon number in *unc-33* mutants, nor were axons converted into dendrites by morphological criteria. Instead, we found that axons and dendrites were morphologically recognizable, but profoundly defective in their cytoskeletal organization and protein localization. A likely explanation for this apparent discrepancy is the complexity of the mammalian CRMP family, which consists of several paralogous genes with multiple splice forms (Quinn et al., 2003); as a result, complete disruption of CRMP function has not been attempted in mammalian neurons.

Similarly, most of the properties of *unc-44* mutants were unexpected. Mammalian ankyrinG prevents the entry of dendritic proteins into axons (Hedstrom et al., 2008; Sobotzik et al., 2009; Winckler et al., 1999), a function that it shares with *unc-44,* and we found that *unc-44* also excludes axonal proteins from dendrites, generating a bidirectional

barrier. More significantly, the widespread microtubule defects in *unc-44* mutants indicate that UNC-44 organizes the microtubule cytoskeleton in axons and dendrites, a function not previously ascribed to ankyrin. This function is likely to arise from the ability of *unc-44* to localize UNC-33L to axons, especially because of the striking phenotypic similarities between *unc-33* and *unc-44* mutants.

The effects of UNC-33 on asymmetric protein transport, UNC-104 localization, and tubulin immunoreactivity, along with its early action and its localization to the axon, suggest that UNC-33 functions primarily to organize unique classes of axonal microtubules. CRMP2 stimulates microtubule polymerization *in vitro* and promotes axonal transport of tubulin (Fukata et al., 2002; Kimura et al., 2005), functions that could contribute to the axonal microtubule defects in *unc-33* mutants. Indirect measurements of microtubule polarity suggests that microtubules in *C. elegans* axons, like those in mammalian neurons, may be oriented with distal plus-ends, whereas dendritic microtubules are less polarized (Ou et al., 2010). The developmental requirement for *unc-33* in PVD suggests that polarized properties arise during a discrete time period, which could be characterized to provide insight into the construction of cytoskeletal asymmetry.

The UNC-33L-enriched zone of *C. elegans* axons bears analogies with the vertebrate axon initial segment, which organizes the microtubule cytoskeleton and divides neurons into functional compartments. In most vertebrate neurons, the axon initial segment is a clearly demarcated diffusion boundary and the site of action potential initiation (Grubb and Burrone, 2010). In invertebrate neurons, the nature of the axon initial segment is less clear: a single process can split into axonal and dendritic regions far from the cell body, and spike zones can be distant from the soma (Bucher et al., 2003;

Meyrand et al., 1992; Rolls et al., 2007). *C. elegans* does not have classical sodium-based action potentials, so its neurons are not predicted to have spike initiating zones, but they do have distinct axonal and dendritic regions. *unc-44* represents a molecular connection to ankyrinG at the axon initial segment, and the region of UNC-33L enrichment represents a plausible subcellular site for the axon-dendrite boundary in several *C. elegans* neurons. Moreover, the vertebrate axon initial segment is enriched in unusual microtubule fascicles that are absent from other neuronal compartments (Palay et al., 1968), an observation that may relate to the microtubule-stabilizing functions of UNC-33 and CRMP2.

Although UNC-33L protein is largely excluded from dendrites, *unc-33* mutant dendrites accumulate axonal proteins and excessive microtubules (Hedgecock et al., 1985) and lose some dendritic proteins. Thus *unc-33* establishes a distinction between axons and dendrites that is essential for the molecular integrity of both compartments, either through self-organizing features of the cytoskeleton or through cascades of inappropriate protein sorting. Our results suggest that UNC-33L protects dendrites from axonal proteins by capturing the axonal kinesin UNC-104 and limiting its activity to axons. We speculate that UNC-33 may affect other kinesin motors as well, since CRMP2 acts as an adaptor for axonal Kinesin-1-dependent traffic (Arimura et al., 2005; Kawano et al., 2005; Kimura et al., 2005). *C. elegans* Kinesin-1/*unc-116* has a relatively minor role in PVD compared to *unc-33* and *unc-44* ((Tsuboi et al., 2005) and our data not shown), but a further examination of microtubules and microtubule-dependent traffic in *unc-33* mutants may support or extend this hypothesis.

Acknowledgements

We thank C. Ghenoiu, P. Nurse, Y. Saheki, S. Shaham, T. Starich, M. Tsunozaki, M. Heiman, A. Kelly and members of our labs for thoughtful advice and comments on the manuscript, C. Janke and B. Edde for antibodies, and the *Caenorhabditis* Genetics Center (CGC) for strains. C.I.B. and K.S. are Investigators of the Howard Hughes Medical Institute. This work was supported by the Howard Hughes Medical Institute.

References

Altun-Gultekin, Z., Andachi, Y., Tsalik, E.L., Pilgrim, D., Kohara, Y., and Hobert, O. (2001). A regulatory cascade of three homeobox genes, ceh-10, ttx-3 and ceh-23, controls cell fate specification of a defined interneuron class in C. elegans. Development *128*, 1951-1969.

Arimura, N., and Kaibuchi, K. (2007). Neuronal polarity: from extracellular signals to intracellular mechanisms. Nat Rev Neurosci *8*, 194-205.

Arimura, N., Menager, C., Kawano, Y., Yoshimura, T., Kawabata, S., Hattori, A., Fukata, Y., Amano, M., Goshima, Y., Inagaki, M.*, et al.* (2005). Phosphorylation by Rho kinase regulates CRMP-2 activity in growth cones. Mol Cell Biol *25*, 9973-9984.

Arnold, D.B. (2009). Actin and microtubule-based cytoskeletal cues direct polarized targeting of proteins in neurons. Sci Signal *2*, pe49.

Baas, P.W., Deitch, J.S., Black, M.M., and Banker, G.A. (1988). Polarity orientation of microtubules in hippocampal neurons: uniformity in the axon and nonuniformity in the dendrite. Proc Natl Acad Sci U S A *85*, 8335-8339.

Barnes, A.P., and Polleux, F. (2009). Establishment of axon-dendrite polarity in developing neurons. Annu Rev Neurosci *32*, 347-381.

Brenner, S. (1974). The genetics of Caenorhabditis elegans. Genetics *77*, 71-94.

Brot, S., Rogemond, V., Perrot, V., Chounlamountri, N., Auger, C., Honnorat, J., and Moradi-Ameli, M. CRMP5 interacts with tubulin to inhibit neurite outgrowth, thereby modulating the function of CRMP2. J Neurosci *30*, 10639-10654.

Bucher, D., Thirumalai, V., and Marder, E. (2003). Axonal dopamine receptors activate peripheral spike initiation in a stomatogastric motor neuron. J Neurosci *23*, 6866-6875.

Burton, P.R. (1985). Ultrastructure of the olfactory neuron of the bullfrog: the dendrite and its microtubules. J Comp Neurol *242*, 147-160.

Burton, P.R., and Paige, J.L. (1981). Polarity of axoplasmic microtubules in the olfactory nerve of the frog. Proc Natl Acad Sci U S A *78*, 3269-3273.

Conde, C., and Caceres, A. (2009). Microtubule assembly, organization and dynamics in axons and dendrites. Nat Rev Neurosci *10*, 319-332.

Crump, J.G., Zhen, M., Jin, Y., and Bargmann, C.I. (2001). The SAD-1 kinase regulates presynaptic vesicle clustering and axon termination. Neuron *29*, 115-129.

Desai, C., Garriga, G., McIntire, S.L., and Horvitz, H.R. (1988). A genetic pathway for the development of the Caenorhabditis elegans HSN motor neurons. Nature *336*, 638-646.

Dwyer, N.D., Adler, C.E., Crump, J.G., L'Etoile, N.D., and Bargmann, C.I. (2001). Polarized dendritic transport and the AP-1 mu1 clathrin adaptor UNC-101 localize odorant receptors to olfactory cilia. Neuron *31*, 277-287.

Dwyer, N.D., Troemel, E.R., Sengupta, P., and Bargmann, C.I. (1998). Odorant receptor localization to olfactory cilia is mediated by ODR-4, a novel membrane-associated protein. Cell *93*, 455-466.

Fukata, Y., Itoh, T.J., Kimura, T., Menager, C., Nishimura, T., Shiromizu, T., Watanabe, H., Inagaki, N., Iwamatsu, A., Hotani, H.*, et al.* (2002). CRMP-2 binds to tubulin heterodimers to promote microtubule assembly. Nat Cell Biol *4*, 583-591.

Goldstein, L.S., and Yang, Z. (2000). Microtubule-based transport systems in neurons: the roles of kinesins and dyneins. Annu Rev Neurosci *23*, 39-71.

Grubb, M.S., and Burrone, J. (2010). Building and maintaining the axon initial segment. Curr Opin Neurobiol.

Hall, D.H., and Hedgecock, E.M. (1991). Kinesin-related gene unc-104 is required for axonal transport of synaptic vesicles in C. elegans. Cell *65*, 837-847.

Hedgecock, E.M., Culotti, J.G., Thomson, J.N., and Perkins, L.A. (1985). Axonal guidance mutants of Caenorhabditis elegans identified by filling sensory neurons with fluorescein dyes. Dev Biol *111*, 158-170.

Hedstrom, K.L., Ogawa, Y., and Rasband, M.N. (2008). AnkyrinG is required for maintenance of the axon initial segment and neuronal polarity. J Cell Biol *183*, 635-640.

Heidemann, S.R., Landers, J.M., and Hamborg, M.A. (1981). Polarity orientation of axonal microtubules. J Cell Biol *91*, 661-665.

Hirokawa, N., and Takemura, R. (2005). Molecular motors and mechanisms of directional transport in neurons. Nat Rev Neurosci *6*, 201-214.

Inagaki, N., Chihara, K., Arimura, N., Menager, C., Kawano, Y., Matsuo, N., Nishimura, T., Amano, M., and Kaibuchi, K. (2001). CRMP-2 induces axons in cultured hippocampal neurons. Nat Neurosci *4*, 781-782.

Jacobson, C., Schnapp, B., and Banker, G.A. (2006). A change in the selective translocation of the Kinesin-1 motor domain marks the initial specification of the axon. Neuron *49*, 797-804.

Jenkins, S.M., and Bennett, V. (2001). Ankyrin-G coordinates assembly of the spectrin-based membrane skeleton, voltage-gated sodium channels, and L1 CAMs at Purkinje neuron initial segments. J Cell Biol *155*, 739-746.

Kawano, Y., Yoshimura, T., Tsuboi, D., Kawabata, S., Kaneko-Kawano, T., Shirataki, H., Takenawa, T., and Kaibuchi, K. (2005). CRMP-2 is involved in kinesin-1-dependent transport of the Sra-1/WAVE1 complex and axon formation. Mol Cell Biol *25*, 9920-9935.

Kimura, T., Watanabe, H., Iwamatsu, A., and Kaibuchi, K. (2005). Tubulin and CRMP-2 complex is transported via Kinesin-1. J Neurochem *93*, 1371-1382.

Kishi, M., Pan, Y.A., Crump, J.G., and Sanes, J.R. (2005). Mammalian SAD kinases are required for neuronal polarization. Science *307*, 929-932.

Kwan, A.C., Dombeck, D.A., and Webb, W.W. (2008). Polarized microtubule arrays in apical dendrites and axons. Proc Natl Acad Sci U S A *105*, 11370-11375.

Li, W., Herman, R.K., and Shaw, J.E. (1992). Analysis of the Caenorhabditis elegans axonal guidance and outgrowth gene unc-33. Genetics *132*, 675-689.

Meyrand, P., Weimann, J.M., and Marder, E. (1992). Multiple axonal spike initiation zones in a motor neuron: serotonin activation. J Neurosci *12*, 2803-2812.

Nakata, T., and Hirokawa, N. (2003). Microtubules provide directional cues for polarized axonal transport through interaction with kinesin motor head. J Cell Biol *162*, 1045-1055.

Nonet, M.L., Staunton, J.E., Kilgard, M.P., Fergestad, T., Hartwieg, E., Horvitz, H.R., Jorgensen, E.M., and Meyer, B.J. (1997). Caenorhabditis elegans rab-3 mutant synapses exhibit impaired function and are partially depleted of vesicles. J Neurosci *17*, 8061-8073.

Ogawa, Y., Schafer, D.P., Horresh, I., Bar, V., Hales, K., Yang, Y., Susuki, K., Peles, E., Stankewich, M.C., and Rasband, M.N. (2006). Spectrins and ankyrinB constitute a specialized paranodal cytoskeleton. J Neurosci *26*, 5230-5239.

Oren-Suissa, M., Hall, D.H., Treinin, M., Shemer, G., and Podbilewicz, B. (2010). The fusogen EFF-1 controls sculpting of mechanosensory dendrites. Science *328*, 1285-1288.

Otsuka, A.J., Franco, R., Yang, B., Shim, K.H., Tang, L.Z., Zhang, Y.Y., Boontrakulpoontawee, P., Jeyaprakash, A., Hedgecock, E., Wheaton, V.I.*, et al.* (1995). An ankyrin-related gene (unc-44) is necessary for proper axonal guidance in Caenorhabditis elegans. J Cell Biol *129*, 1081-1092.

Ou, C.Y., Poon, V.Y., Maeder, C.I., Watanabe, S., Lehrman, E.K., Fu, A.K., Park, M., Fu, W.Y., Jorgensen, E.M., Ip, N.Y.*, et al.* (2010). Two cyclin-dependent kinase pathways are essential for polarized trafficking of presynaptic components. Cell *141*, 846-858.

Pack-Chung, E., Kurshan, P.T., Dickman, D.K., and Schwarz, T.L. (2007). A Drosophila kinesin required for synaptic bouton formation and synaptic vesicle transport. Nat Neurosci *10*, 980-989.

Palay, S.L., Sotelo, C., Peters, A., and Orkand, P.M. (1968). The axon hillock and the initial segment. J Cell Biol *38*, 193-201.

Quinn, C.C., Chen, E., Kinjo, T.G., Kelly, G., Bell, A.W., Elliott, R.C., McPherson, P.S., and Hockfield, S. (2003). TUC-4b, a novel TUC family variant, regulates neurite outgrowth and associates with vesicles in the growth cone. J Neurosci *23*, 2815-2823.

Rolls, M.M., Satoh, D., Clyne, P.J., Henner, A.L., Uemura, T., and Doe, C.Q. (2007). Polarity and intracellular compartmentalization of Drosophila neurons. Neural Dev *2*, 7.

Sengupta, P., Chou, J.H., and Bargmann, C.I. (1996). odr-10 encodes a seven transmembrane domain olfactory receptor required for responses to the odorant diacetyl. Cell *84*, 899-909.

Setou, M., Seog, D.H., Tanaka, Y., Kanai, Y., Takei, Y., Kawagishi, M., and Hirokawa, N. (2002). Glutamate-receptor-interacting protein GRIP1 directly steers kinesin to dendrites. Nature *417*, 83-87.

Siddiqui, S.S., Aamodt, E., Rastinejad, F., and Culotti, J. (1989). Anti-tubulin monoclonal antibodies that bind to specific neurons in Caenorhabditis elegans. J Neurosci *9*, 2963-2972.

Siddiqui, S.S., and Culotti, J.G. (1991). Examination of neurons in wild type and mutants of Caenorhabditis elegans using antibodies to horseradish peroxidase. J Neurogenet *7*, 193-211.

Sobotzik, J.M., Sie, J.M., Politi, C., Del Turco, D., Bennett, V., Deller, T., and Schultz, C. (2009). AnkyrinG is required to maintain axo-dendritic polarity in vivo. Proc Natl Acad Sci U S A *106*, 17564-17569.

Song, A.H., Wang, D., Chen, G., Li, Y., Luo, J., Duan, S., and Poo, M.M. (2009). A selective filter for cytoplasmic transport at the axon initial segment. Cell *136*, 1148-1160.

Srayko, M., Kaya, A., Stamford, J., and Hyman, A.A. (2005). Identification and characterization of factors required for microtubule growth and nucleation in the early C. elegans embryo. Dev Cell *9*, 223-236.

Sulston, J.E., and Horvitz, H.R. (1977). Post-embryonic cell lineages of the nematode, Caenorhabditis elegans. Dev Biol *56*, 110-156.

Treinin, M., Gillo, B., Liebman, L., and Chalfie, M. (1998). Two functionally dependent acetylcholine subunits are encoded in a single Caenorhabditis elegans operon. Proc Natl Acad Sci U S A *95*, 15492-15495.

Troemel, E.R., Sagasti, A., and Bargmann, C.I. (1999). Lateral signaling mediated by axon contact and calcium entry regulates asymmetric odorant receptor expression in C. elegans. Cell *99*, 387-398.

Tsalik, E.L., Niacaris, T., Wenick, A.S., Pau, K., Avery, L., and Hobert, O. (2003). LIM homeobox gene-dependent expression of biogenic amine receptors in restricted regions of the C. elegans nervous system. Dev Biol *263*, 81-102.

Tsuboi, D., Hikita, T., Qadota, H., Amano, M., and Kaibuchi, K. (2005). Regulatory machinery of UNC-33 Ce-CRMP localization in neurites during neuronal development in Caenorhabditis elegans. J Neurochem *95*, 1629-1641.

White, J.G., Southgate, E., Thomson, J.N., and Brenner, S. (1986). The structure of the nervous system of the nematode Caenorhabditis elegans. Philos Trans R Soc Lond B Biol Sci *314*, 1-340.

Winckler, B., Forscher, P., and Mellman, I. (1999). A diffusion barrier maintains distribution of membrane proteins in polarized neurons. Nature *397*, 698-701.

Witte, H., Neukirchen, D., and Bradke, F. (2008). Microtubule stabilization specifies initial neuronal polarization. J Cell Biol *180*, 619-632.

Wolff, A., de Nechaud, B., Chillet, D., Mazarguil, H., Desbruyeres, E., Audebert, S., Edde, B., Gros, F., and Denoulet, P. (1992). Distribution of glutamylated alpha and beta-tubulin in mouse tissues using a specific monoclonal antibody, GT335. Eur J Cell Biol *59*, 425-432.

Yonekawa, Y., Harada, A., Okada, Y., Funakoshi, T., Kanai, Y., Takei, Y., Terada, S., Noda, T., and Hirokawa, N. (1998). Defect in synaptic vesicle precursor transport and neuronal cell death in KIF1A motor protein-deficient mice. J Cell Biol *141*, 431-441.

Yoshimura, T., Kawano, Y., Arimura, N., Kawabata, S., Kikuchi, A., and Kaibuchi, K. (2005). GSK-3beta regulates phosphorylation of CRMP-2 and neuronal polarity. Cell *120*, 137-149.

Zhou, D., Lambert, S., Malen, P.L., Carpenter, S., Boland, L.M., and Bennett, V. (1998). AnkyrinG is required for clustering of voltage-gated Na channels at axon initial segments and for normal action potential firing. J Cell Biol *143*, 1295-1304.

Zhou, H.M., Brust-Mascher, I., and Scholey, J.M. (2001). Direct visualization of the movement of the monomeric axonal transport motor UNC-104 along neuronal processes in living Caenorhabditis elegans. J Neurosci *21*, 3749-3755.

Chapter 3

Regulation of Chemoreceptor ODR-10 transport to sensory cilia by ODR-8/UfSP2 and UFM1

Abstract

The biosynthetic transport of GPCRs from the ER to specific sub-cellular locations is a highly regulated process. While critical in regulating the surface levels of these vital signaling receptors, this process remains not well understood. Previous work had identified *odr-8* as an important regulator of odorant receptor transport in *C. elegans*, whose identity was not known. Here, we report that *odr-8* encodes the *C. elegans* homolog of mammalian *UfSP2*, a cysteine-protease specific for the ubiquitin-like molecule UFM1. We found that *odr-8* and *ufm-1*/ *UFM1* are both required for the proper regulation of chemoreceptor localization at the *C. elegans* chemosensory cilia. ODR-8, while diffusely distributed in neurons, showed ER-enrichment. *odr-8* mutants defective for ciliary localization of ODR-10 diacetyl receptor, displayed ER-retention of ODR-10. *ufm-1* mutants displayed a converse up-regulation of ODR-10 localization at the cilia. Double mutants resembled *ufm-1* animals, suppressing ER-retention defects and instead showing ODR-10 ciliary enrichment. Together, these results suggest that a balance between UFM-1-conjugation and ODR-8/UfSP2–mediated deconjugation at the ER controls the rate of ODR-10 ER-exit and thereby dictates ODR-10 surface expression at the cilia.

Introduction

Cell polarization is a ubiquitous phenomenon by which cells organize subcellular domains that serve distinct functions. Neurons are striking examples of polarized cells, whose most fundamental division is the presence of a single axon and one or more dendrites, each of which typically elaborates further compartments. Axons specialize in neurotransmitter release and signal propagation, whereas the primary function of dendrites is to gather information; neural function depends on the proper regulation of these domains(Barnes and Polleux, 2009). Since the functional properties of these compartments are defined by their constituent proteins, understanding the mechanisms that control polarized protein localization may provide significant insight into the regulation of neuronal function.

G-protein coupled receptors (GPCRs) represent a major group of proteins whose expression and distribution specify functional properties of cellular domains(Dong et al., 2007). GPCRs comprise the largest family of signaling receptors in animals and respond to a wide range of external stimuli and intercellular cues. A growing number of GPCRs are known to localize in an asymmetric fashion in neurons and in other polarized cells such as epithelial cells. For example, A1 adenosine receptors localize to the apical surface of epithelial cells, whereas β-adrenergic receptors localize to the basolateral surface(Wozniak et al., 1997; Wozniak and Limbird, 1996). Furthermore, GPCRs can show distinct distributions in different cell types: the μ-opioid receptor 1 shows dendritic enrichment in CNS neurons, but axonal targeting in primary afferent neurons(Arvidsson et al., 1995). The biosynthetic processes by which GPCRs are transported from the ER to specific

subcellular compartments remain poorly understood and require further investigation, especially considering that GPCR transport defects are associated with the pathogenesis of human diseases such as retinitis pigmentosa and nephrogenic diabetes insipidus(Morello and Bichet, 2001; Stojanovic and Hwa, 2002).

Recent studies indicate that the export of GPCRs from the ER to the Golgi complex, and subsequently from the Golgi complex to the correct plasma membrane domain is highly regulated. A number of cis-acting motifs, such as phenylalanine-based and dileucine-based cytoplasmic signals promote export from the ER(Dong et al., 2007). Trans-acting accessory proteins, which typically affect a small set of GPCRs, can promote GPCR export from the ER to the plasma membrane and may also act in subsequent steps of vesicle transport or receptor regulation at the cell surface. For example, *ninaA*, the *Drosophila* cyclophilin homolog, is required for the export of rhodopsin Rh1 from the ER and its transport along the biosynthetic pathway(Baker et al., 1994; Colley et al., 1991). The cyclophilin-related protein, RanBP2, may play an analogous chaperoning and escort role for mammalian red/green opsin(Ferreira et al., 1996).

Chemoreceptors are a large and divergent set of GPCRs involved in olfaction and taste(Bargmann, 2006). Mice have about ~1200 chemoreceptors including ~900 odorant receptors (ORs), humans have ~350 odorant receptors, and the nematode *C. elegans* has the highest number reported in any species, 1700-2100 predicted chemosensory receptors(Bargmann, 2006). In *C. elegans*, a screen for chemotaxis-defective mutants, followed by an examination of odorant receptor localization, identified *odr-4* as the first accessory molecule identified for odorant receptors(Dwyer et al., 1998). *odr-4* encodes a transmembrane protein required for the transport of multiple chemoreceptors, including the

diacetyl receptor ODR-10, from the ER to the sensory cilia. ODR-4 localizes to subcellular organelles and perhaps transport vesicles, but not to the cilia themselves. A functional role similar to that of ODR-4 is suggested for three small transmembrane proteins (RTP1, RTP2 and REEP1) that are expressed in mammalian olfactory sensory neurons. They associate with a subset of mammalian ORs and enhance their surface expression in heterologous cells(Saito et al., 2004).

Mutants for *odr-8*, another regulator of odorant receptor localization, share numerous phenotypes with *odr-4* mutants(Dwyer et al., 1998). *odr-4* and *odr-8* mutants are defective in chemotaxis to a common subset of odorants, sensed by AWA and AWC chemosensory neurons. *odr-8* and *odr-4* mutants also share defects in localizing a common subset of chemoreceptors, including the odorant receptor ODR-10. In *odr-4* and *odr-8* mutant animals, these receptors are retained in the cell body rather than being enriched in cilia. While multiple screens led to the isolation of five mutant alleles, the molecular identity of *odr-8*, possibly encoding another accessory molecule or a new class of molecule critical for GPCR transport to sensory cilia, remained to be discovered.

Here, we report the identification of *odr-8* as the *C. elegans* homolog of UfSP2 (UFM1-specific protease 2), a potential regulator of UFM1 (ubiquitin-fold modifier 1). UFM1 is a conserved small protein belonging to the ubiquitin-like protein (UBL) family, with no sequence similarity but significant structural homology to ubiquitin(Komatsu et al., 2004), and E1, E2, and E3-like enzymes for conjugation to other proteins(Komatsu et al., 2004; Tatsumi et al., 2010). UfSP2 and UfSP1 encode cysteine proteases specific for UFM1, activities that could either process mature UFM1 from its inactive precursor, or remove UFM1 from its conjugated substrates(Kang et al., 2007). Only a single UFM1-

modified substrate has been identified, the DDRGK1 (C20orf116) protein of unknown function, and the physiological function of UFM1 is unknown(Tatsumi et al., 2010). UBA5, the UFM1-specific E1 enzyme, is essential for mouse hematopoietic development. Uba5 knockout mice are severely anemic, show marked defects in differentiation of erythroid progenitors, and die by E13.5(Tatsumi et al., 2011).

Here we analyze *odr-8* (*UfSP2*) and *zk652.3/ufm-1* (*UFM1*) single and double mutants and show that UfSP2 aids in the transport of odorant receptors such as ODR-10 from the ER to the cilia, whereas UFM1 conjugation antagonizes receptor transport from the ER.

Results

odr-8 encodes the *C. elegans* homolog of UFM1-specific protease 2 (UfSP2)

Genetic screens for olfactory mutants had previously identified four alleles of *odr-8* (*ky26, ky28, ky31* and *ky41*), and a direct screen for the localization of the GPCR ODR-10 yielded a fifth allele, *ky173(Dwyer et al., 1998)*. Recombinant mapping performed by Noelle Dwyer using visible genetic markers and genetic deficiencies had placed *odr-8(ky31)* on chromosome IV in between *lin-45* and *deb-1*, markers with genetic positions +3.23 and +3.29 respectively. However, prior attempts to rescue *odr-8* with DNA from this region proved unsuccessful. We employed whole genome sequencing to identify the causative mutation underlying the *odr-8* phenotype. Illumina-Solexa sequencing of *odr-8(ky31)* genomic DNA yielded ~35 bp sequence reads that were aligned against the N2 (wild type) reference genomic sequence to identify putative single nucleotide

polymorphisms (SNPs) and other genetic changes. To distinguish the *odr-8* mutation from extraneous SNPs present in the strain backgrounds used for mutagenesis or outcrossing, the following criteria were used: 1.) The SNP should be a C->T or a G->A change, characteristic of EMS mutagenesis; 2.) The SNP should not have been detected in unrelated strains from the lab that were previously sequenced.

These criteria led to the identification of three putative SNPs in the 3.3 Mb interval between *lin-45* and *deb-1* on chromosome IV: a C->T non-coding SNP just downstream of *H34C03.2*; a C->T non-coding SNP in an intron of gene *C17H12.13*; and a G->A coding SNP at position 6850375 in *R13H7.2*, predicted to result in a Glu->Lys missense change in the corresponding amino acid sequence. Two lines of experimental evidence indicated that none of these three SNPs was likely to be the mutation underlying *odr-8(ky31)*. First, fosmid transgenes and PCR product transgenes corresponding to each of the three genes failed to rescue the defect in localization of the GPCR ODR-10::GFP in *odr-8(ky31)* mutants. Second, sequencing of the exons and splice junctions of these three genes did not reveal any mutations in two other *odr-8* mutants, *odr-8(ky28)* and *odr-8(ky41)*.

These negative results raised the possibility that the *odr-8*(*ky31)* lesion had been incorrectly assigned to the interval between *lin-45* and *deb-1*. So the analysis of the whole genome sequence was expanded to SNPs located outside but near that genetic interval. Indeed, a G->A change in the coding region of *F38A5.1*, located on chromosome IV at +3.21, was predicted to result in the premature termination of the corresponding protein. Sanger sequencing of PCR products confirmed the putative *F38A5.1* SNP identified by whole genome sequencing of *odr-8(ky31)*, and also identified missense or nonsense mutations in four additional *odr-8 ky31* (Fig. 3.1.c). Transgenes corresponding to the

F38A5.1 genomic region rescued the ODR-10::GFP localization defects of *odr-8(ky31)* animals, restoring bright labeling of AWA cilia by ODR-10::GFP (Fig. 3.1.a). These results identify F38A5.1 as *odr-8*.

F38A5.1 is the *C. elegans* homolog of UfSP2, a conserved gene found in most multicellular organisms (Fig. 3.1.b). Mammalian UfSP2 encodes a cysteine protease specific for Ubiquitin-fold modifier 1 (UFM1), a ubiquitin-like molecule conjugated to various cellular proteins(Kang et al., 2007; Komatsu et al., 2004). UfSP2 is divided into two structural domains: a C-terminal catalytic domain that is similar to that of UfSP1, whereas an N-terminal domain of unique structure important for the interaction of UfSP2 with its substrate, C20orf116(Ha et al., 2011; Tatsumi et al., 2010). The *odr-8* locus encodes two near-identical isoforms with alternative lengths of their N-termini. Four of the five *odr-8* alleles encode nonsense mutations affecting both isoforms, whereas the fifth allele (*ky26*) is a missense mutation changing a conserved histidine residue to a tyrosine in both isoforms.

odr-8 is expressed in head and tail neurons, and acts cell autonomously to localize ODR-10::GFP to AWA olfactory cilia

GFP reporter genes with short (1.6-2.6 kb) regions upstream of the *odr-8* start site were consistently expressed in chemosensory neurons in the head and tail, likely to be amphid and phasmid neurons whose identities remain to be confirmed (Fig. 3.2.a). Transgenes driving expression of mCherry::ODR-8A or mCherry::ODR-8B cDNA using the AWA-specific *odr-7* promoter (Sengupta et al., 1994) restored ciliary localization of

Figure 3.1. *odr-8* encodes the *C. elegans* homolog of UFM1-specific protease 2 (UfSP2).

(a) Representative images of ODR-10 localization in wild type and *odr-8* mutants. Yellow arrowhead points to cilia enrichment of ODR-10; white arrowhead points to cell body distribution. Scale bar, 10 μm.

(b,c) Schematic representation of (b) *odr-8* gene structure and (c) protein isoforms with positional information about mutant alleles (red arrowheads denote nonsense mutations; black arrow signifies a misses mutation affecting a conserved histidine.)

(d) Sequence alignment of ODR-8A, UfSP2 and UfSP1 sequences from other species, neighboring the catalytic cysteine (red asterisk, top) and around the catalytic aspartate and histidine residues (red asterisks, bottom).

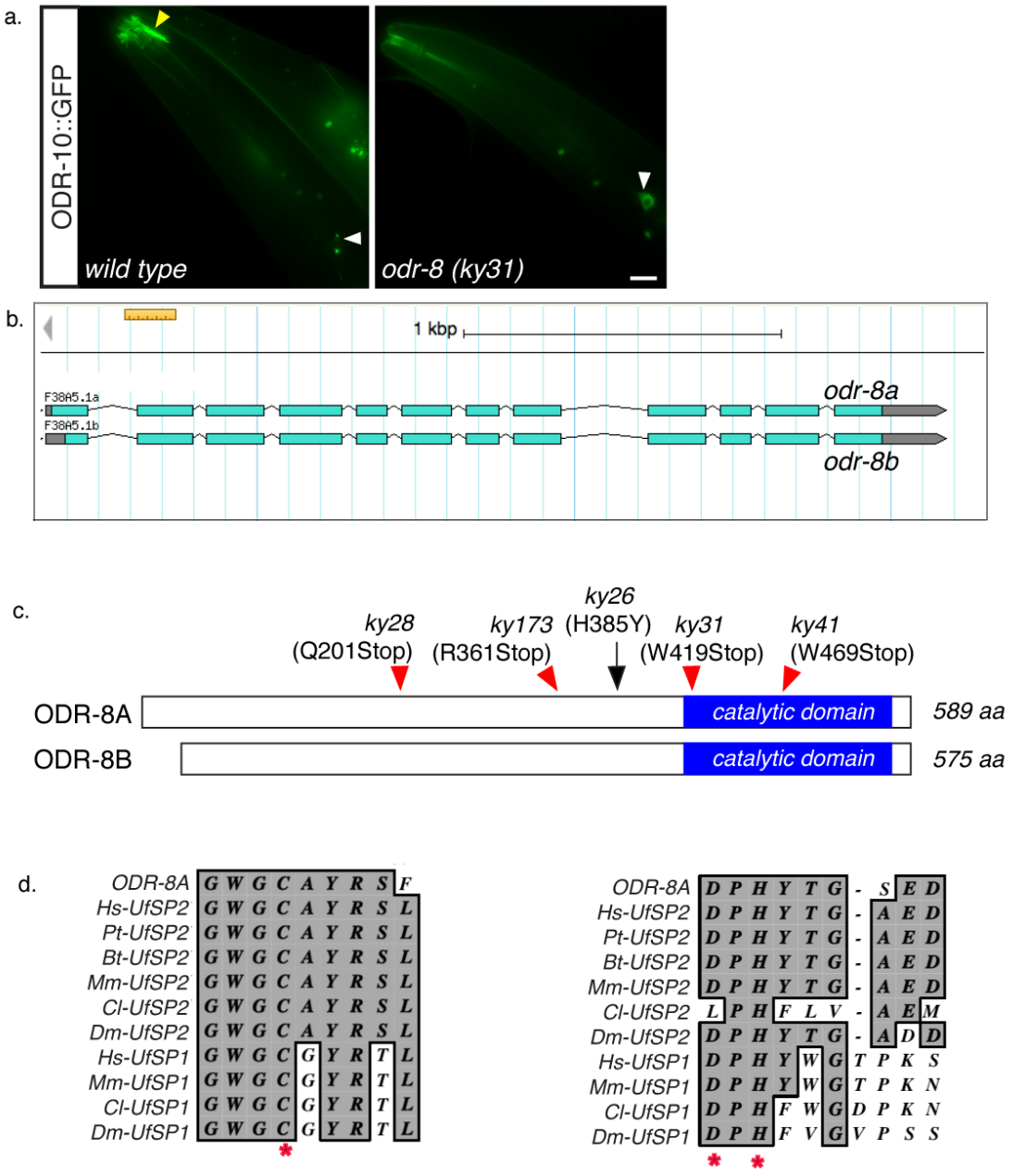
a.
ODR-10::GFP
wild type
odr-8 (ky31)
b.
1 kbp
F38A5.1a
F38A5.1b
odr-8a
odr-8b
c.
ky28
(Q201Stop)
ky173
(R361Stop)
ky26
(H385Y)
ky31
(W419Stop)
ky41
(W469Stop)
ODR-8A
catalytic domain
589 aa
ODR-8B
catalytic domain
575 aa
d.
ODR-8A G W G C A Y R S F
Hs-UfSP2 G W G C A Y R S L
Pt-UfSP2 G W G C A Y R S L
Bt-UfSP2 G W G C A Y R S L
Mm-UfSP2 G W G C A Y R S L
Cl-UfSP2 G W G C A Y R S L
Dm-UfSP2 G W G C A Y R S L
Hs-UfSP1 G W G C G Y R T L
Mm-UfSP1 G W G C G Y R T L
Cl-UfSP1 G W G C G Y R T L
Dm-UfSP1 G W G C G Y R T L
ODR-8A D P H Y T G - S E D
Hs-UfSP2 D P H Y T G - A E D
Pt-UfSP2 D P H Y T G - A E D
Bt-UfSP2 D P H Y T G - A E D
Mm-UfSP2 D P H Y T G - A E D
Cl-UfSP2 L P H F L V - A E M
Dm-UfSP2 D P H Y T G - A D D
Hs-UfSP1 D P H Y W G T P K S
Mm-UfSP1 D P H Y W G T P K N
Cl-UfSP1 D P H F W G D P K N
Dm-UfSP1 D P H F V G V P S S

Figure 3.1

ODR-10::GFP in *odr-8(ky31)* animals, suggesting a cell autonomous role for ODR-8 (Fig. 3.2.b,c).

Both mCherry::ODR-8A and mCherry::ODR-8B, each of which could rescue ODR-10 localization, were primarily localized to the cell body, and could not be detected in AWA cilia. The distribution of mCherry::ODR-8 in the cell body was irregular and punctate, and puncta typically showed co-localization with ODR-10::GFP puncta (Fig.3.2.b). At higher expression levels, mCherry::ODR-8 was broadly distributed throughout the cytoplasm as well as the nucleus.

A transgene driving expression of ODR-8A cDNA, under the control of a heat-shock promoter, was used to ask when in development *odr-8* acts to regulate ODR-10 expression. A heat-shock pulse provided during late L4 or adult stages completely rescued ODR-10::GFP localization in *odr-8(ky31)* animals (Fig. 3.2.d), with bright labeling of AWA cilia within 6 hours after heat-shock. This result suggests that ODR-8 acts acutely in mature neurons to regulate ODR-10::GFP localization.

Genetic interactions between *odr-8*, *odr-4* and *unc-101* (μ-adaptin)

In animals mutant for UNC-101, the μ1 subunit of the AP1 adaptin complex, ODR-10::GFP is no longer enriched at the AWB cilia, and instead shows bright labeling of the entire cell surface (Fig. 3.3.a) (Dwyer et al., 2001). *unc-101(m1); odr-8(ky31)* and *unc-101(m1); odr-8(ky173)* double mutants resembled *odr-8* single mutants in that ODR-10::GFP was primarily retained in the cell body (Fig. 3.3.a). A similar localizatio pattern was observed in *unc-101; odr-4* double mutants (Fig. 3.3.a) These results suggest that

Figure 3.2. ODR-8 acts cell autonomously to localize ODR-10::GFP to the cilia.

(a) Representative images of *odr-8*promoter::GFP expression in head (left) and tail (right) neurons.

(b) Representative showing rescued localization of ODR-10::GFP and mCherry::ODR-8A. In (Top) AWA neurons olfactory cilia and to the cell body (dashed box in top panels; also showed at a higher magnification in the bottom panels). Scale bar 10 μm.

(c) Fraction of animals displaying bright labeling of AWA cilia with ODR-10::GFP.

(d) Fraction of *odr-8(ky31);kyIs53* animal rescued for ODR-10::GFP localization after a 2 hour heat-shock at 33°C.

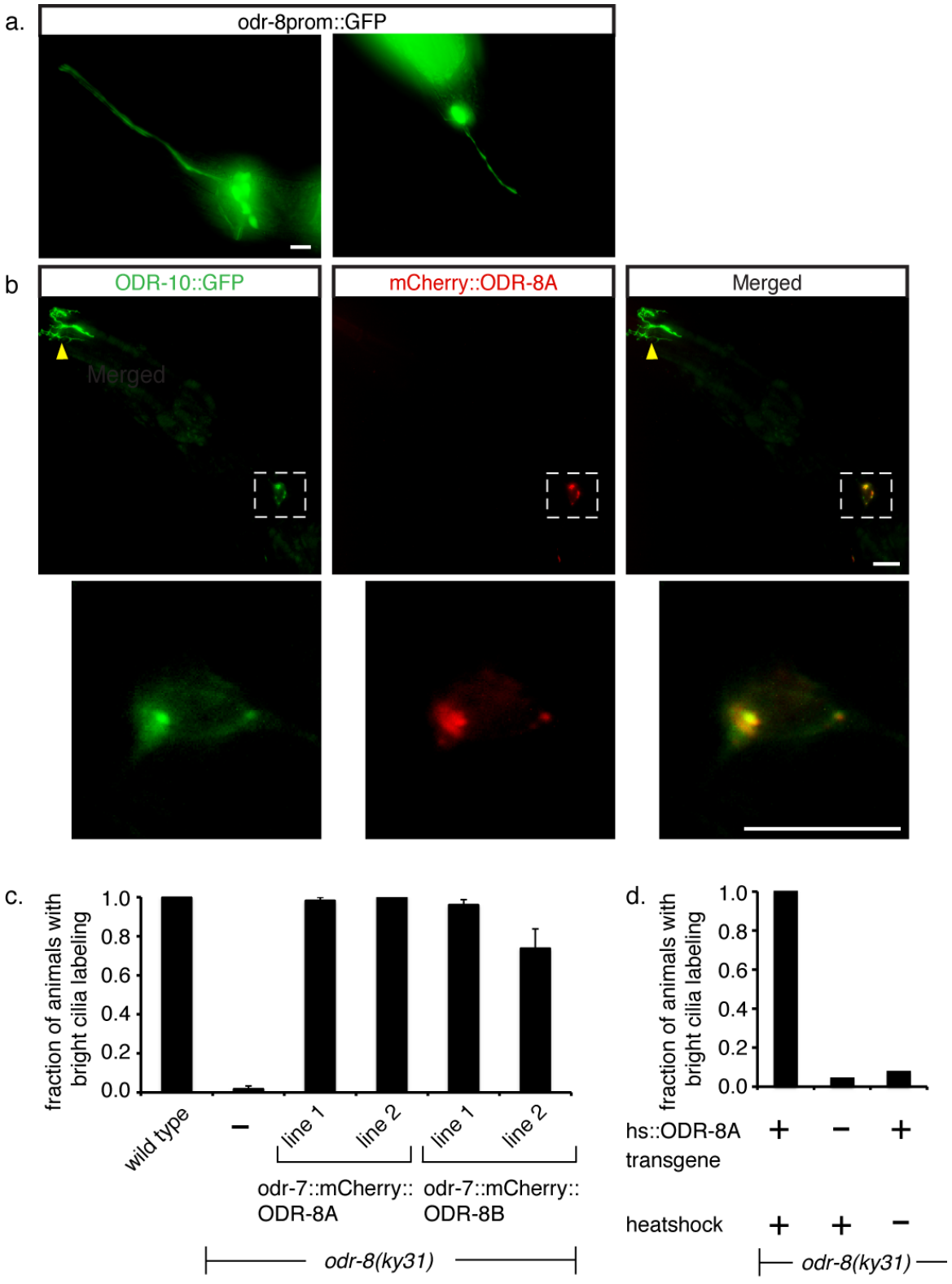
a.
odr-8prom::GFP
b
ODR-10::GFP
mCherry::ODR-8A
Merged
Merged
c.
fraction of animals with bright cilia labeling
1.0
0.8
0.6
0.4
0.2
0.0
wild type
−
line 1
line 2
line 1
line 2
odr-7::mCherry:: ODR-8A
odr-7::mCherry:: ODR-8B
odr-8(ky31)
d.
fraction of animals with bright cilia labeling
1.0
0.8
0.6
0.4
0.2
0.0
hs::ODR-8A transgene
+
−
+
heatshock
+
+
−
odr-8(ky31)

Figure 3.2

ODR-8 and ODR-4 function in a compartment required for delivery to cilia and for constitutive delivery to the plasmam membrane, perhaps the ER.

The similar phenotypes of *odr-4 and* odr-8 single and double mutants prompted an examination of potential interactions between them. *odr-8* mutants were not rescued by overexpression of ODR-4 (Dwyer et al., 1998), and conversely *odr-4* mutants were not rescued by overexpression of ODR-8 (0 animals rescued, n>=38 animals each for three independent lines). Localization of mCherry::ODR-8 was not different in wild type and *odr-4* mutants (Fig. 3.3.b).

ODR-10::GFP co-localizes with endosomal and Golgi markers in the cell bodies of *wild type* neurons, but shows ER retention in *odr-8* mutants

To gain a better understanding of the step in ODR-10 transport that is regulated by ODR-8, the localization of ODR-10::GFP in AWA neurons of *odr-8* mutant animals was compared with that of a Golgi marker (α-mannosidase - MANS), several ER proteins (CP450, cb5 and TRAPβ)(Rolls et al., 2002), and RAB proteins marking overlapping but distinct sets of internal structures(Grant and Donaldson, 2009). In wild type neurons, ODR-10::GFP was localized to cilia and to punctate structures in the cell body. The somatic puncta showed modest co-localization with the Golgi marker, MANS::mCherry (Fig. 3.4.b), and more significant co-localization with the cilia-targeting marker, mCherry::RAB-8 and the endosomal marker mCherry::RAB-10 (Fig. 3.4.a). In *odr-8* mutants, ODR-10::GFP was distributed throughout the soma rather than being punctate, and showed perinuclear enrichment that colocalized with the ER markers CP450::mCherry

Figure 3.3. Genetic interactions between *odr-8*, *odr-4* and unc-101.

(a) *odr-8* and *odr-4* act upstream of *unc-101*(μ1 AP1-adaptin) in a genetic pathway regulating ODR-10 localization. Representative epifluorescence images showing ODR-10::GFP localization in various mutants. Scale bar 10 μm. n>50 examined for each genotype.

(b) mCherry::ODR-8 localization is unaffected in *odr-4*(*n2144*) mutants, and ODR-8 overexpression cannot rescue ODR-10 localization in *odr-4*(*n2144*) mutants. Scale bar 10 μm.

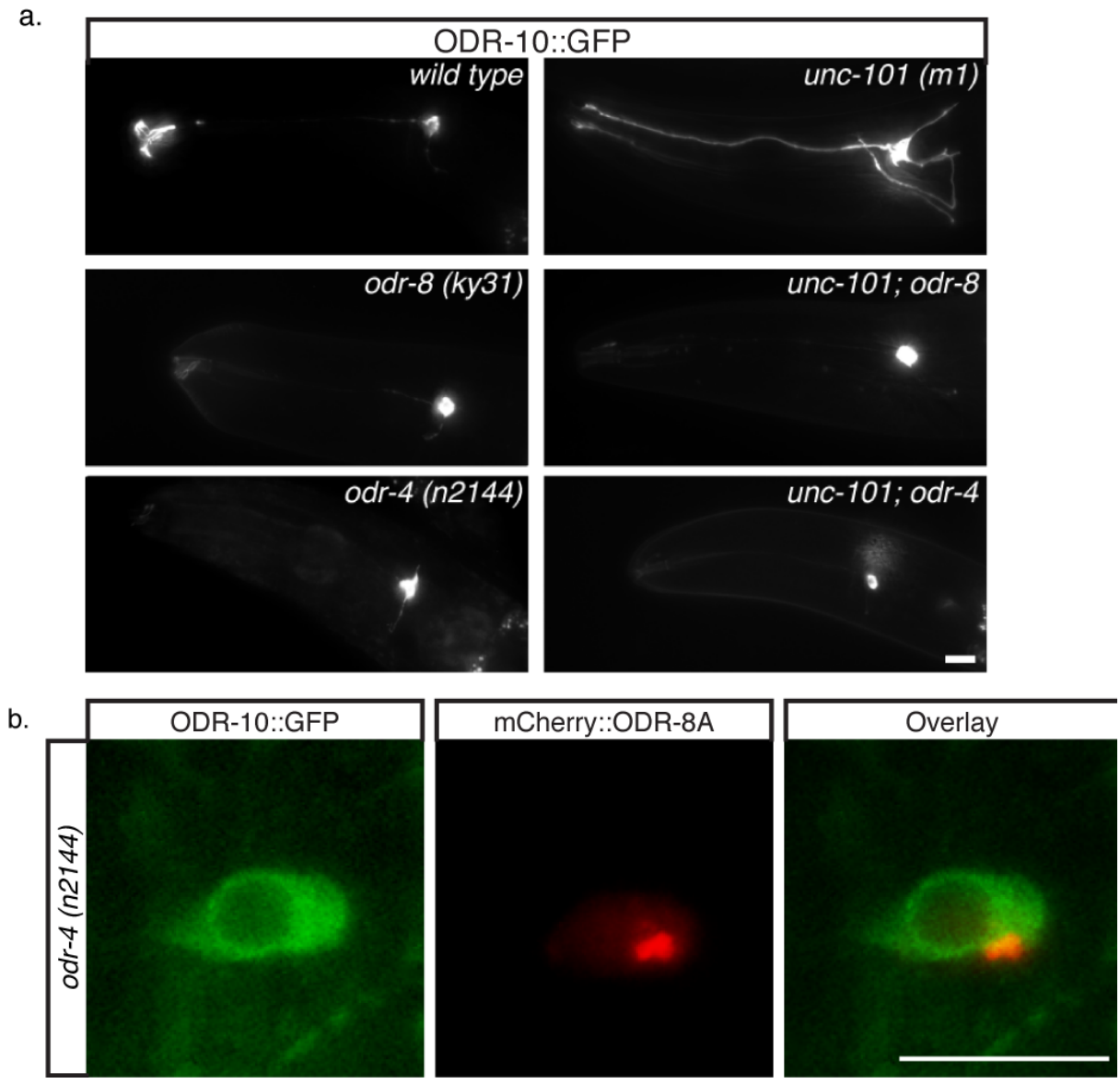
a.
ODR-10::GFP
wild type
unc-101 (m1)
odr-8 (ky31)
unc-101; odr-8
odr-4 (n2144)
unc-101; odr-4
b.
ODR-10::GFP
mCherry::ODR-8A
Overlay
odr-4 (n2144)

Figure 3.3

and TRAPβ::mCherry(Fig. 3.4.c,d). These results are consistent with the hypothesis that ODR-8 regulates ODR-10::GFP exit from the ER.

To further investigate the site at which ODR-8 acts to regulate ODR-10 transport, the subcellular localization of ODR-8 was examined. In wild type AWA neurons GFP::ODR-8A and mCherry ODR-8A were distributed throughout the cytoplasm with perinuclear enrichment (Fig. 3.5). The pattern is consistent with ER localization but should be confirmed with ER markers. In AWA wild type neurons that expressed ODR-10::GFP, mCherry ODR-8 colocalized with ODR-10 puncta, suggesting that the overexpressed ODR-10 protein could redirect the distribution of ODR-8, and supports an interaction between the two proteins.

UFM1 negatively regulates ODR-10::GFP transport to the cilia, and a deletion in *ufm1* rescues the ODR-10 ER retention phenotype of *odr-8* mutants

UfSP1 and UfSP2 proteases can play a role in the production of mature UFM1 and in the removal of UFM1 from its cellular substrates(Ha et al., 2011; Kang et al., 2007; Tatsumi et al., 2010). So the defects in *odr-8* mutants could either arise from a reduction in UFM1 protein or from a defect in UFM-1 deconjugation. The *ufm-1(gk879)* deletion allele was employed to ask whether and how *ufm-1* contributes to GPCR traffic and how it interacts with *odr-8*. *gk379* disrupts both the sole *C. elegans* UFM1 homolog *ZK652.3*, and the adjacent gene *coq-5,* which encodes a methyltransferase in ubiquinone biosynthesis (Asencio et al., 2003; Rodriguez-Aguilera et al., 2003). *ufm-1 (gk379)* homozygotes arrest

Figure 3.4. ODR-10::GFP colocalizes with RAB protein and Golgi marker in wild type animal, but with ER markers in *odr-8* mutants.

(a) Representative confocal images of ODR-10::GFP showing a high degree of colocalization with RAB-8 (top) and partial colocalization with RAB-10 (bottom) in wild type animals.

(b-d) Representative epifluorescence images showing colocalization of ODR-10::GFP with (b) Golgi marker, MANS::mCherry, and ER markers (c) CP450::mCherry and (d) TRAPβ::mCherry. Scale bar 10 μm.

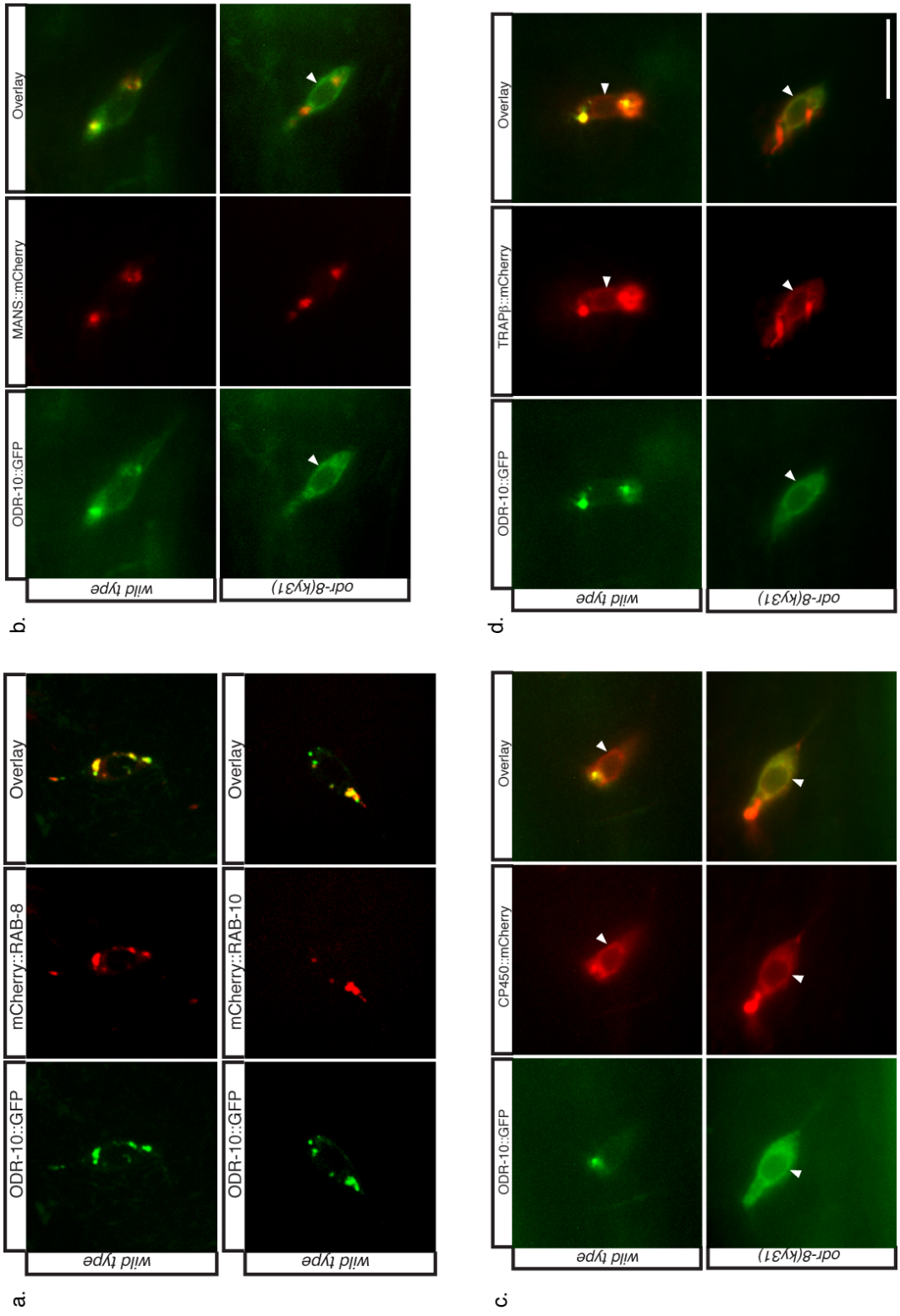
a.
wild type
odr-8(ky31)
ODR-10::GFP
mCherry::RAB-8
mCherry::RAB-10
Overlay
b.
MANS::mCherry
c.
CP450::mCherry
d.
TRAPβ::mCherry

Figure 3.4

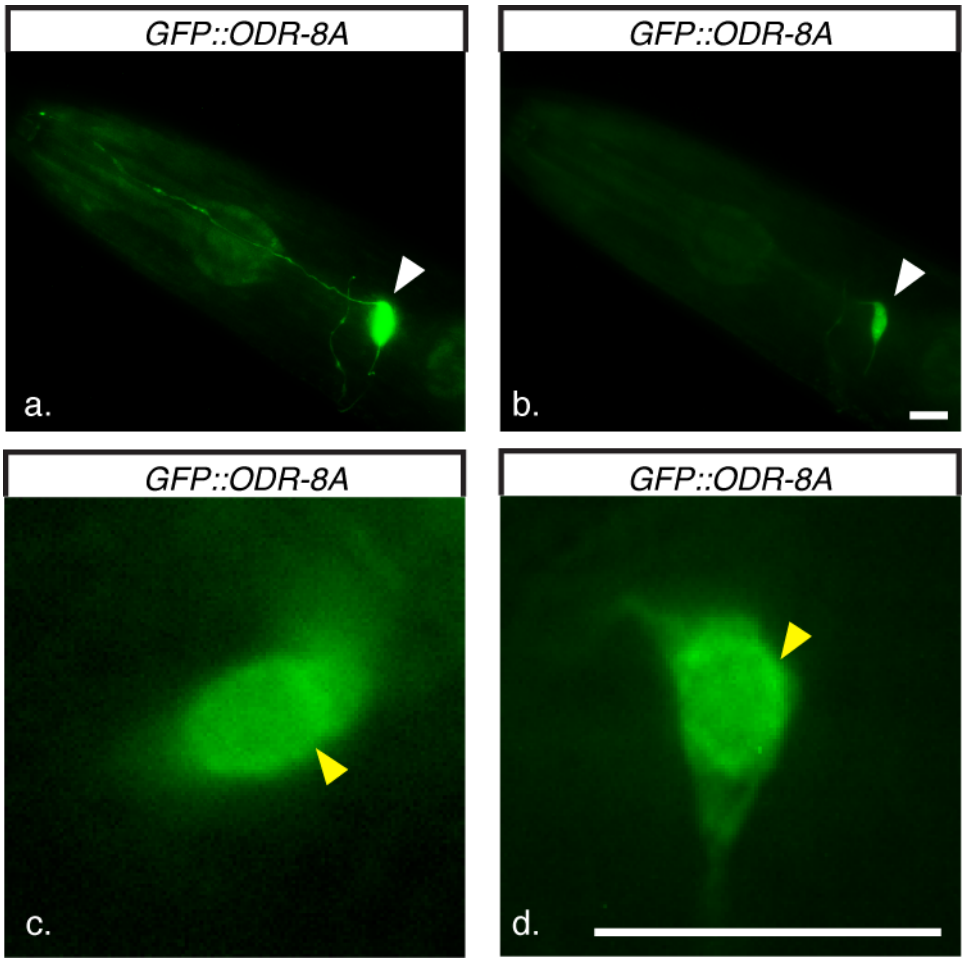

Figure 3.5. GFP::ODR-8 is localized throughout the cytoplasm and the nucleus, and exhibits perinuclear enrichment indicative of ER association.

(a,b) Two representative images of GFP::ODR-8 localization in AWA neurons at (a) high and (b) low expression levels.

(c,d) Two representative images of GFP::ODR-8 localization; white arrowheads point to AWA cell bodies; yellow arrowheads point to perinuclear enrichment. Scale bar 10 μm.

or die at larval early larval stages at which point ODR-10::GFP expression is relatively AWA. Therefore to examine effects of *ufm-1* on chemoreceptor localization, we used an AWB::ODR-10::GFP transgene that is strongly expressed in young animals and regulated by *odr-8*. Compared to wild type L1-stage larvae, *ufm-1(gk379)* larvae showed significantly higher levels of ODR-10::GFP in AWB cilia, and lower levels of ODR-10::GFP in the cell body (Fig.3.6.a-f). Moreover, the ODR-10::GFP in the AWB cell body of *ufm-1(gk379) larvae* appeared near the plasma membrane and not in the puncta seen in wild type animals (Fig. 3.6.c). In a few animals, ODR-10::GFP was present at the plasma membrane throughout the cell, a phenotype resembling *unc-101*(μ1 adaptor) mutants. Collectively, these results suggest that UFM-1 negatively regulates the transport of ODR-10 from the cell body to the cilia, and perhaps the surface level and distribution of ODR-10.

In *gk379; odr-8(ky173)* double mutants, ODR-10::GFP instead shows bright AWB cilia labeling, in contrast with the ER retention observed in *odr-8* alone (Fig. 3.6.b,e,f). This striking suppression (Fig. 3.6.g) suggests that UFM1 conjugation is responsible for the ER retention of ODR-10 in *odr-8* mutants. Collectively, these results indicate that *odr-8 (UfSP2)* and *ZK652.3 (UFM-1)* have antagonistic roles in the regulation of ODR-10 transport, and therefore one consistent with the possibility that the ODR-10 localization defect in *odr-8* is due to a defect in UFM1 deconjugation from substrate proteins.

T03F1.1 encodes the predicted *C. elegans* homolog of Uba5, an E1 enzyme for UFM1(Komatsu et al., 2004). A putative null allele for *T03F1.1*(*ok3364*) did not show a marked change in ODR-10::GFP distribution in AWA neurons compared to wild type (Fig. 3.7). Similarly the *T03F1.1*(*ok3364*) deletion did not suppress the ODR-10::GFP

Figure 3.6. *ufm-1* is required for ER retention of ODR-10::GFP in *odr-8* mutants.
(a-f) Representative images depicting ODR-10::GFP distribution in AWB neurons of L1 larvae of indicated genotypes. Two examples each are provided for *ufm-1(gk379)* (c,d) and *ufm-1:odr-8* (e,f) to show the variations in degree of ODR-10::GFP distribution along the processes, and ODR-10::GFP surface labeling of the soma. *kyIs156* transgene was used to drive ODR-10::GFP in AWB neurons. Scale bar 10 μm.
(g) Fluorescence quantification of ODR-10::GFP localization in AWA cilia and cell body represented as a ratio. 12-18 animals used per genotype for fluorescence quantification. Error bars, SEM. Compared using Dunn's multiple comparison test.

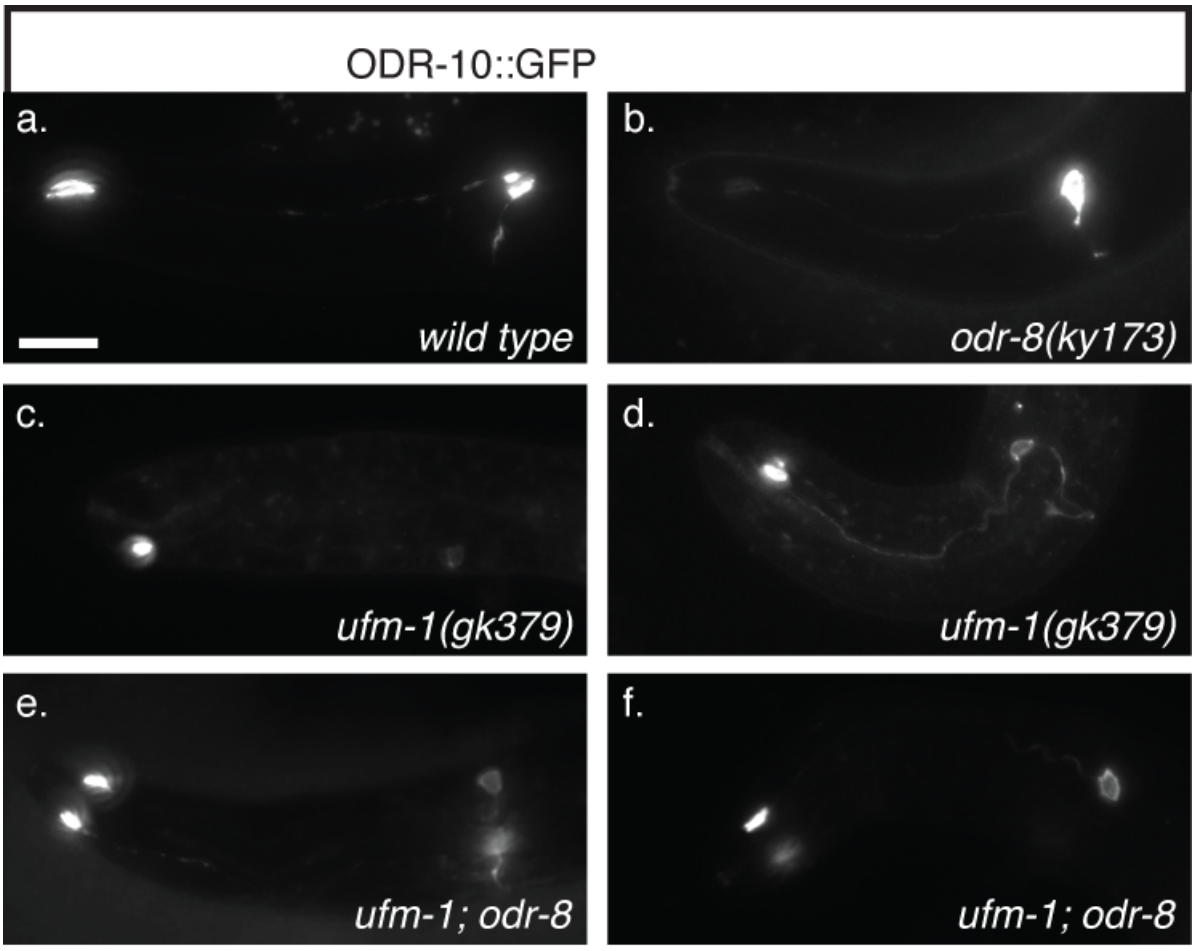
ODR-10::GFP
a.
wild type
b.
odr-8(ky173)
c.
ufm-1(gk379)
d.
ufm-1(gk379)
e.
ufm-1; odr-8
f.
ufm-1; odr-8

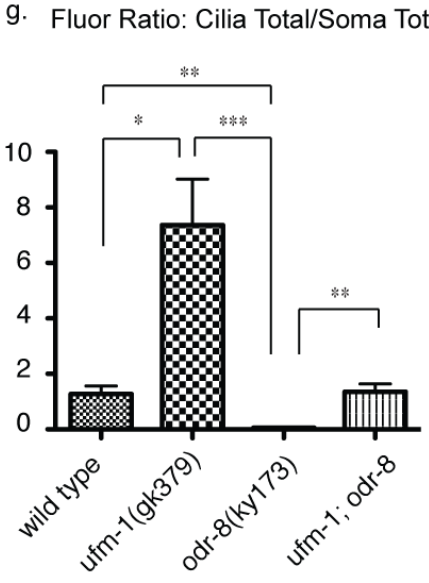
g.
Fluor Ratio: Cilia Total/Soma Total
**
*
***
**
10
8
6
4
2
0
wild type
ufm-1(gk379)
odr-8(ky173)
ufm-1; odr-8

Figure 3.6

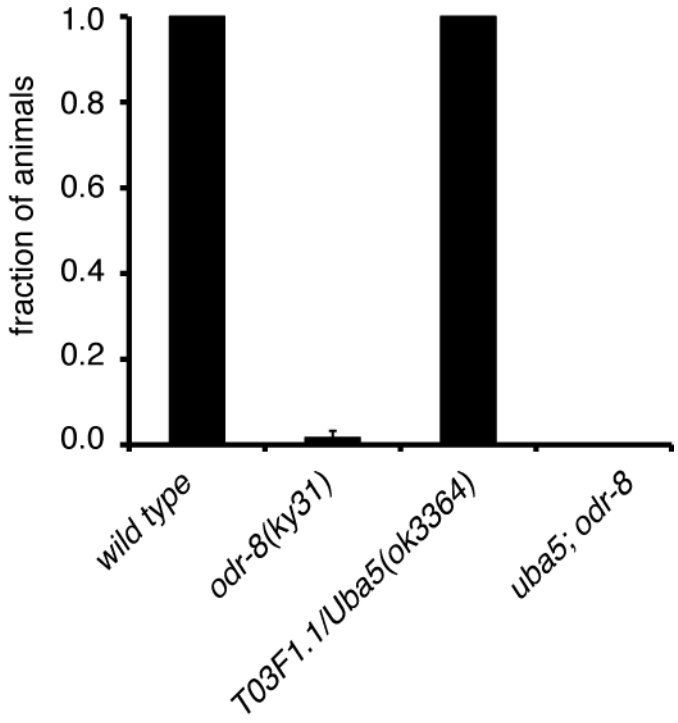

Figure 3.7. A deletion in *T03F1.1/Uba5* (the putative E1 enzyme for UFM1) did not lead to a marked change in ODR-10::GFP localization. Fraction of animals displaying ODR-10::GFP enrichment at AWA cilia. (n>50 animals for all genotypes).

localization defect of *odr-8(ky31)* mutants (Fig. 3.7). *T03F1.1*(*ok3364*) animals are viable and healthy, in contrast to the early larval arrest and lethality of *ufm-1(gk379)* mutants, suggesting that *T03F1.1* is not the only E1 enzyme for UFM-1.

odr-8 mutants show an increase in UFM1 immunoreactivity, suggesting a defect in UFM1 deconjugation

In addition to the genetic analysis mentioned above, a molecular approach was employed to ask whether *odr-8* mutants fail to remove UFM1 from its substrates or to conjugate it in the first place. Wild type and *odr-8(ky31)* animals were lysed to obtain protein extracts that were subsequently centrifuged to obtain cytosolic and membrane fractions, which were probed for immunoreactivity against UFM1 (Fig. 3.8). Preliminary results revealed the presence of a 9kDa band in the cytosolic fraction of both genotypes, the predicted size of unconjugated UFM1 protein. Additional higher molecular weight bands were detected in the cytosolic and membrane fractions of both genotypes. These bands may represent endogenous target proteins with UFM1-conjugation, and their presence in *odr-8* protein extracts suggests that *ufm-1* can be conjugated to substrates in *odr-8* mutants. Moreover, a subset of the UFM1-immunoreactive bands, appeared to increase in *odr-8* protein extracts, the pattern expected for a potential target of ODR-8 (Fig 3.8.a,b).

Figure 3.8. UFM1 immunoreactivity may be upregulated in *odr-8* mutants.

(a) Western blot probed for immunoreactivity against UFM1. The presence of UFM1 and UFM1 conjugated proteins was assessed in the cytosolic and membrane fractions extracted from either wild type worms or *odr-8* mutants. [*kyIs156=str-1::ODR-10::GFP*, driving expression of ODR-10::GFP in AWB neurons].

The red and yellow arrowheads point to bands that appear upregulated in *odr-8* mutants. See (b) for a close up of these bands from the cytosolic fraction along with a loading control. The star denotes BSA added to the membrane fraction. (Representative of n=2 experiments).

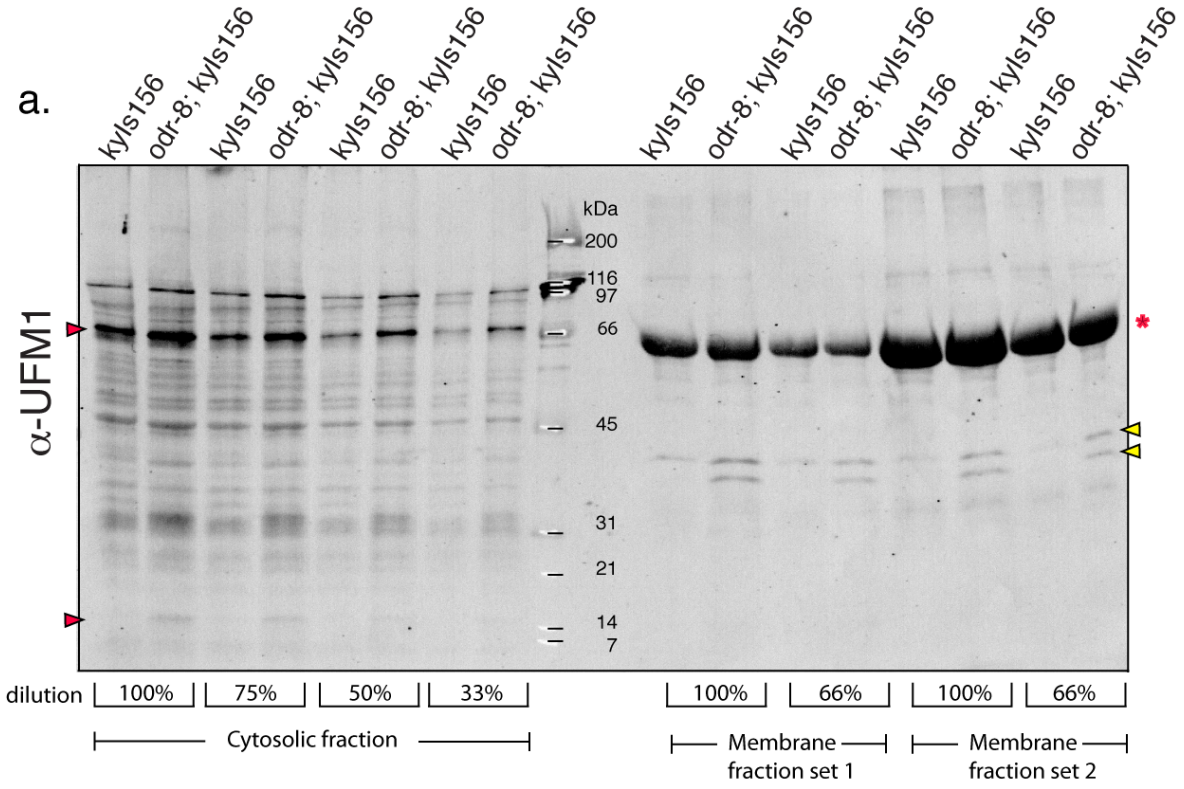
a.
kyIs156
odr-8; kyIs156
α-UFM1
kDa
200
116
97
66
45
31
21
14
7
dilution
100%
75%
50%
33%
100%
66%
100%
66%
Cytosolic fraction
Membrane fraction set 1
Membrane fraction set 2

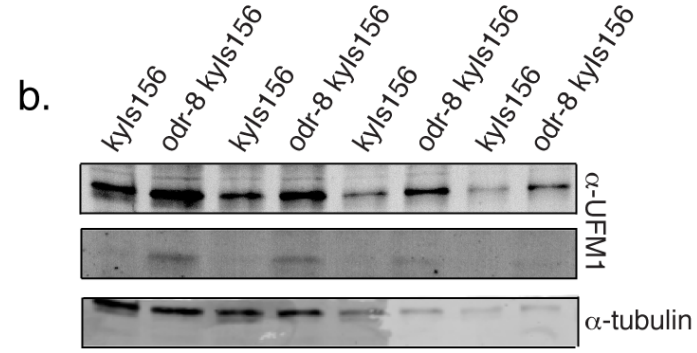
b.
kyIs156
odr-8 kyIs156
α-UFM1
α-tubulin

Figure 3.8

Discussion

Both *odr-8 (UfSP2)* and *ufm-1 (zk652.3/UFM1)* affect localization of the GPCR ODR-10 to *C. elegans* chemosensory cilia. *odr-8* mutants display ER retention of the tagged ODR-10 odorant receptor, whereas *ufm-1* mutant animals show increased ODR-10 localization in the cilia near the cell surface in the soma, and occasionally in axon and dendrite processes. *ufm-1* is epistatic to *odr-8* in double mutants, such that ODR-10 is no longer retained in the ER. This result suggests that UFM-1 conjugation of substrates is required for the ODR-10 ER retention phenotype of *odr-8* mutants. UFM-1 conjugation to one or more substrates may inhibit ODR-10 transport from the ER, whereas ODR-8 mediated deconjugation of UFM-1 alleviates this inhibition, leading to the ER exit of ODR-10 and entry into the ciliar transport pathway. A regulated balance of these two activities may be a mechanism to control surface levels of chemoreceptors like ODR-10.

Subcellular distribution of ODR-10 diacetyl receptor in wild type and *odr-8* animals

Colocalization analyses with tagged reporter proteins for different subcellular organelles revealed ODR-10 enrichment in cilia and in somatic compartments marked with an endosomal marker and a Golgi marker. A previous study identified a steady-state pool of ODR-10 in RAB-8 positive compartments in AWB chemosensory neurons (Kaplan et al., 2010), consistent with this observation. On the other hand, in *odr-8* mutants, ODR-10::GFP showed perinuclear colocalizing with two ER markers, a pattern that was not seen in wild type. ER retention resulting in poor surface expression is often associated with transmembrane proteins that exhibit improper folding or incomplete oligomeric assembly,

and regulation of ER exit represents a common step for accessory protein action (Bush and Hall, 2008; Dong et al., 2007). For example, mammalian odorant receptors and pheromone receptors are poorly expressed and trapped in the ER of heterologous cells, unless coexpressed with accessory proteins such as RTPs or members of the M10 family of MHC molecules(Loconto et al., 2003; Saito et al., 2004).

odr-8/*UfSP2* and *ufm-1*/*UFM1* mutant phenotypes reveal a physiological role for the UFM1-conjugation system

UFM1 is a recently identified member of the growing class of ubiquitin-like (UBL) molecules that is highly conserved across eukaryotic species, including most sequenced multi-cellular animals and plants, but not in yeast (Komatsu et al., 2004). Likewise, the enzymes involved in its conjugation cascade (E1 UBA5, E2 UFC1, E3 UFL1) are also well conserved(Komatsu et al., 2004; Tatsumi et al., 2010). Analogous to the role played by de-ubiquitinating (DUB) enzymes for ubiquitin, UfSP2 and UfSP1 encode two UFM-1-specific cysteine proteases. UfSP2, the longer of the two proteases, is found in most if not all multicellular organisms including plants, whereas UfSP1 is not present in nematodes and plants(Ha et al., 2011; Kang et al., 2007). While recent studies reflect a growing biochemical and structural characterization of the enzymatic cascade for UFM1 conjugation, a biological function for UFM1 was not known.

Previous work identified *odr-8* as an important regulator of chemoreceptor transport to the cilia, and my efforts revealed its molecular identity as the nematode

homolog of UfSP2, suggesting a physiological significance of UFM1 conjugation in this process. While *odr-8* mutants exhibit defects in chemotaxis and in the localizaton of a subset of chemoreceptors to sensory cilia, mutant animals seem superficially healthy and do not display any striking defects in development, morphology or locomotion. Furthermore, rather than a more general role in cilia development or ciliary protein transport, *odr-8* mutations disrupt chemoreceptor distribution without affecting localization of G-proteins, TRP channels and cGMP-gated ion channels at the cilia(Dwyer et al., 1998). Consistent with a restricted function, expression of *odr-8* was detected only in a subset of chemosensory neurons in the head and the tail, a pattern analogous to that observed for *odr-4 (Dwyer et al., 1998)*, which in turn matches well with the two mutants displaying identical phenotypes.

GFP::ODR-8 protein was detected throughout the cytoplasm and the nucleus but not at the cilia, and was particularly enriched in the perinuclear region associated with ER proteins. Given the ODR-10 ER retention phenotype of *odr-8* mutants, the association of ODR-8 with the ER may be relevant for regulating chemoreceptor transport from the ER to the cilia. Providing further support to this idea, a similar localization pattern, including nuclear presence as well as ER-enrichment, was observed for mammalian UfSP2 when expressed in heterologous cells(Ha et al., 2011).

The distribution of mCherry::ODR-8 protein fusion, however, only partly matched that of the GFP::ODR-8 protein or that of the mammalian myc::UfSP2 in HEK cells, with a less prominent ER enrichment of mCherry::ODR-8, and a more punctate distribution in the cell body. The mCherry::ODR-8 protein has only been examined in cells expressing a high level of ODR-10::GFP and its puncta showed a very high degree of colocalization

with coexpressed ODR-10::GFP sites in the soma. In an interesting scenario, ODR-8 protein may be redistributed by overexpressed ODR-10::GFP. Additional experiments in progress should test these possibilities.

UFM-1 limits ODR-10 transport from the ER, regulating surface expression at the cilia

C. elegans ufm-1(gk379) homozygotes arrest or die as early larvae. The knockout phenotype for mouse Uba5, the E1 enzyme is also lethal but since the *gk379* deletion also disrupts an adjacent gene (*coq-5*), rescue experiments are needed to clarify whether the lethality reflects a requirement for *ufm-1* or *coq-5*.

ODR-10::GFP cilia expression showed a marked increase in *ufm-1(gk379)* animals, with a corresponding decrease in the soma. This observation suggests that UFM-1 negatively regulates ODR-10 transport to cilia. Moreover, ODR-10::GFP that remained at the soma in these mutant animals appear to localize on or near the cell surface. *ufm1(gk379)* suppressed the ODR-10::GFP localization defect of *odr-8* animals. These results suggest that UFM1 is required for the ER retention of ODR-10 in *odr-8* mutants. Our model for chemoreceptor traffic would suggest that UFM1 acts at the ER to restrict the rate of ODR-10 exit. Indeed, cell-fractionation experiments have demonstrated the presence of UFM1, UFM1-conjugates, and the E3 enzyme UFL1 in fractions enriched for ER proteins(Kang et al., 2007; Tatsumi et al., 2010). Hence, a balance between UFM1 function and ODR-8/UfSP2 activity may control the net movement of ODR-10 from the ER to the cilia.

In addition to the genetic argument, preliminary results using an antibody against human UFM1 suggest increased immunoreactivity against UFM1-modified proteins in

odr-8(ky31) mutants. Identification of these substrates may shed further light into the means by which UFM1 controls ODR-10 transport. ODR-10 itself and ODR-4 are prime candidates for UFM-1 conjugation, and are under investigation. The only UFM1 target identified thus far, DDRGK1, could also be involved, but there is no existing mutant allele for this gene in *C. elegans*.

While mutants for the UFM1 E2 and E3 enzymes are not available, examination of a putative *C. elegans* E1 for UFM1, *T03F1.1/Uba5(ok3364)* mutants, showed neither an increase nor a decrease in ODR-10 transport to the cilia. While this phenotype is surprising and the reason behind it remains unclear, it is likely that another E1, perhaps the closely related protein Uba4 (known as MOC-3/UBA-4 in *C. elegans*) may act redundantly with UBA-5.

References

Arvidsson, U., Riedl, M., Chakrabarti, S., Lee, J.H., Nakano, A.H., Dado, R.J., Loh, H.H., Law, P.Y., Wessendorf, M.W., and Elde, R. (1995). Distribution and targeting of a mu-opioid receptor (MOR1) in brain and spinal cord. J Neurosci *15*, 3328-3341.

Asencio, C., Rodriguez-Aguilera, J.C., Ruiz-Ferrer, M., Vela, J., and Navas, P. (2003). Silencing of ubiquinone biosynthesis genes extends life span in Caenorhabditis elegans. FASEB J *17*, 1135-1137.

Baker, E.K., Colley, N.J., and Zuker, C.S. (1994). The cyclophilin homolog NinaA functions as a chaperone, forming a stable complex in vivo with its protein target rhodopsin. EMBO J *13*, 4886-4895.

Bargmann, C.I. (2006). Comparative chemosensation from receptors to ecology. Nature *444*, 295-301.

Barnes, A.P., and Polleux, F. (2009). Establishment of axon-dendrite polarity in developing neurons. Annu Rev Neurosci *32*, 347-381.

Bush, C.F., and Hall, R.A. (2008). Olfactory receptor trafficking to the plasma membrane. Cell Mol Life Sci *65*, 2289-2295.

Colley, N.J., Baker, E.K., Stamnes, M.A., and Zuker, C.S. (1991). The cyclophilin homolog ninaA is required in the secretory pathway. Cell *67*, 255-263.

Dong, C., Filipeanu, C.M., Duvernay, M.T., and Wu, G. (2007). Regulation of G protein-coupled receptor export trafficking. Biochim Biophys Acta *1768*, 853-870.

Dwyer, N.D., Adler, C.E., Crump, J.G., L'Etoile, N.D., and Bargmann, C.I. (2001). Polarized dendritic transport and the AP-1 mu1 clathrin adaptor UNC-101 localize odorant receptors to olfactory cilia. Neuron *31*, 277-287.

Dwyer, N.D., Troemel, E.R., Sengupta, P., and Bargmann, C.I. (1998). Odorant receptor localization to olfactory cilia is mediated by ODR-4, a novel membrane-associated protein. Cell *93*, 455-466.

Ferreira, P.A., Nakayama, T.A., Pak, W.L., and Travis, G.H. (1996). Cyclophilin-related protein RanBP2 acts as chaperone for red/green opsin. Nature *383*, 637-640.

Grant, B.D., and Donaldson, J.G. (2009). Pathways and mechanisms of endocytic recycling. Nat Rev Mol Cell Biol *10*, 597-608.

Ha, B.H., Jeon, Y.J., Shin, S.C., Tatsumi, K., Komatsu, M., Tanaka, K., Watson, C.M., Wallis, G., Chung, C.H., and Kim, E.E. (2011). Structure of Ubiquitin-fold Modifier 1-specific Protease UfSP2. J Biol Chem *286*, 10248-10257.

Kang, S.H., Kim, G.R., Seong, M., Baek, S.H., Seol, J.H., Bang, O.S., Ovaa, H., Tatsumi, K., Komatsu, M., Tanaka, K.*, et al.* (2007). Two novel ubiquitin-fold modifier 1 (Ufm1)-specific proteases, UfSP1 and UfSP2. J Biol Chem *282*, 5256-5262.

Kaplan, O.I., Molla-Herman, A., Cevik, S., Ghossoub, R., Kida, K., Kimura, Y., Jenkins, P., Martens, J.R., Setou, M., Benmerah, A.*, et al.* (2010). The AP-1 clathrin adaptor facilitates cilium formation and functions with RAB-8 in C. elegans ciliary membrane transport. J Cell Sci *123*, 3966-3977.

Komatsu, M., Chiba, T., Tatsumi, K., Iemura, S., Tanida, I., Okazaki, N., Ueno, T., Kominami, E., Natsume, T., and Tanaka, K. (2004). A novel protein-conjugating system for Ufm1, a ubiquitin-fold modifier. EMBO J *23*, 1977-1986.

Loconto, J., Papes, F., Chang, E., Stowers, L., Jones, E.P., Takada, T., Kumanovics, A., Fischer Lindahl, K., and Dulac, C. (2003). Functional expression of murine V2R pheromone receptors involves selective association with the M10 and M1 families of MHC class Ib molecules. Cell *112*, 607-618.

Morello, J.P., and Bichet, D.G. (2001). Nephrogenic diabetes insipidus. Annu Rev Physiol *63*, 607-630.

Rodriguez-Aguilera, J.C., Asencio, C., Ruiz-Ferrer, M., Vela, J., and Navas, P. (2003). Caenorhabditis elegans ubiquinone biosynthesis genes. Biofactors *18*, 237-244.

Rolls, M.M., Hall, D.H., Victor, M., Stelzer, E.H., and Rapoport, T.A. (2002). Targeting of rough endoplasmic reticulum membrane proteins and ribosomes in invertebrate neurons. Mol Biol Cell *13*, 1778-1791.

Saito, H., Kubota, M., Roberts, R.W., Chi, Q., and Matsunami, H. (2004). RTP family members induce functional expression of mammalian odorant receptors. Cell *119*, 679-691.

Sengupta, P., Colbert, H.A., and Bargmann, C.I. (1994). The C. elegans gene odr-7 encodes an olfactory-specific member of the nuclear receptor superfamily. Cell *79*, 971-980.

Stojanovic, A., and Hwa, J. (2002). Rhodopsin and retinitis pigmentosa: shedding light on structure and function. Receptors Channels *8*, 33-50.

Tatsumi, K., Sou, Y.S., Tada, N., Nakamura, E., Iemura, S., Natsume, T., Kang, S.H., Chung, C.H., Kasahara, M., Kominami, E.*, et al.* (2010). A novel type of E3 ligase for the Ufm1 conjugation system. J Biol Chem *285*, 5417-5427.

Tatsumi, K., Yamamoto-Mukai, H., Shimizu, R., Waguri, S., Sou, Y.S., Sakamoto, A., Taya, C., Shitara, H., Hara, T., Chung, C.H.*, et al.* (2011). The Ufm1-activating enzyme Uba5 is indispensable for erythroid differentiation in mice. Nat Commun *2*, 181.

Wozniak, M., Keefer, J.R., Saunders, C., and Limbird, L.E. (1997). Differential targeting and retention of G protein-coupled receptors in polarized epithelial cells. J Recept Signal Transduct Res *17*, 373-383.

Wozniak, M., and Limbird, L.E. (1996). The three alpha 2-adrenergic receptor subtypes achieve basolateral localization in Madin-Darby canine kidney II cells via different targeting mechanisms. J Biol Chem *271*, 5017-5024.

Chapter 4

Conclusion and Future Directions

Summary

As masters of cell compartmentalization, neurons are polarized into two primary domains that are morphologically and functionally distinct: a single long axon and one or more dendrites. The distinct properties of these two compartments rely on the differences in their molecular composition. Hence, understanding the mechanisms that target constituent proteins to specific domains is a fundamental question for neuronal cell biology and function.

Here, I have described my thesis work aimed at understanding these mechanisms that regulate the transport of neuronal proteins to their respective subcellular destinations. I established an *in vivo* system to visualize axon-dendrite compartmentalization in *C. elegans* neurons by expressing two fluorescently-tagged presynaptic molecules in PVD mechanosensory neurons. A visual screen for mutants identified *unc-33/CRMP*, a homolog of mammalian Collapsin Response Mediator Proteins (CRMPs), as a major regulator that establishes the restricted localization of axonal as well as dendritic molecules. Furthermore, a candidate approach revealed that *unc-44/ankyrin* mutants share the phenotypes of *unc-33/CRMP* mutants. The loss of axon and dendrite identities seem to result from misdirected transport: in mutants, the axonal kinesin UNC-104/KIF1A actively transports axonal proteins to both axons and dendrites, and the distinctive organization of axonal and dendritic microtubules is altered. UNC-33 is axonally localized, and through the action of UNC-44 shows further enrichment in a proximal axonal region, reminiscent

of the axon initial segment – a spatial and physiological landmark with emerging roles in neuronal polarity.

Next, in order to further characterize dendritic protein transport, and potentially identify the motor protein responsible for GPCR transport to sensory cilia, I focused on understanding the role of *odr-8*. *odr-8* mutants were identified in *C. elegans* screens for olfactory mutants or defective GPCR localization. Mutants are defective at localizing chemoreceptors such as ODR-10, the diacetyl receptor, to the chemosensory cilia in neurons. Using Illumina/Solexa whole genome sequencing, I identified *odr-8* as a gene encoding the *C. elegans* homolog of UfSP2. Mammalian UfSP2 acts as a cysteine-protease specific for UFM1, a ubiquitin-like molecule, whose function remains to be identified. *odr-8* mutants exhibit ER retention of ODR-10::GFP. In contrast, *ufm-1* mutants show enhanced levels of ODR-10 at the cilia and cell body surface. Double mutants show suppression of the *odr-8* phenotype, rescuing ODR-10 ciliary enrichment. *odr-8* functions cell autonomously to regulate ODR-10 transport. GFP::ODR-8, diffusely distributed throughout the cytosol and the nucleus, shows peri-nuclear enrichment suggesting ER association. This suggests that ODR-8 may act at the ER in opposition to UFM-1 function to regulate ODR-10 transport from the ER to the cilia.

Future Directions

Screen: Additional regulators of axon-dendrite compartmentalization

Considering the possibility that mutants with defects in neuronal polarity may also have defects in other polarized cell types, we reasoned that these animals might be

extremely sick or even lethal, making it likely that one would fail to isolate these in a non-clonal pool of F2s. Hence, I performed an EMS-based F1 clonal screen examining ~40 F2 progeny from each cloned F1 for the localization of mCherry::RAB-3 and SAD-1::GFP in PVD as well as FLP neurons. This screen that led to the identification of *unc-33(ky880)* was a particularly small screen, examining ~4000 animals representing ~200 mutagenized genomes. This work established RAB-3 and SAD-1 distribution in PVD neurons as a suitable system to examine axon-dendrite compartmentalization. Clearly, further pursuance of this screen is likely to yield additional important regulators of axon-dendrite polarization.

i.) Extracellular cues: Given the documented roles of *unc-6*/netrin, *slt-1*/Slit and WNTs in regulating neuronal polarity(Ou and Shen, 2011), it would be interesting to see if they act in regulating PVD axon-dendrite polarization. Since PVD polarity is aligned along the dorsal-ventral axis, *unc-6* and *slt-1* are prime candidates for orienting PVD axon-dendrite development.

While extracellular information has been shown to spatially organize axon-dendrite development and regulate protein transport in *C. elegans* neurons, its requirement for axon or dendrite growth per se requires further examination. Future experiments can help identify cues that are required for PVD axon growth, and thereby assess if the same set of cues or distinct cues function together to co-ordinate morphological polarization and molecular composition of axons versus dendrites.

ii.) Regulation of UNC-33/CRMP function

The work presented in Chapter 2 suggests that UNC-44/ankyrin localizes UNC-33/CRMP to axons, where they may function together to organize axonal microtubules so as to differentially recruit axonal kinesins. Given the observation that the N-terminus of UNC-33L is required for its polarized localization, it is possible that UNC-44 or its unidentified downstream effector recruits UNC-33L by interacting with its N-terminus. A yeast-two-hybrid approach with this N-terminus or an UNC-33L pull-down experiment may test this hypothesis and identify the binding partner. This would shed light on the mechanism by which UNC-33 localization and hence activity is regulated in *C. elegans* neurons. In mammals, the significance of ankyrins in regulating CRMP localization remains to be tested.

Experiments using cultured hippocampal neurons have shown that GSK-3β is a major regulator of CRMP-2. GSK-3β phosphorylates the C-terminus of CRMP-2 at Thr-514 and Thr-518, once Cdk5 kinase primes the substrate at Ser-522(Yoshimura et al., 2005). These phosphorylation events result in a diminished affinity of CRMP-2 for microtubules, thereby regulating axon versus dendrite levels of CRMP-2 function (Yoshimura et al., 2005). While the phosphorylation residues do not appear to be conserved in the C-terminus of UNC-33, alternative sites are likely given the consensus motif for GSK-3β (S/T-X-X-X-S/T). Thus, it remains to be seen if GSK-3β is also an important regulator of polarized protein transport in *C. elegans*, acting through UNC-33.

iii.) Regulation of UNC-44/ankyrin function

A complete understanding of axon-dendrite compartmentalization would require connecting the relevant extracellular cues to UNC-44 as well as UNC-33 localization. The mechanisms defining UNC-44 localization are unknown, mainly due to the complexity of the *unc-44* locus that is characterized by a multitude of isoforms varying from 3 kb to ~25 kb in length (Boontrakulpoontawee and Otsuka, 2002; Otsuka et al., 2002; Otsuka et al., 1995). However, recent advances in fosmid recombineering may allow the development of a translational GFP fusion reporter for UNC-44 that could be used for a forward genetic or a candidate screening approach. Such reporters, in combination with α-UNC-44 immunofluorescence experiments, can be used to test whether UNC-44 and UNC-33 are interdependent for their localization.

As is true for *C. elegans* UNC-44, we know next to nothing about how ankyrinG is targeted to the AIS in mammalian neurons, and what determines the position of the AIS. Recent evidence indicates that the regulation of IκBα, an inhibitor of the transcription factor NFκB, may play a role in AIS formation and ankyrinG clustering . IκBα is enriched in the proximal axonal region along with ankyrinG, and inhibiting the phosphorylation of IκBα prevents AIS formation and ankyrinG clustering. It remains to be seen whether this is a permissive function or an instructive role in spatially defining ankyrinG location.

Understanding the effect of UNC-33 and UNC-44 on microtubules

A central observation in the work presented in Chapter 2 is that UNC-44 and UNC-33 are necessary for the proper organization of axonal and dendritic microtubules that are known to have distinct properties. Axonally localized UNC-33 and UNC-44 seem to

stabilize and organize axonal microtubules that may allow the differential recruitment of kinesins towards axons while preventing dendritic kinesin-cargo complexes. While it has been shown that UNC-33 and mammalian CRMP proteins can promote microtubule assembly *in vitro(Fukata et al., 2002)*, the mechanism of UNC-33 action on microtubule regulation needs further analysis. 1.) It will be important to ask whether UNC-33 promotes microtubule polymerization by bundling microtubules or by inhibiting catastrophe or by actively promoting addition of tubulin heterodimers. Consistent with the last of the three scenarios, mammalian CRMP proteins can bind tubulin heterodimers in addition to their microtubule binding property. Assessing UNC-33 distribution on microtubules will provide additional information that may inform our understanding of its function. 2.) An interesting possibility to consider is whether microtubules polymerized in presence of UNC-33 differ from those polymerized without UNC-33. If so, such differences may reveal the fundamental cytoskeletal differences between axonal and dendritic microtubules that may regulate polarized transport. Given that axonal microtubules are more stable than dendritic microtubules in mammalian neurons(Witte et al., 2008), one could ask whether the microtubules formed with the aid of UNC-33 are more resistant to cold-induced or nocodazole-induced deplymerization, compared to microtubules formed without UNC-33. 3.) Ultimately, it will be important to connect any UNC-33 induced microtubule feature to regulation of kinesin-binding or kinesin-motility. Considering that this may or may not be direct, it represents an important but challenging question that will need addressing.

The significance of UNC-44 in organizing neuronal microtubules may either be purely due to its effect on UNC-33 distribution, or UNC-44 may have additional roles in

regulating microtubule organization, perhaps directly. Indeed, mammalian ankyrins in the brain and erythrocytes can interact with microtubules(Bennett and Davis, 1981, 1982; Davis and Bennett, 1984), the significance of which remains to be identified. *Drosophila* giant ankyrin, *Ank2-L,* is also able to bind microtubules, and promotes microtubule stabilization through its extended C-terminal domain(Pielage et al., 2008). Similar C-terminal extensions also exist in mammalian ankyrinG and ankyrinB as well as *C. elegans* UNC-44, and their significance in binding and stabilizing microtubules will require further investigation.

Regulation of ODR-10 transport: Identification of UFM-1 substrates

The studies on ODR-10 transport regulation by *odr-8*, presented in Chapter 3, show that while *odr-8* is required for ER exit of ODR-10, UFM-1 may act to limit ODR-10 transport from the ER to chemosensory cilia. While the genetic argument in this analysis may be convincing, much work needs to be done, such as the verification of preliminary results concerning UFM-1 immunoreactivity, and continued characterization of ODR-10 and ODR-8 subcellular localization. In addition, one of the most interesting questions is the one raised by the *ufm-1(gk379);odr-8(ky173)* double mutant analysis. The suppression of the *odr-8* phenotype by *ufm-1(gk379)* suggests that UFM1 conjugation is required for ODR-10 ER retention in *odr-8* mutans. Therefore, one important direction for future experiments would be the identification of UFM1-modified substrates in neurons, and testing if these could result in ER retention of ODR-10. The significance of ODR-4 for ODR-10 transport combined with its subcellular localization, makes ODR-4 a prime candidate whose modification by UFM1 may be functionally relevant. Alternatively,

ODR-10 itself may be under direct control of UFM1 modification. Thus, a candidate-based approach combined with an unbiased LC-MS/MS analysis of UFM1-pull down samples is likely to yield the identity of the relevant UFM1-substrate that may control transport of chemoreceptors such as ODR-10.

Significance of odr-8 and ufm-1: A potential Quantity Control and a Quality Control mechanism?

The results presented in Chapter 3 support, but not prove, the roles of ODR-8 and UFM-1 in a quantity control mechanism, where a balance of the two activities regulates the level of ODR-10 enrichment at the cilia. While *odr*-8 is required for ER exit of ODR-10, it would be useful to ask whether overexpression of ODR-8 can increase ODR-10 cilia localization. Similarly, *ufm-1(gk379)* single mutants clearly show that *ufm-1* negatively regulates ODR-10 transport from the ER to the cilia. However, a converse experiment of assessing the effect of UFM-1 overexpression on ODR-10 transport may prove informative. Such an experiment may provide further support to the proposed role of UFM-1 in regulating ODR-10 surface levels. Taking these experiments one step further, overexpression of UFM1 combined with ODR-8 overexpression can examine the importance of relativel levels as opposed to absolute levels in the regulation of ODR-10 transport.

ER retention is often associated with misfolded proteins or partly assembled complexes(Dong et al., 2007). The system, regulating protein folding and transport from the ER, is referred to as the Quality Control mechanism(Ellgaard and Helenius, 2003). The efficient function of the Quality Control system ensures only mature, functional

proteins exit the ER for transport to their respective destinations, whereas the misfolded proteins get eventually targeted for proteasomal destruction via the ER-associated degradation (ERAD) pathway. The experimental analyses of *odr-8* and *ufm-1* mutants are also consistent with a Quality Control function of the UFM1-modification system; this intriguing role, however, is purely speculative and may warrant further investigation. It would be interesting to see if UFM1-conjugation of ODR-10/ODR-4/another substrate serves as a mark to label immature ODR-10 protein, causing it to be retained in the ER. On the other hand, proper conformational assembly, sensed directly or indirectly by ODR-8/UfSP2, might result in UFM1-removal, allowing ER exit. Examination of the conformational stability and functional capability of ODR-10 or other chemoreceptors in *odr-8* and *ufm-1* mutants could be used to test this model. While direct examination of this model remains to be done, it is interesting that UFM1, its E3 ligase UFL1, and their lone substrate DDRGK1 show marked upregulation in response to elevated ER stress, induced by chemical ER stressors or in genetic models of ischemic heart disease and diabetes mellitus 2 (Azfer et al., 2006).

Concluding Remarks

The studies presented here show the value of using *C. elegans* genetics along with single-cell resolution analysis of its well-defined nervous system to identify molecules that are *in vivo* regulators of polarized protein transport in neurons. In addition, examination of genetic interactions and subcellular reporter distribution can provide further insight into the mechanism by which such molecules control protein targeting. As in the case of UNC-33, UNC-44 as well as for ODR-8, the combination of such studies in *C. elegans* neurons, with

biochemical as well as genetic experiments in additional systems will likely yield a complete picture regarding the mechanisms of asymmetric protein transport in neurons.

References

Azfer, A., Niu, J., Rogers, L.M., Adamski, F.M., and Kolattukudy, P.E. (2006). Activation of endoplasmic reticulum stress response during the development of ischemic heart disease. Am J Physiol Heart Circ Physiol *291*, H1411-1420.

Bennett, V., and Davis, J. (1981). Erythrocyte ankyrin: immunoreactive analogues are associated with mitotic structures in cultured cells and with microtubules in brain. Proc Natl Acad Sci U S A *78*, 7550-7554.

Bennett, V., and Davis, J. (1982). Immunoreactive forms of human erythrocyte ankyrin are localized in mitotic structures in cultured cells and are associated with microtubules in brain. Cold Spring Harb Symp Quant Biol *46 Pt 2*, 647-657.

Boontrakulpoontawee, P., and Otsuka, A.J. (2002). Mutational analysis of the Caenorhabditis elegans ankyrin gene unc-44 demonstrates that the large spliceoform is critical for neural development. Mol Genet Genomics *267*, 291-302.

Davis, J.Q., and Bennett, V. (1984). Brain ankyrin. A membrane-associated protein with binding sites for spectrin, tubulin, and the cytoplasmic domain of the erythrocyte anion channel. J Biol Chem *259*, 13550-13559.

Dong, C., Filipeanu, C.M., Duvernay, M.T., and Wu, G. (2007). Regulation of G protein-coupled receptor export trafficking. Biochim Biophys Acta *1768*, 853-870.

Ellgaard, L., and Helenius, A. (2003). Quality control in the endoplasmic reticulum. Nat Rev Mol Cell Biol *4*, 181-191.

Fukata, Y., Itoh, T.J., Kimura, T., Menager, C., Nishimura, T., Shiromizu, T., Watanabe, H., Inagaki, N., Iwamatsu, A., Hotani, H*., et al.* (2002). CRMP-2 binds to tubulin heterodimers to promote microtubule assembly. Nat Cell Biol *4*, 583-591.

Otsuka, A.J., Boontrakulpoontawee, P., Rebeiz, N., Domanus, M., Otsuka, D., Velamparampil, N., Chan, S., Vande Wyngaerde, M., Campagna, S., and Cox, A. (2002). Novel UNC-44 AO13 ankyrin is required for axonal guidance in C. elegans, contains six highly repetitive STEP blocks separated by seven potential transmembrane domains, and is localized to neuronal processes and the periphery of neural cell bodies. J Neurobiol *50*, 333-349.

Otsuka, A.J., Franco, R., Yang, B., Shim, K.H., Tang, L.Z., Zhang, Y.Y., Boontrakulpoontawee, P., Jeyaprakash, A., Hedgecock, E., Wheaton, V.I*., et al.* (1995). An ankyrin-related gene (unc-44) is necessary for proper axonal guidance in Caenorhabditis elegans. J Cell Biol *129*, 1081-1092.

Ou, C.Y., and Shen, K. (2011). Neuronal polarity in C. elegans. Dev Neurobiol.

Pielage, J., Cheng, L., Fetter, R.D., Carlton, P.M., Sedat, J.W., and Davis, G.W. (2008). A presynaptic giant ankyrin stabilizes the NMJ through regulation of presynaptic microtubules and transsynaptic cell adhesion. Neuron *58*, 195-209.

Witte, H., Neukirchen, D., and Bradke, F. (2008). Microtubule stabilization specifies initial neuronal polarization. J Cell Biol *180*, 619-632.

Yoshimura, T., Kawano, Y., Arimura, N., Kawabata, S., Kikuchi, A., and Kaibuchi, K. (2005). GSK-3beta regulates phosphorylation of CRMP-2 and neuronal polarity. Cell *120*, 137-149.

Materials and Methods

Strains and Transgenes

Wild type nematodes were *C. elegans* variety Bristol, strain N2. Strains were cultured using standard techniques (Brenner, 1974) at 21-23 C. Some strains were provided by the *Caenorhabditis* Genetics Center. The following mutants were used: *unc-33(e204, e1193, ky869, ky880, mn407)* IV*; unc-34(e315)* V*; unc-104(e1265)* II*; unc-44(e362, ky110)* IV, *odr-8(ky26, ky28, ky31, ky41, ky173)* IV; *odr-4(n2144)* III; *unc-101(m1)* I; *Zk652.3*/*ufm-1(gk379)* III; *T03F1.1/Uba5(ok3364*) I.

Germline transformation was carried out as described (Mello and Fire, 1995) using *odr-1::DsRed* (25 ng/μl) or *unc-122::DsRed* (20 ng/μl) as co-injection markers.

Standard molecular biology techniques were used to generate expression plasmids and cDNAs used for transgenes.

Isolation and characterization of *unc-33(ky880)* and *unc-33(ky869)*

A strain expressing RAB-3::mCherry and SAD-1::GFP in PVDs (*kyIs445*) was mutagenized using ethylmethane sulfonate (EMS) according to standard procedures (Anderson, 1995). F1s were cloned onto individual plates, and 40-60 F2 progeny from each F1 parent were screened under a compound fluorescence microscope. Mutants were chosen on the basis of dendritic mislocalization of RAB-3::mCherry and SAD-1::GFP, as detected by a Plan-Neofluar 40x objective on a Zeiss Axioplan2 microscope, resulting in the isolation of *ky880*.

Similarly, a strain expressing RAB-3::mCherry and UNC-2::GFP in AWCs (*kyIs442*) was mutagenized using EMS. Through an analogous F1 clonal screen, *ky869* was isolated by Y. Saheki as a mutant that showed reduced axonal localization of RAB-3::mCherry and UNC-2::GFP in AWC neurons. Further characterization uncovered a significant increase in dendritic localization of both markers in AWCs.

Mapping and rescue of *ky880* and *ky869*

ky880 and *ky869* were mapped to the middle of LGIV using single nucleotide polymorphisms in the CB4856 strain (Wicks et al., 2001) and sequenced to identify *unc-33* mutations. Both mutants failed to complement *unc-33(e1193)* and *unc-33(mn407)* null alleles for *Unc* and *Egl* behavior and for localization of RAB-3::mCherry and SAD-1::GFP in PVD and FLP neurons, but complemented the hypomorphic allele *unc-33(e204)* for all phenotypes. This intragenic complementation suggests that *unc-33* has two interdependent functions, and is consistent with the reported oligomerization of UNC-33/CRMP proteins (Tsuboi et al., 2005; Wang and Strittmatter, 1997). A plasmid driving the expression of an UNC-33L cDNA under the regulation of the pan-neuronal *tag-168* promoter rescued uncoordinated movement, egg-laying behavior, and RAB-3::mCherry and SAD-1::GFP localization in PVD neurons in *unc-33(ky880)* and *unc-33(mn407)* mutants.

Cloning of *odr-8*

Mixed stage CX2386 *odr-8(ky31)* animals were collected and genomic DNA was isolated through proteinase K digestion, followed by phenol-chloroform extraction and ethanol precipitation. Thereafter, purified genomic DNA was submitted to the Rockefeller

Genomics Resource Center for Illumina-Solexa whole genome sequencing. Scott Dewell and colleagues at the Genomics Resource Center prepared the library from the genomic DNA sample, obtained ~35 bp sequence reads, and aligned it against the worm wild type (N2 strain) reference genome to identify putative SNPs. Patrick McGrath performed further alignment against sequence reads obtained for previously sequenced lab strains so as to eliminate putative SNPs common to lab strains that may have been used for EMS mutagenesis or outcrossing of *odr-8(ky31)*.

As mentioned in the results section of Chapter 3, the abovementioned sequence alignment led to the identification of putative SNPs that may be responsible for the *odr-8* phenotype. Three of these that resided within the *lin-45* and *deb-1* interval were experimentally tested and excluded based on lack of rescue upon injection of corresponding fosmids (5 ng/ul) and PCR amplified gene products (25 ng/ul). Subsequently, the candidate G->A SNP affecting the gene F38A5.1 was considered that was predicted to result in a nonsense mutation (W419Stop), disrupting the putative protease just before its catalytic cysteine residue (C421). 1.) Sanger sequencing of three independent PCR products amplifying the putatively affected F38A5.1 region in *odr-8(ky31)* animals confirmed the G->A SNP corresponding to W419. 2.) PCR amplification of F38A5.1 exons and splice junctions from the four additional *odr-8* alleles identified mutations in F38A5.1 that were either nonsense changes or a missense change affecting a conserved histidine. 3.) F38A5.1 genomic region was PCR amplified with its exons, introns, 3' UTR, and either 1.6 kb or 2.6 kb upstream region. These two PCR products were injected at ~25 ng/ul (along with Coel:: DsRED co-injection marker at ~20 ng/ul) into *odr-8(ky31); kyIs53* animals, where *kyIs53* is the reporter driving ODR-10::GFP in

AWA neurons. L4s or young adults from multiple lines were scored for both sets of injections. For both PCR products injected, animals with the transgene exhibited wild type patterns of ODR-10::GFP localization, compared to animals without the transgene that showed cell body retention of ODR-10::GFP in AWA neurons. Based on these three lines of evidence, it was concluded that F38A5.1 corresponds to *odr-8*.

Analysis of ODR-10::GFP localization in *ufm-1(gk379)* animals

ufm-1(gk379) homozygous animals are either arrested or dead at an early stage in L1. Hence, using a balancer, they are maintained as heterozygotes *ufm-1(gk379)/hT2*. For the analysis of ODR-10::GFP expressed in *ufm-1* single mutants or *ufm-1; odr-8* double mutants, 20-30 *ufm-1* heterozygous adults were allowed to lay eggs for 2 hours or 4 hours. After about 11-13 hours, most embryos had hatched at room temperature. These progeny were allowed to grow for 1-2 days before the balancer-positive non-arrested progeny was removed from the plate. No balancer-negative animal escaped the L1 arrest. These *ufm-1* homozygous progeny, with or without the *odr-8(ky173)* mutation were examined for ODR-10::GFP about 3-4 days post-hatching. The reason for doing so was to bypass a potential maternal contribution of UFM-1. In case of wild type and *odr-8(ky173)* single mutant animals, the hatch-off technique was used to obtained synchronized L1s. Animals were examined at roughly 3 hour intervals. Fluorescence quantification data for these genotypes corresponds to 5-7 hour-old L1s.

Fluorescence microscopy and quantification

Animals were mounted on 2% agarose pads in 10 mM sodium azide. For *unc-33* experiments, L4 larvae or young adult animals were used for analysis of fluorescently tagged markers in PVD, whereas L1 stage and L4 stage larvae were examined for the analysis of ODR-10::GFP in AWB neurons (*kyIs156* transgene). Wild type animals generally showed >15 bright RAB-3::mCherry and SAD-1::GFP puncta in PVD axons, no dendritic puncta, and faint or nonexistent fluorescence in the primary dendrites, with modest variations depending on expression level of the transgene. Animals were scored as having reduced axonal labeling if there were fewer than 12 bright puncta in PVD axons, and were scored as having ectopic dendritic labeling if bright RAB-3::mCherry or SAD-1::GFP puncta were present in PVD secondary dendrite branches. Several independent transgenic lines were examined for each transgene in each genetic background.

For *odr-8* experiments, animals were mounted on 2% agarose pads in 400uM tetramisole or 10 mM sodium azide. L4 and adult animals were analyzed for ODR-10::GFP distribution in AWA neurons, whereas L1 staged as well as L4/adults were examined for ODR-10::GFP localization in AWB neurons.

Z-stacks of fluorescent images were acquired on a Zeiss Axioplan2 imaging system or on a Zeiss LSM510 META laser scanning confocal imaging system. Wide-field and confocal z-stacks were processed using Metamorph or ImageJ (NIH) to obtain maximum intensity projections.

For the quantification of fluorescence intensities of RAB-3::mCherry and SAD-1::GFP in PVD axons and dendrites, fluorescent z-stacks were acquired under consistent

detector settings using a Hamamatsu Photonics C2400 CCD camera and Metamorph software, under a 40x Plan-Neofluar on the Zeiss Axioplan2 imaging system. ImageJ was used to measure fluorescence intensities. We obtained maximum projections of axonal focal planes and dendritic focal planes for one PVD in each animal. Background intensity was subtracted and fluorescent clusters with signals above an arbitrary threshold were scored for total fluorescent intensity. Identical thresholds were used for the quantification of each image. 10-17 worms per genotype were scored.

Using the same process, ODR-10::GFP fluorescence quantification was performed on the soma and cilia of AWB neurons in wild type, *odr-8(ky173)*, *ufm-1(gk379)* and ufm-1;odr-8 animals. Using ImageJ (NIH), background fluorescence was estimated and subtracted for each of the subcellular regions, and the outlines of cell body and cilia were traced to obtain information about the fluorescence profile.

For the quantification of UNC-33::GFP in PVD axonal domains, fluorescent z-stacks were obtained as above, using the 63x Plan-Apochromat objective on the Zeiss Axioplan2 system, and fluorescence measurements were performed using Metamorph. Z-stack planes with 'axonal proximal domain' and 'axonal initial domain' in focus were selected for maximum intensitiy projections. Background fluorescence was substracted for each image, and a line tool was used to measure the fluorescence along the axonal domains. This average fluorescence for each axonal segment was used to calculate the 'axon initial'/'axon proximal' ratio for Figure 2.3e.

Heat-shock experiments

For *unc-33* experiments, animals were synchronized by allowing bleached eggs to hatch overnight in M9 buffer (22 mM KH_2PO_4, 22 mM Na_2HPO_4, 85 mM NaCl, 1 mM $MgSO_4$) without food; the resulting larvae, synchronized at the L1 larval stage, were then fed and allowed to develop at 21-23°C. Animals were provided a 2 hour pulse of heat-shock at 33°C at varying time points, then recovered at 21-23°C. For each heat-shock time point, a corresponding group of animals was examined using DIC on the Zeiss Axioplan2 microscope to confirm the developmental stage at which animals were being heat-shocked. Adult animals were scored for the localization of RAB-3::mCherry and SAD-1::GFP in PVDs.

ODR-10::GFP localization defect in *odr-8(ky31)* animals was rescued by providing a 2 hour pulse of 33°C heat-shock to L4s or young adults. Animals were allowed to recover at 21-23°C for 8 hours, before examining them for enrichment of ODR-10::GFP in AWA cilia.

Immunofluorescence

Antibodies used as well as their corresponding dilutions are as follows: DM1A anti-α-tubulin (mouse monoclonal, Sigma) 1:400, GT335 anti-glutamylated tubulin (mouse monoclonal, a gift from C. Janke and B. Edde, CNRS) 1:500, 6-11B-1 anti-acetylated-α-tubulin (mouse monoclonal, Sigma) 1:500, AB3201 anti-detyrosinated-α-tubulin (rabbit polyclonal, Millipore) 1:200, TUB-1A2 anti-tyrosinated- α-tubulin (mouse monoclonal,

Sigma) 1:200, 24H11 anti-UNC104 (mouse monoclonal, S. Koushika, unpub.) 1:250. Rabbit polyclonal antisera (Q3201 and Q3203) against an UNC-33L – specific fragment of UNC-33 (amino acid 29 to amino acid 128 of UNC-33L sequence) were generated using genomic antibody technology by Strategic Diagnostics, DE, and used at 1:250 dilution for immunostaining. Antisera from both rabbits yielded similar UNC-33L localization results. The secondary antibodies, Alexa Fluor 488-conjugated goat anti-mouse IgG and Alexa Fluor 488-conjugated goat anti-rabbit IgG, (Invitrogen) were used at 1:400 or 1:500 dilutions.

Whole mount immunostaining was performed according to the peroxide tube fixation protocol (Duerr JS, Wormbook 2006), except that animals were fixed in 2% paraformaldehyde as described previously (Ruvkun and Giusto, 1989). Briefly, nematodes were rocked in the fixation solution for 20 min at room temperature prior to freezing, and overnight at 4°C post freezing. Fixed animals were permeabilized in TTB buffer (100 mM Tris pH 7.4, 1% Triton X-100, 1 mM EDTA buffer) containing 1% β-mercaptoethanol for 2 hrs at 37 C, washed with BO_3 buffer (10 mM H_3BO_3 pH 9.4, 0.1 % Triton X-100), reduced by 15 min incubation with 10 mM dithiothreitol in BO_3 buffer at 37°C, washed with BO_3 buffer, and sulfhydryl groups were oxidized by gentle agitation treatment with BO_3 buffer containing 1% H_2O_2 for 1 hour at 25°C. Samples were washed and incubated for 15-30 min with ABB buffer (PBS containing 0.5 % Triton X-100, 1 mM EDTA, 0.05% sodium azide and 0.1% BSA), and stored at 4°C in ABA buffer (PBS containing 0.5 % Triton X-100, 1 mM EDTA, 0.05% sodium azide and 1% BSA) until further use. Animals were gently rocked and incubated overnight at 4°C in primary antibody solutions in ABA buffer, washed with ABB buffer; rocked in secondary antibody solutions in ABA buffer

for 2 hours at room temperature, and washed with ABB buffer. The resulting animals were mounted on 2% agarose pads containing 50 mM Tris (pH 8.5) and 5 mM $MgCl_2$ for visualization under the microscope.

Sub-cellular Fractionation and Western Blotting using anti-human UFM1

Preparation of worm extracts and sub-cellular fractionation was performed according to Burbea et al. (Burbea et al., 2002) with some modifications. Briefly, mixed stage worms were collected and extracts were prepared using a Barocycler in Buffer A (50 mM Hepes pH 7.7, 50 mM Potassium Acetate, 2 mM Magnesium Acetate, 1 mM EDTA, 250 m M sucrose) containing protease inhibitors (leupeptin, chymostatin, elastatinal, pepstatin A, PMSF). Cytosolic and membrane fractions were isolated by spinning at 55,000 rpm in a Ti70 rotor (Beckman). The supernatant from this spin was the cytosolic fraction, used directly for western blotting. The membrane fraction pellets were resuspended in Buffer A, supplemented with 7mM β-mercaptoethanol. These were solubilized with (50 mM TRIS-HCl (pH 8.5), 1% SDS, 2 mM DTT) and diluted with 5 volumes of 50 mM Hepes (pH 7.7) buffer containing BSA to be used for western blotting or immunoprecipitation experiments. Standard techniques were used for SDS-PAGE electrophoresis, transfer to nitrocellulose membranes and incubationg with primary and seconday antibodies. The primary antibodies used were anti-human UFM1 (rabbit polyclonal, Boston Biochem, 1:200) and DM1A anti-α-tubulin (mouse monoclonal, Sigma, 1:10000).

References:

Brenner, S. (1974). The genetics of Caenorhabditis elegans. Genetics *77*, 71-94.

Burbea, M., Dreier, L., Dittman, J.S., Grunwald, M.E., and Kaplan, J.M. (2002). Ubiquitin and AP180 regulate the abundance of GLR-1 glutamate receptors at postsynaptic elements in C. elegans. Neuron *35*, 107-120.

Mello, C., and Fire, A. (1995). DNA transformation. Methods Cell Biol *48*, 451-482.

Tsuboi, D., Hikita, T., Qadota, H., Amano, M., and Kaibuchi, K. (2005). Regulatory machinery of UNC-33 Ce-CRMP localization in neurites during neuronal development in Caenorhabditis elegans. J Neurochem *95*, 1629-1641.

Wang, L.H., and Strittmatter, S.M. (1997). Brain CRMP forms heterotetramers similar to liver dihydropyrimidinase. J Neurochem *69*, 2261-2269.

Wicks, S.R., Yeh, R.T., Gish, W.R., Waterston, R.H., and Plasterk, R.H. (2001). Rapid gene mapping in Caenorhabditis elegans using a high density polymorphism map. Nat Genet *28*, 160-164.